Accident Risk reduCtion of vulnerAble RoaD usErs: an interdisciplinary – multiperspective approach (ARCADE)

Deliverable 3

WP2 - Experimental design at driving/riding/pedestrian simulators

WP3 - Experimental investigation at driving/riding/walking simulators on case studies, also considering the countermeasures

---

Version:	1
Date	26 September 2025
Drafted:	Vennarucci A. (UniRM3); Tefa L. (PoliTO); Bruno G. (UniPD)
Validate	Francesco Bella (Principal Investigator – UniRM3) Marco Bassani (Resp. research unit PoliTO) Andrea Spoto (Resp. research unit UniPD)
Authors/members RU	RU-UniRM3: Bella F., Calvi A., D'Amico F., De Blasiis M. R., Gagliardi V., Vennarucci A. , Manalo J.R.D. RU-PoliTO: Bassani M., Tefa L., Lioi A., Hassani Barbin A. RU-UniPD: Spoto A., Bruno G.
Keywords:	Road Safety, Vulnerable Road Users, Human Factors, Surrogate Safety Measures, Multiperspective, Biopsychology

WP2 - Experimental design at driving/riding/pedestrian simulators (Method #2)

WP3 - Experimental (before/after) investigation at driving/riding/walking simulators on case studies (Method #2), also considering the countermeasures

Contents

1 Introduction

This document provides a brief description of the activities carried out by the Research Unities (RU) of Roma Tre University, Polytechnic of Turin and the University of Padua within the following WPs of the ARCADE project:

- WP2 - Experimental design at driving/riding/pedestrian simulators (Method #2)
- WP3 - Experimental (before/after) investigation at driving/riding/walking simulators on case studies (Method #2), also considering the countermeasures

Considering the specificities of the simulation systems used by 3 RUs and the peculiar driver-VRU interactions analysed by 3 RUs, the document describes for each Research Unit the activities related to design of experiments, 3D modelling of the selected case scenario, BIM model formation of driving scenarios, identification of countermeasures, formation of test participant samples, driving/riding/walking simulation tests with driver/rider/pedestrian's behaviour (spatio-temporal trajectories) and psychophysiological data acquisition.

Referring to the sections below for details, it is highlighted here that the experimental designs developed, the experimental campaigns carried out, and the multidisciplinary approach adopted have allowed a multi-perspective assessment of the interactions between road users (drivers, motorcyclists, cyclists, pedestrians), considering also the central role of human factors in the occurrence of accident events involving VRU.

It should be highlighted in particular that the study of the conflicting interaction involving drivers and VRU carried out from different road users' points of view represents an original contribution to the current road safety literature.

The outcomes of the studies will be showed in the Deliverable 4 together with the practical implications of the obtained results.

2 Simulation studies RU UniRM3

2.1 Simulation Scenario

The driving simulation scenario was developed to accurately reproduce a real urban traffic configuration that had previously been identified as a hazardous road location. This identification was based on accident data analyses presented in Deliverable 1 and on field inspections documented in Deliverable 2, which highlighted a high level of conflict between motor vehicles and vulnerable road users. The selected scenario corresponds to the intersection between Via delle Medaglie d'Oro and Via Prisciano, located in the city of Rome. The choice of this site was further supported by stakeholder consultations conducted within the framework of the PRIN ARCADE research project, ensuring that the simulated environment reflects both empirical evidence and local expertise regarding critical safety issues.

The intersection geometry reflects the actual layout of the study area, including lane widths, curb alignments, visibility constraints, and surrounding urban elements. Particular attention was devoted to replicating the real spatial configuration that influences drivers' perception and decision-making processes, such as building setbacks, roadside obstacles, parking arrangements, and the alignment of approach legs. This detailed geometric reconstruction ensured a high degree of ecological validity and allowed the simulator to reproduce realistic sight distances and conflict points.

The current existing configuration of the site of interest (Scenario 0) was reconstructed in the Building Information Modelling (BIM) virtual environment (Figure 0) and then implemented into the driving simulator scenarios.

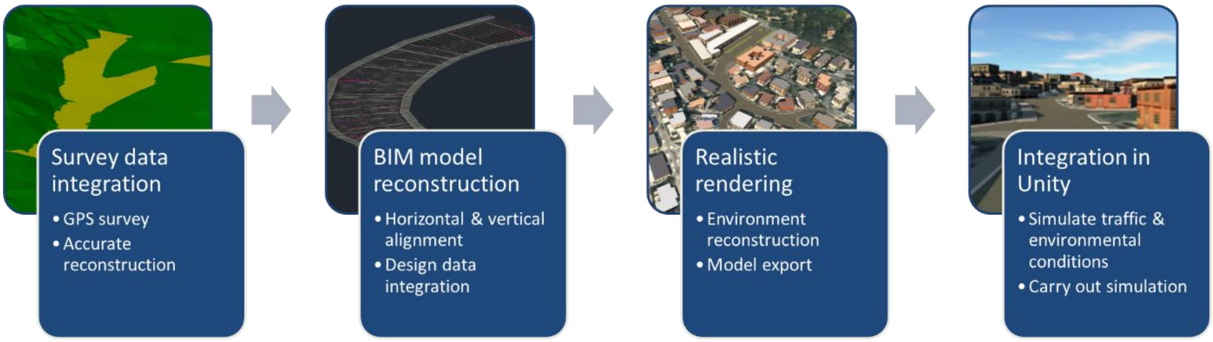

Figure 0 - BIM model process

Two design scenarios (Scenario 1 and Scenario 2) with infrastructural safety measures were defined in agreement with Roma Servizi per la Mobilità - RSM), considering the evidence provided by the observational investigations (deliverable 2). Similarly to Scenario 0, they were modelled in BIM environment and then implemented in the simulator systems.

Their features are briefly described below:

- **Scenario 0 (Current Existing Configuration)**

  This scenario represents the existing state of the intersection, without any modifications, as reported in the following *Figure 1*. It includes the original roadway geometry, lane configurations, pedestrian crossings, parking layout, and traffic control devices as observed in the real environment. Scenario 0 serves as the baseline condition against which the performance of alternative design solutions is assessed.

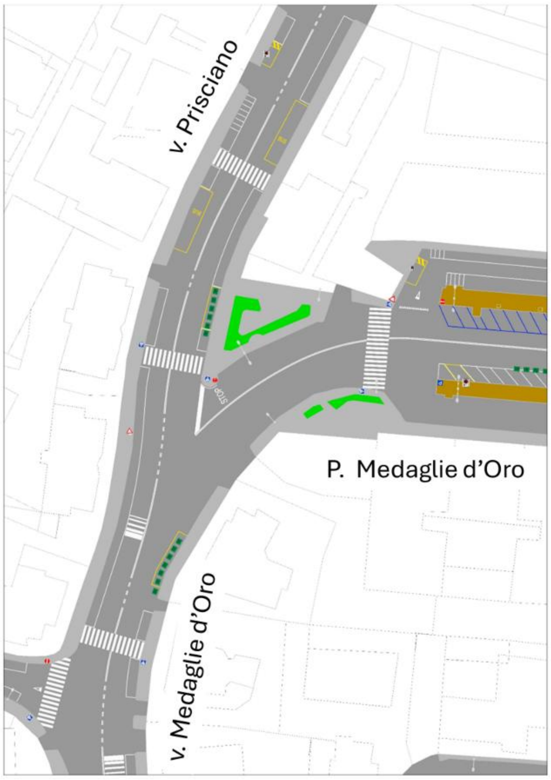

Figure 1 - ARCADE Scenario 0

- **Scenario 1**

  The first design scenario, reported in the following Figure 2, introduces a set of targeted infrastructural countermeasures aimed at improving visibility and reducing conflict severity. These measures include curb extensions, traffic islands, relocation and reconfiguration of pedestrian crossings, and minor geometric adjustments intended to moderate vehicle speeds and improve drivers' visual fields. The objective of this scenario is to assess whether relatively low-impact interventions can produce measurable improvements in safety-related indicators.

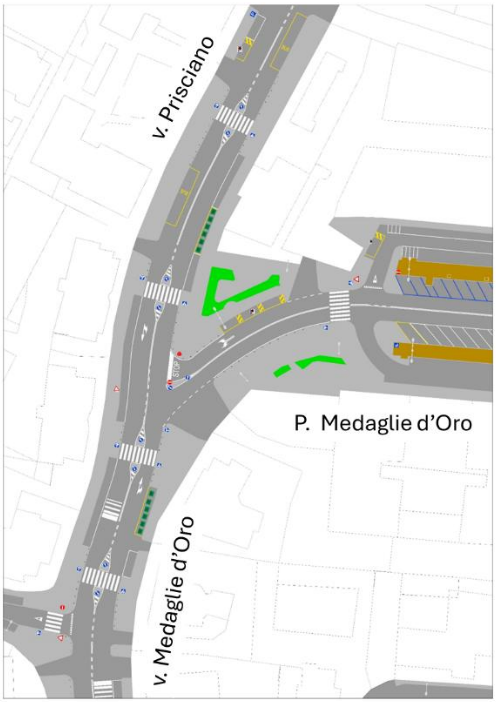

Figure 2 - ARCADE Scenario 1

- **Scenario 2**

  The second design scenario builds upon Scenario 1 by incorporating more substantial modifications to the road platform, as reported in the following Figure 3. These include a redesigned cross-section with on-street parking arrangements to visually narrow the carriageway, as well as the introduction of raised pedestrian crossings to enhance traffic calming effects. Scenario 2 represents a more comprehensive approach to safety-oriented urban design, aimed at inducing behavioural adaptation through perceptual and geometric cues.

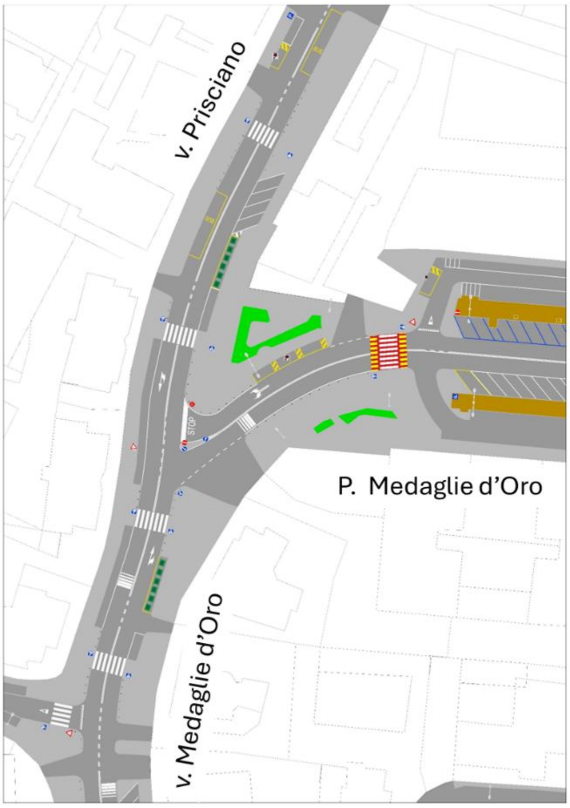

Figure 3 - ARCADE Scenario 2

Each of the three scenarios was simulated under both daytime and nighttime lighting conditions. The inclusion of lighting variability allowed the analysis of the interaction between infrastructural design and environmental visibility, recognising the significant role played by illumination in urban driving behaviour and risk perception. Nighttime scenarios were carefully calibrated to reproduce realistic lighting conditions, including street lighting intensity and contrast, in order to assess potential changes in gap acceptance, speed profiles, and safety margins. Traffic flow conditions within the simulation were defined based on empirical data collected through field surveys. The opposing traffic stream was modelled as a platoon of vehicles composed of passenger vehicles, travelling at a constant speed representative of real-world conditions. Overall, the simulation scenario was designed to provide a controlled, repeatable, and immersive environment in which users' behaviour could be observed under varying infrastructural and environmental conditions. By reproducing a real-world hazardous intersection and systematically modifying its design features, the scenario enables a robust quantitative assessment of the effectiveness of infrastructural countermeasures in reducing potential conflicts between vehicles and vulnerable road users in urban contexts.

To ensure smooth and continuous scenario management, a continuous driving path was initially implemented to allow the user vehicle to be transferred between different areas of the virtual environment. However, this approach required the introduction of artificial curvilinear segments, which generated undesired visual and kinematic effects and increased the risk of simulation sickness. To address this issue, a Spatial Transition System was designed and implemented, as reported in the following Figure 4. The system enables the instantaneous spatial translation of the user vehicle between predefined locations within the study area, while preserving the subjective continuity of the driving experience and eliminating the need for artificial connecting road segments. To prevent disorientation and ensure a seamless transition, the spatial relocation was performed during a controlled stop phase, enforced by a red traffic signal. This context-consistent pause masks the spatial transition and ensures that the relocation occurs without perceptible discontinuities. As a result, the Spatial Transition System contributes to a significant reduction in visuo-vestibular conflicts, thereby mitigating simulation sickness and improving user comfort, without compromising the ecological validity of the driving scenarios.

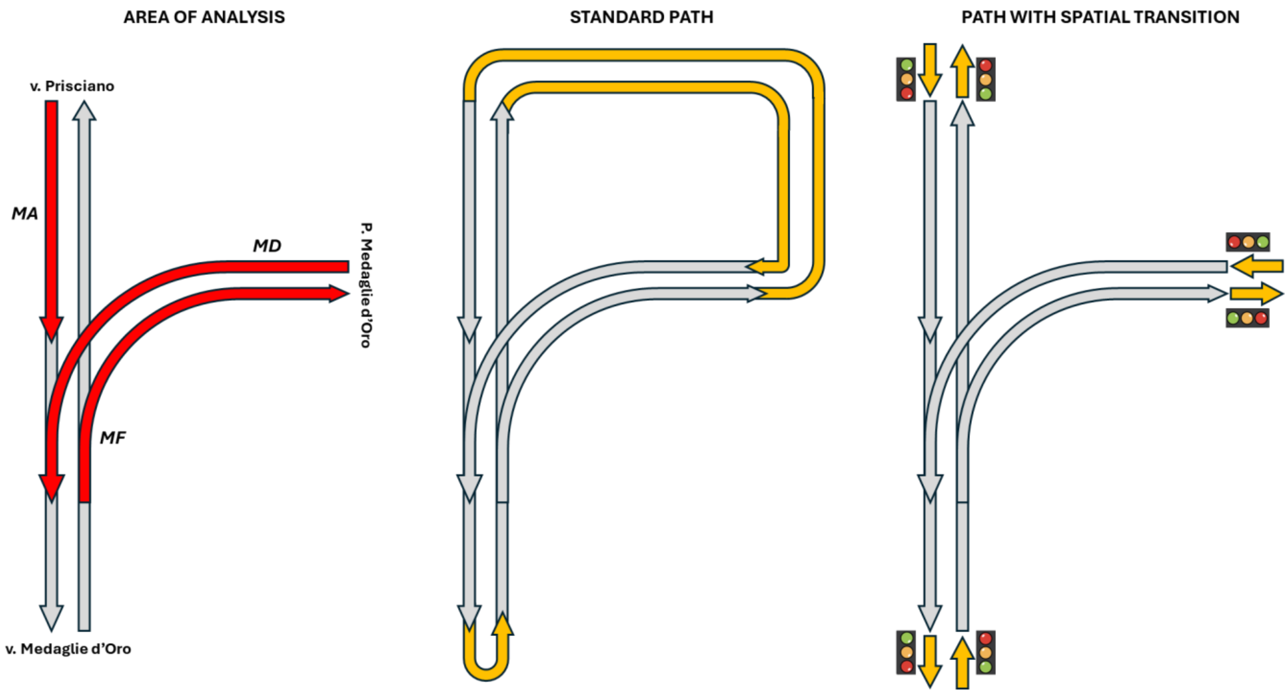

Figure 4 - Manoeuvres and path analysed during simulations.

2.1.1 Vehicle-vehicle/Vehicle-motorcycle interaction area

The vehicle–vehicle and vehicle–motorcycle interaction area analysed is centred on the left-turn manoeuvre from Piazzale delle Medaglie d'Oro towards Viale delle Medaglie d'Oro, with interference from the vehicular flows travelling along the main traffic stream on Viale delle Medaglie d'Oro and Via Prisciano, as reported in the following Figure 5. In this context, the criticality does not arise solely from the presence of conflicting traffic, but rather from the combined effects of intersection geometry, functional organisation of the road space, and typical visual obstructions of a T-shaped urban intersection. These elements directly influence risk perception, gap assessment, and the quality of manoeuvre execution.

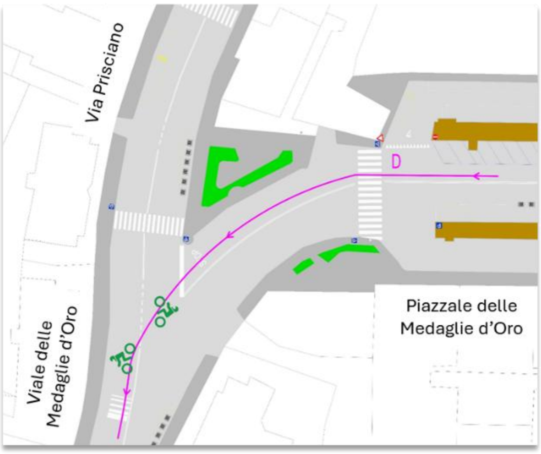

Figure 5 - Vehicle-Vehicle and Vehicle-Motorcycle interaction

In Scenario 0, the intersection exhibits a configuration that tends to generate unfavourable operational conditions. A first critical aspect is represented by the relatively high operating speeds of the main traffic stream: vehicles approaching along Viale delle Medaglie d'Oro and Via Prisciano may maintain speeds that significantly reduce the available temporal window for safe decision-making. This condition increases the sensitivity of the left-turn manoeuvre to errors in estimating the arrival time of conflicting vehicles, while also increasing both crash risk and potential crash severity.

A second aspect concerns visibility constraints at the stop position and within the merging area. The visibility available to drivers intending to cross the main traffic stream is affected by multiple factors:

- roadside vegetation and urban furniture, which can partially obstruct sight lines;
- waste collection containers, which in certain conditions constitute relevant fixed visual obstacles;
- on-street parked vehicles, which introduce dynamic screening effects that may limit both longitudinal and lateral visibility depending on the viewing direction.

These elements result in a scenario in which the acquisition of information required to correctly assess approaching traffic is often progressive and partially obstructed, leading to increased perceptual and decision-making workload during the scanning phase prior to entry.

A third critical issue relates to the overall geometry of the intersection, characterised by wide carriageways and extended crossing distances. The large roadway widths and the need to traverse a relatively long distance during the left-turn manoeuvre increase the time spent within the conflict area. Moreover, wide carriageways tend to reduce the perceived level of constraint and may encourage less guided trajectories, resulting in greater variability in crossing positions and turn execution.

Overall, Scenario 0 combines high speeds of conflicting traffic, limited visibility due to physical obstacles (vegetation, waste containers, parked vehicles), and wide geometric layouts that prolong exposure within the critical zone. This combination makes the scenario particularly suitable for a controlled and comparable evaluation of the effectiveness of infrastructural countermeasures aimed at reducing both conflict probability and potential severity, with specific attention to interactions involving motorcycles.

Scenario 1 preserves the general layout of the intersection while introducing a set of targeted interventions aimed at improving safety through better spatial organisation and, above all, enhanced perceptual quality of the road environment. A first group of countermeasures concerns the reduction of the effective lane width (from approximately 4.8 m to 3.5 m), as reported in the following Figure 6, achieved through lane narrowing and the introduction of refuge islands in correspondence with pedestrian crossings. This approach indirectly affects the vehicular interaction area as well: narrower lanes and the presence of central physical elements make the main traffic stream more constrained, promoting speed moderation and increased driver attention in the vicinity of the intersection.

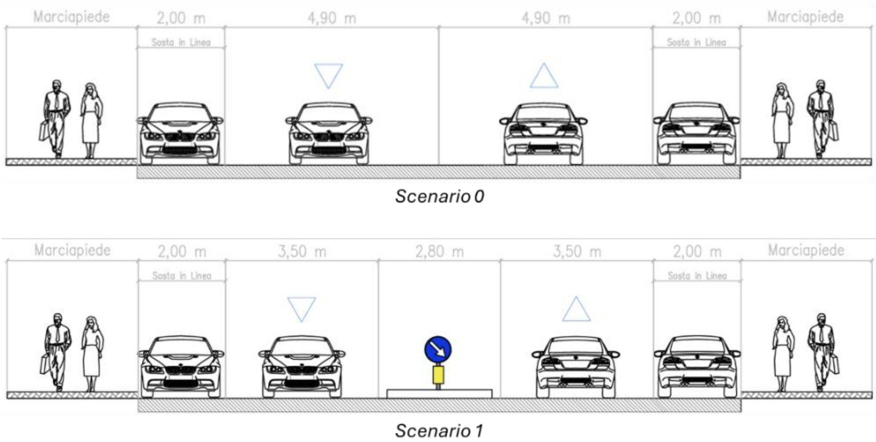

Figure 6 - Comparison of road section between Scenario 0 and Scenario 1

A second group of interventions, reported in the following Figure 7, focuses on improving visibility and intersection legibility. Kerb realignment and the advancement of the stop line produce a key effect by relocating the operational waiting and decision point to a position more favourable for observing approaching traffic. This reduces situations in which drivers are forced to incrementally advance in order to gain visibility.

In parallel, kerb reprofiling along the entrance and exit areas of the Piazzale discourages improper parking behaviour and contributes to maintaining the critical area free from visual obstructions. Finally, the introduction of a channelisation island at the intersection and directional pavement markings enhances perceptual guidance. These measures reduce trajectory variability, limit excessively free movements, and minimise overlaps between manoeuvres. The expected outcome is a reduction in ambiguous situations and greater consistency between intended and actual trajectories, with a potential decrease in lateral conflicts and overall manoeuvre complexity during the left turn.

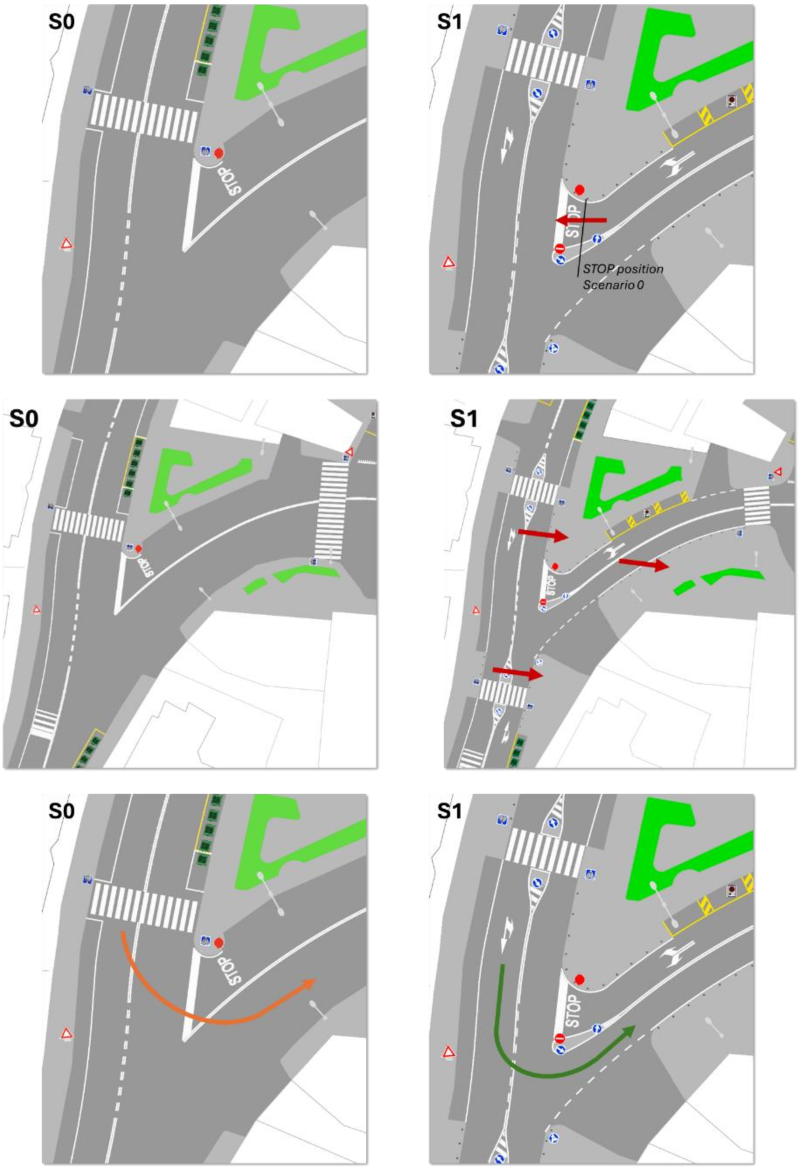

Figure 7 - Interventions introduced in Scenario 1 compared with Scenario 0.

In Scenario 2, the main geometric modifications introduced in Scenario 1 are maintained and consolidated, particularly those aimed at improving visibility, reducing operating speeds, and rationalising vehicular trajectories near the intersection. These interventions directly affect the approach conditions of vehicles travelling along the main traffic stream as well as those performing the left-turn manoeuvre from the Piazzale, contributing to a more legible and predictable intersection layout from a driving behaviour perspective. Scenario 2 introduces a more substantial and continuous reorganisation of the road cross-section along Viale delle Medaglie d'Oro and Via Prisciano, systematically addressing lane width along the entire length of the analysed segments. The reduction in cross-sectional width is not limited to isolated points within the intersection area but is applied continuously through a transversal redistribution of the road platform. In particular, carriageway widths are reduced from values on the order of 4.8 m to approximately 3.5 m, as reported in the following Figure 8, resulting in a section more consistent with the urban context and traffic calming objectives. The uniform reduction in lane width along the entire stretch contributes to containing operating speeds of the main traffic stream already during the approach phase, producing a more controlled and progressive entry into the intersection. This intervention directly affects drivers' perception of available space, encouraging more cautious driving behaviour and reducing the tendency to maintain high speeds near the conflict area.

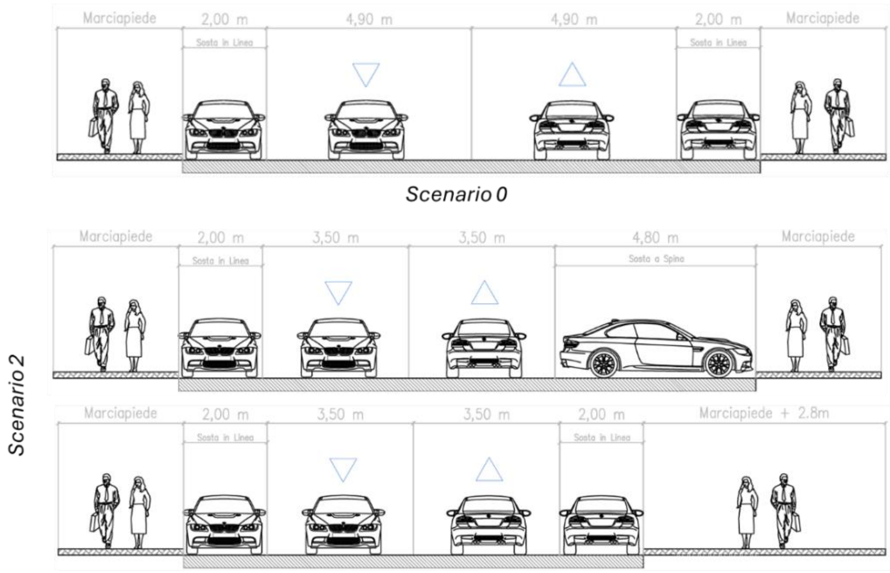

Figure 8 - Comparison of road section between Scenario 0 and Scenario 2.

Another key element is represented by kerb reprofiling and the consequent advancement of the stop line at the intersection entry, as reported in the following Figure 9. This configuration significantly improves visibility conditions for turning vehicles by reducing visual interference caused by lateral elements and by the original intersection geometry. A further qualifying intervention in Scenario 2 is the implementation of a raised pedestrian crossing near the intersection, conceived as a speed reduction measure for vehicles approaching from the Piazzale. The introduction of a vertical discontinuity along the vehicular path induces an early and progressive deceleration, reducing vehicle speeds before entering the conflict area. This measure is particularly effective in limiting speeds along the segment immediately preceding the turning manoeuvre, thereby contributing to a reduction in the potential severity of vehicular interactions. Scenario 2 is completed by traffic flow channelisation measures and improvements in intersection legibility, achieved through trajectory simplification and the introduction of visual guidance elements. These solutions reduce the likelihood of improper manoeuvres, limit overlaps between vehicular paths, and promote driving behaviour that is more regular and consistent with the intersection geometry.

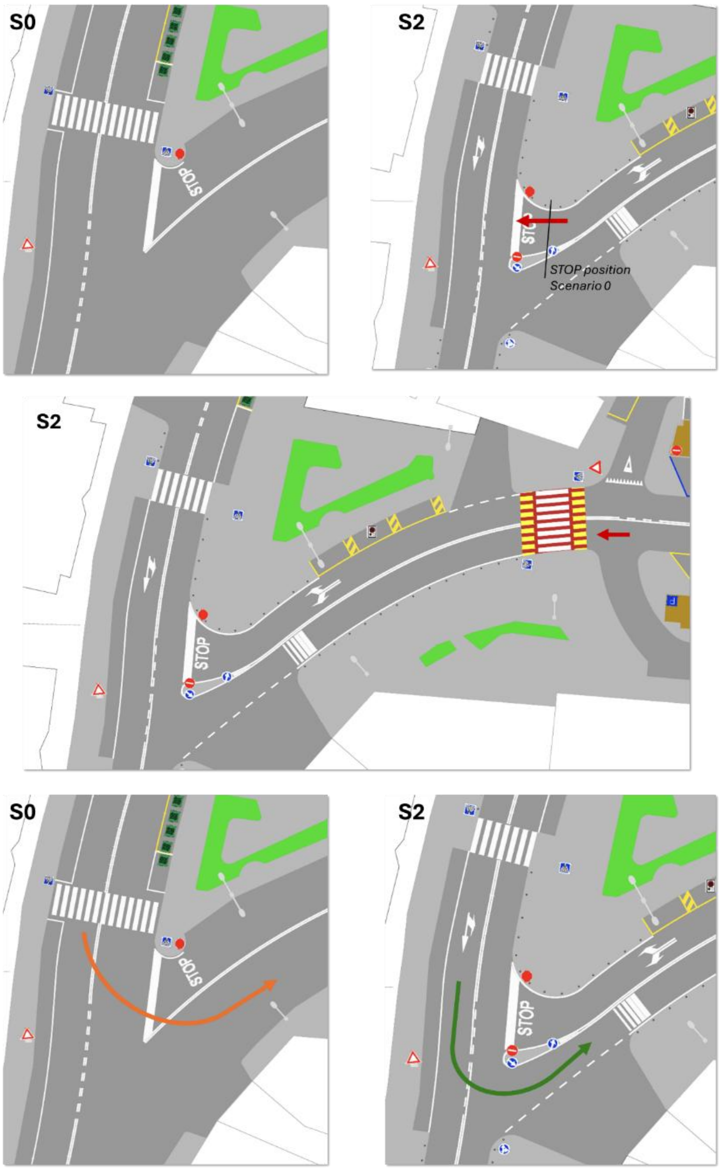

Figure 9 - Interventions introduced in Scenario 2 compared with Scenario 0.

Overall, Scenario 2 represents a design solution with greater impact compared to Scenario 1, capable of systematically addressing both geometric conditions and speed dynamics, as well as vehicular interaction patterns. As a result, it enhances overall intersection safety and reduces the risk associated with left-turn manoeuvres.

2.1.2 Vehicle-pedestrian interaction area on Piazzale delle Medaglie d'Oro

The following Figure 10 represents the baseline (as-is) configuration of the study site on Piazzale delle Medaglie d'Oro, Scenario 0, and reproduces the existing urban layout without the introduction of any infrastructural countermeasures. The scenario is characterised by a complex intersection geometry embedded in a dense urban context, with mixed vehicular and pedestrian flows and limited visual openness. The pedestrian crossing is located along a curved roadway segment and is marked by a zebra crossing connecting two sidewalk areas characterised by roadside vegetation and street furniture. The presence of trees and urban elements partially constrains sight lines, potentially affecting the mutual visibility between approaching drivers and pedestrians waiting to cross. The crossing is uncontrolled, with no traffic signals or active pedestrian priority devices, and relies exclusively on driver yielding behaviour. Vehicular traffic follows predefined lanes aligned with the existing road curvature, with vehicles approaching the crossing at operating speeds typical of an urban arterial context. The curvature of the approach, combined with the proximity of parked vehicles and roadside obstacles, contributes to a progressive exposure of the pedestrian crossing, rather than a fully unobstructed view. This configuration creates conditions in which driver perception, anticipation, and decision-making play a critical role in determining yielding behaviour.

Figure 10 - Simulated representation of the pedestrian crossing at Piazzale delle Medaglie d'Oro under Scenario 0.

The Scenario 1, reported in the following Figure 11, represents a modified geometric configuration of the vehicle–pedestrian interaction area on Piazzale delle Medaglie d'Oro, obtained through the implementation of passive infrastructural countermeasures aimed at improving pedestrian safety. Compared to the baseline condition, this scenario introduces sidewalk extensions (curb advancements) in correspondence with the pedestrian crossing, while preserving the overall intersection layout and traffic scheme. The advancement of the sidewalks reduces the effective roadway width in the vicinity of the crossing and results in the elimination of on-street parking spaces adjacent to the pedestrian conflict zone. This intervention shortens the pedestrian crossing distance and removes visual obstructions caused by parked vehicles, thereby improving mutual visibility between approaching drivers and pedestrians waiting to cross. The pedestrian crossing remains located along the curved roadway segment and continues to operate as an uncontrolled crosswalk, without the introduction of traffic signals or active pedestrian priority devices. However, the geometric reconfiguration modifies the spatial relationship between the vehicular trajectory and the pedestrian space, making the crossing area more compact and clearly defined within the roadway environment. Vehicular traffic continues to follow the existing curved alignment, but the reduced roadway width and the absence of parking near the crossing contribute to a more constrained approach geometry, which is expected to influence driver behaviour in terms of speed adaptation and anticipation.

Figure 11 - Simulated representation of the pedestrian crossing at Piazzale delle Medaglie d'Oro under Scenario 1.

Scenario 2, reported in the following Figure 12, represents the most advanced design configuration of the vehicle–pedestrian interaction area on Piazzale delle Medaglie d'Oro, building upon the geometric modifications introduced in Scenario 1 and further enhancing pedestrian safety through additional functional and perceptual countermeasures. In this configuration, the pedestrian crossing is implemented as a raised crosswalk, clearly distinguishable from the surrounding roadway surface through a contrasting pavement treatment. The elevation of the crossing introduces a vertical deflection in the vehicular path, physically reinforcing pedestrian priority and acting as a traffic-calming measure. This intervention increases the perceptual salience of the crossing area while simultaneously encouraging speed reduction through geometric constraint rather than regulatory enforcement. As in Scenario 1, sidewalk extensions are maintained on both sides of the crossing, resulting in a reduced crossing length and the permanent removal of on-street parking spaces in the vicinity of the pedestrian conflict zone. The combined effect of sidewalk advancement and vertical elevation produces a compact and clearly delimited pedestrian space, improving mutual visibility between drivers and pedestrians and reducing exposure time during crossing. Vehicular traffic continues to follow the existing curved alignment; however, the raised crossing modifies the continuity of the roadway profile, introducing a localized vertical discontinuity that influences driver behaviour during the approach phase. The crossing remains uncontrolled, with no traffic signals or active pedestrian priority devices, thereby allowing the assessment of driver yielding behaviour under enhanced geometric and perceptual conditions.

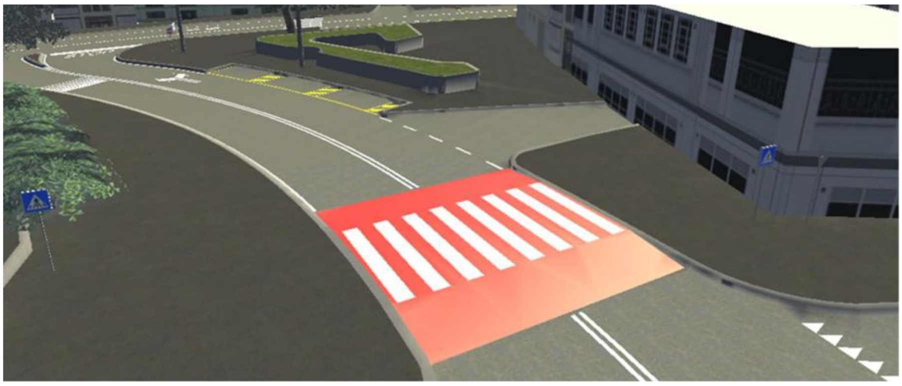

Figure 12 - Simulated representation of the pedestrian crossing at Piazzale delle Medaglie d'Oro under Scenario 2.

2.1.3 Vehicle-pedestrian interaction area on Via Prisciano

The following Figure 13 represents the baseline (as-is) configuration of the study site on Via Prisciano, Scenario 0, and reproduces the existing urban layout without the introduction of any infrastructural countermeasures. The scenario is characterised by a linear roadway segment with a longitudinal slope, embedded in a dense urban context with residential and institutional buildings aligned along the street frontage. The pedestrian crossing is located along the roadway and is marked by a standard zebra crossing connecting two sidewalks running parallel to the carriageway. The crossing is uncontrolled, with no traffic signals or active pedestrian priority devices, and relies exclusively on driver yielding behaviour. On-street parallel parking is present in close proximity to the crossing, particularly along the approach segment, potentially affecting sight distance and pedestrian conspicuity. Vehicular traffic follows a straight alignment with operating speeds typical of an urban collector road. The presence of a longitudinal gradient, combined with the availability of curbside parking and the linear geometry of the approach, influences driver perception and speed regulation when approaching the pedestrian crossing. The approach configuration allows relatively long forward visibility; however, parked vehicles and roadside elements may partially obstruct the lateral visibility of pedestrians waiting to cross.

Figure 13 - Simulated representation of the pedestrian crossing at Via Prisciano under Scenario 0.

Scenario 1 represents a geometric reconfiguration of the vehicle–pedestrian interaction area on Via Prisciano, obtained through the introduction of passive infrastructural countermeasures aimed at improving pedestrian safety while preserving the overall roadway function. Compared to the baseline configuration, this scenario introduces sidewalk extensions (curb advancements) in correspondence with the pedestrian crossing. The sidewalk advancements reduce the effective roadway width at the crossing location and lead to the removal of on-street parking spaces in the immediate vicinity of the pedestrian conflict zone. As a result, the pedestrian crossing distance is shortened and the spatial definition of the crossing area is enhanced, improving mutual visibility between approaching drivers and pedestrians waiting to cross. The pedestrian crossing remains uncontrolled, with no traffic signals or active pedestrian priority devices, and continues to rely on driver yielding behaviour. However, the geometric modification alters the spatial relationship between the vehicular trajectory and the pedestrian space, making the crossing area more compact and clearly delineated within the roadway environment. Vehicular traffic continues to follow a linear alignment along a longitudinally sloped roadway, as in the baseline scenario. The narrowing of the carriageway at the crossing location introduces a localized geometric constraint, which is expected to influence driver behaviour by encouraging earlier speed adaptation and increased attention during the approach phase. Overall, Scenario 1 represents a low-intrusiveness geometric intervention, focused on pedestrian protection through space reallocation and crossing distance reduction, without altering traffic priority rules or introducing active control measures.

Figure 14 - Simulated representation of the pedestrian crossing at Via Prisciano under Scenario 1.

Scenario 2 represents the most advanced design configuration of the vehicle–pedestrian interaction area on Via Prisciano. This configuration introduces a more pronounced geometric simplification of the crossing area, while preserving the overall roadway alignment and traffic function. In this scenario, the sidewalk extensions are maintained, resulting in a permanently reduced carriageway width at the pedestrian crossing. In addition, the on-street parking spaces adjacent to the crossing are completely removed, extending the clear area along the approach segment and further reducing potential visual obstructions caused by parked vehicles. The pedestrian crossing remains marked by a standard zebra crossing, without the introduction of vertical deflections or raised elements. The roadway continues to follow a linear alignment with a longitudinal slope, typical of the Via Prisciano context. The absence of curbside parking and the increased lateral clearance near the crossing create a more open and legible spatial configuration, improving the visibility of pedestrians waiting to cross and the recognisability of the crossing area for approaching drivers.

Figure 15 - Simulated representation of the pedestrian crossing at Via Prisciano under Scenario 2.

2.2 Driving Simulation

2.2.1 Instrument

The experimental study was conducted using a medium-fidelity, fixed-base driving simulator located at the Department of Civil, Computer Science and Aeronautical Technologies Engineering of Roma Tre University, reported in the following Figure 16. The simulator is designed to reproduce realistic and controlled driving conditions, enabling the investigation of driver behaviour and the evaluation of infrastructural countermeasures in an urban context under safe and repeatable conditions. The hardware structure of the driving simulator consists of several integrated components, described below.

The simulator is based on a real Toyota Auris vehicle, configured as a left-hand-drive car and equipped with a complete driving control system, including steering wheel, pedals, and gear lever. These controls are directly connected to the simulation system, which is responsible not only for generating the visual environment but also for recording geometric and kinematic driving parameters. The vehicle interior is also fitted with an audio system that enhances driving realism through sound effects reproducing engine noise, acceleration and braking sounds, as well as audio signals related to navigation, necessary to guide users through scenarios.

Figure 16 - Roma Tre fixed-based and stand-alone Driving Simulator.

The driving scenarios are projected onto a large curved screen with an approximate horizontal field of view of 170 degrees, allowing the driver to feel fully immersed in the simulated environment. The visualisation is achieved through a system of three overhead high-definition projectors, seamlessly blended to provide a continuous and coherent forward and lateral view of the roadway. Additional virtual displays reproduce rear-view and side mirrors, further increasing perceptual realism. The projection system is managed via Vioso software, which ensures geometric correction and image alignment across the curved surface.

The main workstation is directly connected to both the vehicle unit and the projection system. It consists of a dedicated computer running the Unity Graphic Engine, reported in the following Figure 17. Through this station, the driving scenarios are reproduced. In addition to rendering the visual environment, the system enables the acquisition of a wide range of driving performance variables, including speed, acceleration, and vehicle trajectory.

Figure 17 - Simulation Control Station.

A secondary, fully autonomous workstation, reported in the following Figure 18, is also included in the simulator setup. This station consists of a computer, a steering wheel, and a pedal set, and is used during the development and calibration of driving scenarios. Once created, the scenarios are transferred to the main control station for execution during experimental driving sessions.

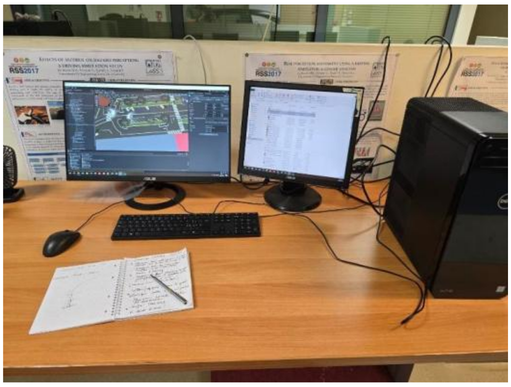

Figure 18 - Scenario modelling and development workstation.

The driving simulation environment was developed using the Unity Graphics Engine, which enables the representation of complex road geometries created through BIM authoring tools, such as Civil 3D and InfraWorks. The simulator allows the reproduction of realistic traffic conditions, including both stochastically generated background traffic and scripted interactive traffic, as well as all the infrastructural layouts required for the experimental scenarios. The platform supports high-frequency data acquisition and detailed performance measurement, making it particularly suitable for behavioural analysis and safety-related research. Previous studies (Calvi and D'Amico, 2006; Bella, 2008; Bella and Silvestri, 2015; Bella and Silvestri, 2017; Calvi, 2015; Calvi, 2018; Calvi et al., 2018; Calvi et al., 2020) have demonstrated the validity of the driving simulator in assessing driving performance in terms of speed, acceleration, and vehicle trajectory across a wide range of driving conditions and road environments. Overall, the integrated hardware–software architecture of the simulator provides a robust and immersive virtual driving environment, making it well suited for evaluating the effectiveness of infrastructural countermeasures and for conducting advanced research on driver behaviour in urban contexts.

2.2.2 Experimental Protocol

The experimental study was conducted following a unified and standardised test protocol designed to investigate multiple interaction phenomena within the same driving simulation session. Specifically, the protocol supported the analysis of both vehicle–motorcycle/vehicle-vehicle interactions at unsignalized intersections and vehicle–pedestrian interactions at uncontrolled pedestrian crossings.

The protocol was structured to ensure repeatability, internal consistency, and comparability across different infrastructural configurations, lighting conditions, and interaction types, while minimising learning effects and behavioural bias.

1. **Participant Preparation and Briefing**

Before the start of the experimental session, each participant received a standardised briefing describing the general objectives of the research, the functioning of the driving simulator, and the overall structure of the experimental trials. Participants were instructed to drive as they would under normal real-world conditions, without adopting overly cautious or deliberately risky behaviour.

To avoid expectancy effects, participants were not informed in advance about the specific interaction events under analysis (e.g., pedestrian appearance or critical turning manoeuvres). Informed consent was obtained from all participants in accordance with ethical research guidelines.

2. **Familiarisation Phase**

A dedicated familiarisation phase was conducted prior to data collection to allow participants to adapt to the simulator environment, vehicle dynamics, control responsiveness, and visual immersion. During this phase, drivers completed a practice route not included in the experimental dataset, featuring the urban road segments without critical interaction events. The familiarisation phase was considered complete once the participant demonstrated stable vehicle control and reported adequate comfort with the simulator.

3. **Experimental Scenarios and Driving Tasks**

The experimental protocol comprised multiple driving trials corresponding to different combinations of infrastructural layout and environmental conditions. Two main categories of interaction were analysed within the same experimental session:

I. **Vehicle–vehicle/vehicle-motorcycle interactions** at an unsignalized T-intersection, reported in the following Figure 19, where the participant was required to perform a left-turn manoeuvre from a secondary road while yielding to opposing traffic on the major road.

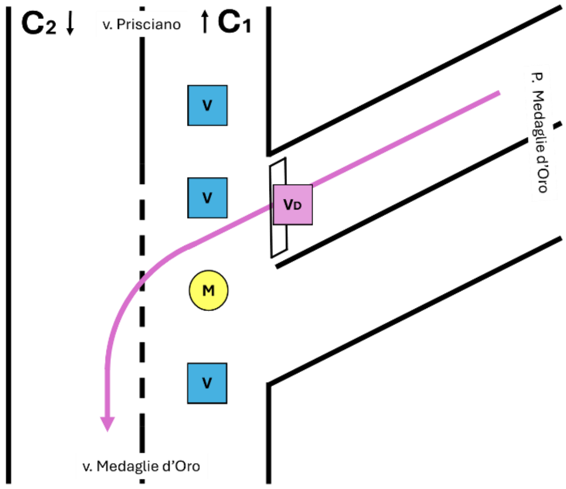

Figure 19 - Vehicle-vehicle and Vehicle-motorcycle interaction.

The vehicle platoons consisted of two cars and one motorcycle and were repeatedly generated over a 60 second period, as reported in the following Figure 20. Two distinct inter-vehicle time gap configurations were implemented between consecutive platoon elements. The time gap values were determined based on a preliminary analysis of field survey data, ensuring consistency with observed real-world traffic behaviour.

VEHICLE PLATOONS												
1	2	3	4	5	6	7	8	9	10	11	12	n
V	V	M	V	V	M	V	V	M	V	V	M	V

Figure 20 - Vehicle platoons configurations.

II. **Vehicle–pedestrian interactions** at uncontrolled pedestrian crossings, involving two pedestrians, one located on Via Prisciano, pedestrian number 1 on the following Figure 21, and the other on Piazzale Medaglie d'Oro, pedestrian number 2, positioned in proximity to the crossing. Pedestrians initiated crossing behaviour according to two predefined Time-to-Zebra conditions, defined as the time remaining before the approaching vehicle reached the crosswalk.

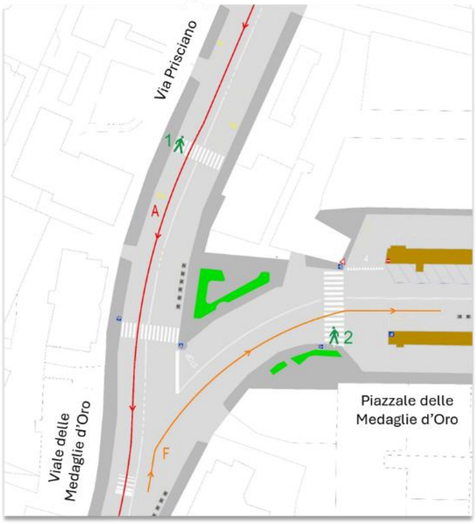

Figure 21 - Vehicle-pedestrian interaction.

For both interaction types, the previous analysed three infrastructural configurations were implemented:

- Scenario 0: baseline configuration;
- Scenario 1: first infrastructural intervention;
- Scenario 2: second infrastructural intervention.

Each scenario was tested under two lighting conditions (daytime and nighttime). Within each lighting condition, the experimental design included the analysis of the following interaction scenarios:

- Vehicle–pedestrian interactions at uncontrolled pedestrian crossings, involving two distinct crossings (one on Via Prisciano and one on Piazzale Medaglie d'Oro), each tested under three pedestrian conditions:
  - Time-to-Zebra (TTZ) = 2.5 s;
  - Time-to-Zebra (TTZ) = 3.5 s;
  - No pedestrian crossing.
- Vehicle–vehicle/vehicle-motorcycle interactions at a left-turn manoeuvre, involving a traffic platoon, tested under three platoon conditions:
  - inter-vehicle GAP time of 5 s;
  - inter-vehicle GAP time of 6 s;
  - no vehicle platoon.

Overall, this design resulted in a total of 18 experimental interaction conditions, corresponding to 9 conditions per lighting configuration. All participants were exposed to the same set of conditions, and the order of scenario presentation was controlled to minimise systematic order effects. An overview of the scenario presentation is provided in the following Table 1.

Table 1 - Simulation submission sequence.

	Simulation Submission Sequence					
	n1	**n2**	**n3**	**n4**	**n5**	**n6**
Daytime	*S0*	*S1*	*S1*	*S2*	*S2*	*S0*
	S1	*S2*	*S0*	*S1*	*S0*	*S2*
	S2	*S0*	*S2*	*S0*	*S1*	*S1*
Nighttime	*N0*	*N1*	*N1*	*N2*	*N2*	*N0*
	N1	*N2*	*N0*	*N1*	*N0*	*N2*
	N2	*N0*	*N2*	*N0*	*N1*	*N1*

4. Traffic and Interaction Modelling

Traffic flows within the simulation were defined based on empirical observations collected at the real study sites. For platoon interactions, opposing traffic platoons were composed of passenger cars and motorcycles travelling at constant approach speed of 45 km/h, representative of real conditions. This speed is representative of regular, uncongested traffic flow, while still allowing for interactions among vehicles. The platoon followed a fixed trajectory and operated in a non-cooperative manner, with no braking or path deviation to facilitate the user vehicle's left-turn manoeuvre. Consequently, incorrect gap assessment by the driver could result in potential collision events. The platoon speed was kept constant at 45 km/h across all three simulation scenarios. Although the implementation of infrastructural countermeasures in scenarios S1 and S2 would be expected to produce a natural reduction in operating speeds under real-world conditions, a constant speed was maintained for methodological consistency. This approach allowed the effects of the geometric and functional reconfiguration of the intersection to be isolated, ensuring that observed safety improvements were not solely attributable to speed reduction.

For vehicle–pedestrian interactions, pedestrian behaviour was controlled through a dynamic Time-to-Zebra (TTZ) triggering mechanism. Pedestrians were continuously present in the scene and positioned near the crosswalk, while the initiation of the crossing manoeuvre was governed by the driver's approach conditions. When the user vehicle entered a control area extending 100 m upstream of the pedestrian crossing, an automated system tracked the vehicle and continuously computed the Time to Zebra (TTZ) based on its instantaneous speed and trajectory. The pedestrian crossing behaviour was triggered when the computed TTZ reached a predefined threshold (2.5 s or 3.5 s), corresponding to different levels of urgency. To ensure scenario consistency and to avoid unrealistically delayed pedestrian activation, a fallback condition was implemented: if the predefined TTZ threshold was not reached due to a low vehicle speed, the pedestrian crossing behaviour was initiated when the distance between the vehicle and the zebra crossing became less than 15 m. This approach ensured a consistent and controlled exposure of drivers to pedestrian crossing events, while preserving the realism of vehicle–pedestrian interactions and avoiding artificial pedestrian appearance effects. An overview of the GAP and TTZ presentation is provided in the following Table 2.

Table 2 - GAP and TTZ distribution across the different scenarios.

Vehicle–Motorcycle Interaction		
Condition:	*Manoeuvre D: Left-turn manoeuvre from Piazzale delle Medaglie d'Oro*	
Scenario 0	Gap 1	Gap 2
Scenario 1	Gap 1	Gap 2
Scenario 2	Gap 1	Gap 2
Gap	5 s	6 s
Platoon Speed		45 km/h

Vehicle–Pedestrian Interaction				
Condition:	*Manoeuvre A: Pedestrian crossing on Via Prisciano*		*Manoeuvre F: Pedestrian crossing on Piazzale delle Medaglie d'Oro*	
Scenario 0	TTZ 1	TTZ 2	TTZ 1	TTZ 2
Scenario 1	TTZ 1	TTZ 2	TTZ 1	TTZ 2
Scenario 2	TTZ 1	TTZ 2	TTZ 1	TTZ 2
Time to Zebra	TTZ 1	2,5 s	TTZ 2	3,5 s

5. Session Completion and Debriefing

At the conclusion of the experimental session, participants were debriefed and asked to report any discomfort, simulator sickness symptoms, or anomalous events experienced during the trials. This information was used to verify data quality and to identify potential exclusions or sensitivity analyses.

Overall, the integrated test protocol allowed multiple safety-related research objectives to be addressed within a single experimental session, ensuring methodological coherence while maximising the informational value of the collected data.

2.2.3 Data Collection

During the experimental sessions, a comprehensive data collection framework was implemented to record both objective driving performance variables and subjective assessments. Data acquisition was fully integrated into the Unity-based driving simulator architecture and was designed to ensure high temporal resolution, accuracy, and consistency across all experimental scenarios and interaction types. The driving simulator continuously recorded vehicle state and motion variables throughout each simulation trial, with data acquisition performed automatically by the simulation software and its associated performance measurement modules.

During the tests, the eye activity of the participants was also observed through eye tracking, as a measure of behavioural monitoring related to attention to space, level of awareness and alertness.

The data acquisition strategy varied according to the type of interaction under analysis. For vehicle–pedestrian interactions, data were collected along predefined trigger sections spaced at an inter-distance of 1.0 m, distributed along a 100 m approach segment upstream of the pedestrian crossing. For vehicle–vehicle and vehicle–motorcycle interactions, data were collected within a predefined trigger volume fully enclosing the intersection under analysis, where vehicle state variables were recorded at a sampling frequency of 0.1 s. This combined approach enabled a fine-grained reconstruction of vehicle dynamics and driver responses across all interaction scenarios.

For vehicle–vehicle and vehicle–motorcycle interactions, the following objective variables were recorded:

- Vehicle position over time: spatial coordinates (X, Y, Z) of the vehicle's centre of mass;
- Vehicle speed: instantaneous linear speed expressed in m/s;
- Absolute time: elapsed time in seconds from the beginning of the simulation trial;
- Platoon vehicle identifier: alphanumeric code identifying each platoon vehicle (e.g., *03_A2*, indicating the third generated platoon vehicle and the second generated car);
- Inter-vehicle distance: distance between the user vehicle and the platoon vehicle in the current frame (in metres), computed as the Euclidean distance between the respective centres of mass.

For vehicle–pedestrian interactions, the following objective variables were recorded:

- Section identifier: alphanumeric code associated with each predefined trigger section;
- Vehicle position: spatial coordinates (X, Y, Z) expressed in a fixed reference frame;
- Lateral offset: lateral deviation of the vehicle from the reference trajectory;
- Vehicle speed;
- Elapsed time: time elapsed from the beginning of the trial at the instant the vehicle crossed each specific trigger section.

In the presence of vehicle–pedestrian, vehicle-vehicle or vehicle-motorcycle collisions, the following additional variables were recorded:

- Collision time: elapsed time from the beginning of the trial at the moment of collision;
- Vehicle speed at impact;
- Pedestrian position at impact;
- Vehicle position at impact.

These continuously recorded variables formed the basis for the subsequent computation of surrogate safety measures (Gettman & Head, 2003; Mahmud et al., 2017; Li et al., 2024) such as Time to Collision (TTC), Minimum Time to Collision (MTTC), Post-Encroachment Time (PET), Time to Zebra (TTZ), Gap Time, and deceleration-based indicators. Importantly, these indicators were not directly recorded, but rather derived offline from the raw kinematic and positional data collected during the simulations

Following data collection, a set of time-based, kinematic, and spatial indicators was computed in order to quantify driver behaviour, conflict severity, and safety-related outcomes across the different interaction scenarios. These indicators were derived from the raw vehicle trajectory, speed, and timing data and are commonly adopted in the analysis of traffic conflicts and surrogate safety measures.

Time-based conflict indicators

Time to Collision (TTC) represents the time remaining before a collision would occur if the current relative speed and trajectory of the interacting entities were maintained unchanged. It is computed as:

$$TTC = \frac{d}{\Delta v}$$

where d is the distance between the vehicle and the conflict point (or another road user), and Δv is the relative speed along the collision path. The minimum value observed during the interaction, denoted as $TTC_{\min}$, was used as an indicator of conflict severity, with lower values indicating more critical situations.

Time Exposed Time to Collision (TET) quantifies the cumulative duration during which the TTC remains below a predefined safety threshold TTC_{th}. It is computed as:

$$TET = \sum_{i=1}^{n} \Delta\, t_i \text{for } TTC_i < TTC_{th}$$

where Δt_i represents each discrete time interval during which the condition is satisfied. TET provides information on the persistence of unsafe conditions during the interaction.

Time Integrated Time to Collision (TIT) accounts for both the magnitude and duration of unsafe proximity by integrating the difference between the safety threshold and the instantaneous TTC:

$$TIT = \int_{TTC<TTC_{th}} (TT\,C_{th} - TTC(t))\, dt$$

Compared to TET, TIT offers a more comprehensive measure of exposure to conflict severity.

Post-Encroachment Time (PET) represents the temporal separation between two interacting road users at a conflict point and is defined as:

$$PET = t_{\text{entry,2}} - t_{\text{exit,1}}$$

where $t_{\text{exit,1}}$ is the time at which the first road user leaves the conflict area and $t_{\text{entry,2}}$ is the time at which the second road user enters it. Lower PET values indicate higher levels of conflict severity.

Gap acceptance and waiting time indicators

Waiting Time (WT) measures the duration between the arrival of the vehicle at a decision point (e.g., stop line or yield point) and the initiation of the manoeuvre:

$$WT = t_{\text{start manoeuvre}} - t_{\text{arrival}}$$

WT is directly related to driver gap acceptance behaviour and decision-making processes.

In scenarios with predefined available gaps, a normalised indicator, the Gap Ratio, was introduced to allow comparison across different gap configurations:

$$Gap_{ratio} = \frac{WT}{GAP}$$

where GAP represents the temporal size of the available gap (e.g., 5 s or 6 s).

Pedestrian-specific indicators

Time to Zebra (TTZ*) represents the time required for the vehicle to reach the pedestrian crossing at its current speed and is computed as:

$$TTZ^* = \frac{d_{zebra}}{v}$$

where $d_{zebra}$is the longitudinal distance between the vehicle and the crossing, and $v$is the vehicle speed. TTZ* was used to classify driver behaviour according to different levels of urgency and aggressiveness, based on predefined thresholds.

Deceleration and severity indicators

Deceleration Rate to Avoid Collision (DRAC) estimates the minimum constant deceleration required to avoid a collision with a conflict point or road user and is defined as:

$$DRAC = \frac{v^2}{2d}$$

where $v$is the vehicle speed at the onset of braking and $d$is the distance to the conflict point.
Pedestrian Safety Distance (PSD) represents the minimum spatial separation between the vehicle and the pedestrian during the interaction and was used as a spatial indicator of conflict severity, with lower values indicating more critical situations.

Speed profile indicators

Several indicators were extracted from the longitudinal speed profiles to characterise vehicle dynamics during the interactions:

- Initial speed (V_i), measured at the onset of the interaction;
- Minimum speed ($V_{\min}$), observed during the interaction;
- Mean deceleration (a_{mean}), computed as:

$$a_{\text{mean}} = \frac{V_i - V_{\min}}{t_{\min} - t_i}$$

where $t_i$is the time at which $V_i$is observed and $t_{\min}$is the time at which $V_{\min}$ occurs.

- Speed Reduction Time (SRT), defined as the time required to reach the minimum speed:

$$SRT = t_{V_{\min}} - t_{V_i}$$

In parallel with objective simulator data, subjective information was collected through standardised questionnaires administered at predefined stages of the experimental session. These data were recorded digitally and stored separately from simulator output files.

The collected subjective data included:

- socio-demographic and driving background information;
- self-reported driving behaviour indicators (Manchester Driver Behaviour Questionnaire);
- perceived realism and credibility of the simulation scenarios;
- perceived workload and task demand (NASA Task Load Index);
- simulator comfort and simulator sickness indicators.

Subjective data were temporally linked to the corresponding simulation sessions but did not interfere with the real-time data acquisition process.

2.2.4 Participants

The experimental study initially involved a total of 58 participants, all holding a valid category B driving license. Participants were recruited on a voluntary basis within the academic community of the Department of Civil, Computer Science and Aeronautical Technologies Engineering of Roma Tre University, including undergraduate and graduate students, academic staff, and researchers.

The sample was predominantly male, consisting of 44 males (76%) and 14 females (24%). Participants' ages ranged from 20 to over 60 years, with a strong prevalence of young drivers. The mean age of the sample was 32.2 years, with a standard deviation of 15.0 years, while the median age was 25 years, reflecting the right-skewed distribution caused by the presence of a limited number of older drivers.

With regard to driving experience, all participants reported regular driving activity. The majority of the sample had held a driving license for less than six years, indicating relatively recent driving experience, while a smaller subset reported long-term experience, extending in some cases beyond 40 years of license holding. In terms of annual mileage, most participants reported driving between 2,000 and 13,200 km per year, with only a few individuals exceeding 18,800 km annually. Participants mainly reported driving in urban and mixed environments, whereas a smaller proportion declared that they primarily drove in extra-urban or motorway contexts. This distribution is consistent with both the age profile of the sample and the urban setting of the experimental scenarios.

Regarding educational background, the sample exhibited a medium-to-high level of education. All participants had completed at least secondary education, and approximately 50% held a university degree, including postgraduate qualifications up to the doctoral level. This composition reflects the academic context in which recruitment took place and the predominance of students and young adults in the sample. Concerning personal conditions relevant to simulation reliability, approximately half of the participants reported using corrective lenses (glasses or contact lenses), while all declared the absence of sensory, motor, or balance impairments that could affect driving performance. No participant reported neurological disorders or conditions incompatible with simulator use. During the experimental sessions, 8 participants (13.8%) interrupted the simulation due to symptoms of simulator sickness and were therefore excluded from subsequent analyses. The incidence of simulator sickness was markedly age-dependent: 46.2% of participants over 45 years of age interrupted the experiment, compared to 4.4% among participants under 45 years of age. After excluding these participants, the datasets available for analysis consisted of 48 valid participants for daytime scenarios and 50 for nighttime scenarios, as two participants completed only nighttime sessions. Additional data cleaning was performed at the manoeuvre level to remove anomalous cases, ensuring a robust and representative final dataset.

Overall, the resulting sample can be described as predominantly young, moderately experienced, and highly educated, with relatively homogeneous driving habits. This controlled degree of homogeneity was intentionally sought in order to limit the influence of confounding factors such as age-related performance differences or extreme variability in driving experience, thereby enhancing the internal validity of the experimental comparisons.

2.3 Pedestrian Simulation

2.3.1 Instrument

The pedestrian simulator was designed as an immersive virtual reality (VR) based simulator, aimed at realistically reproducing the perceptual and decision-making experience of pedestrians in real urban contexts. The system was designed as an immersive virtual reality simulator, in which the user can physically move within the real environment, with movements continuously tracked and faithfully reproduced within the three-dimensional virtual space. The simulator architecture is based on the integration of simulation software, graphics engine, and immersive visualisation hardware, ensuring consistency between the virtual scene, the user's point of view, and the dynamics of environmental elements. The virtual environment was developed using the Unity graphics engine, which enables real-time management of complex three-dimensional scenarios, advanced surface rendering, and dynamic interaction between users and simulated agents.

Immersive visualisation is provided through a Meta Quest 3S virtual reality headset, used as a Head-Mounted Display (HMD) reported in the following Figure 22. The device features a high-resolution stereoscopic display, allowing accurate depth perception and reliable distance representation. The field of view offered by the headset is sufficiently wide to ensure a natural perception of the surrounding environment, enhancing user engagement and reducing tunnel-vision effects. The Meta Quest 3S integrates an inside-out tracking system, based on onboard sensors and cameras, which continuously detects the position and orientation of the user's head in space. This system enables real-time updates of the point of view (POV) within the virtual environment according to the user's natural movements, such as head rotations and small postural adjustments. As a result, the simulator ensures visuo-spatial coherence between real user movements and the virtual scene, a crucial requirement for perceptual reliability. Headset tracking allows the precise definition of the virtual observer's position, which corresponds to the pedestrian's point of view within the scenario. The height of the point of view is set consistently with the average human eye level, ensuring a realistic representation of spatial relationships among pedestrians, vehicles, infrastructure, and other urban elements. This aspect is particularly relevant for analysing mutual visibility between pedestrians and drivers, as well as perception and reaction times.

User interaction with the simulator does not require motion platforms or physical locomotion devices, thereby reducing system hardware complexity and limiting the onset of simulation sickness. The experience is therefore primarily perceptual and cognitive, focusing on traffic observation, distance evaluation, and decision-making regarding the appropriate moment to initiate crossing.

Figure 22 - Meta Oculus Rift 3S Head-Mounted Display

2.3.2 Physical-world assets and embodiment

The physical-world assets, reported in the following Figure 23, were designed as an integral component of the simulator, with the aim of ensuring technical reliability, perceptual coherence, and continuity between physical action and virtual representation. The system employs a wired connection between the virtual reality headset and the processing computer, reported in the Figure 18, a configuration adopted to guarantee high data transfer rates, reduced latency, and increased stability during experimental sessions.

This setup minimises perceptible delays and temporal inconsistencies between physical movement and scene updates, which are particularly critical in the study of pedestrian behaviour. Within the physical interaction space, an ergonomic seating solution was provided and used during the initial setup phase to support the correct positioning and calibration of the HMD. The seat allowed participants to assume a stable and controlled posture while the headset was fitted and aligned with the user's field of view, ensuring consistent initial conditions across participants. Once the calibration phase was completed, participants were free to stand up and move naturally within the available physical space.

A three-dimensional tactile marker fixed to the floor was also introduced as a physical reference element. This marker served a dual purpose: first, it provided haptic feedback enabling participants to perceive the starting point of the available walking area; second, it defined a clear and intuitive spatial boundary corresponding to the pedestrian's initial position prior to crossing. Physical contact with the marker anchored the virtual experience to a real-world reference, reducing spatial uncertainty and improving initial orientation.

This configuration played a significant role in fostering embodiment, understood as the degree to which the user's real body is incorporated into the virtual environment. The possibility of physically moving within the space, combined with tactile references and a controlled ergonomic setup phase, enhanced the sense of presence and agency, promoting alignment between visual perception, body posture, and motor action. In this sense, embodiment was achieved through multisensory coherence between the physical and virtual worlds, rather than through visual realism alone. Overall, the physical asset setup of the simulator extends beyond a purely technical support role and actively contributes to perceptual realism, user comfort, and ecological validity of the experiment, creating the conditions for pedestrian decisions and behaviours to closely reflect those observed in real-world crossing situations.

Figure 23 - Pedestrian Simulator spatial configuration.

2.3.3 Experimental Protocol

The experimental study was conducted according to a standardised protocol specifically designed to investigate pedestrians' intention to cross in urban traffic environments. The protocol focused on analysing pedestrian–vehicle and pedestrian–motorcycle interactions, with the aim of assessing the effect of Vehicle Size Effect and visual salience on pedestrian decision-making processes. The experimental protocol was structured to ensure repeatability, coherence, and internal consistency across all trials, as well as comparability across different infrastructural configurations. Particular attention was devoted to maintaining uniform experimental conditions while systematically varying the key factors under investigation, in order to isolate their influence on pedestrian behaviour. Different interaction scenarios were examined, combining variations in the type of approaching road user (car or motorcycle) with multiple lighting conditions (daytime and nighttime). This design allowed the analysis of pedestrian crossing behaviour under a range of perceptual and environmental contexts, representative of real-world urban conditions.

i. Participant Preparation and Briefing

Before the start of each experimental session, participants received a standardised briefing outlining the general objectives of the study, the functioning of the pedestrian simulator, and the overall structure of the experimental trials. Participants were instructed to cross the road as they would under normal real-world conditions, without adopting overly cautious or deliberately risky behaviour. To minimise expectancy effects, participants were not informed in advance about the specific interaction events under investigation. Informed consent was obtained from all participants in accordance with established ethical research guidelines.

ii. Familiarisation Phase

A dedicated familiarisation phase was conducted prior to data collection to allow participants to adapt to the simulator environment, embodiment responsiveness, and visual immersion. During this phase, participants completed several practice road-crossing trials that were not included in the experimental dataset, featuring urban road segments with different types of interaction events. The familiarisation phase was considered complete once participants demonstrated stable crossing behaviour and reported an adequate level of comfort with the simulator.

iii. Experimental Scenarios and Crossing Tasks

The experimental scenarios were structured around the systematic manipulation of a set of key factors influencing pedestrian decision-making. Specifically, the experimental design considered the crossing configuration, articulated into three distinct scenarios for both Via Prisciano and Piazzale delle Medaglie d'Oro; the lighting condition, defined as daytime or nighttime; and the approaching traffic condition, defined by the type of leading vehicle in the approaching platoon. Accordingly, the number of experimental configurations for each pedestrian crossing resulted from the combination of three crossing configurations, two lighting conditions, and two leading vehicle types, yielding a total of 12 distinct experimental configurations per crossing, as reported in the following Table 3.

Table 3 - Platoon distribution across the different scenarios.

	Codice	Attraversamento	Illuminazione	Gap	Tipo Veicolo	Scenario
1	VP_ATT_D_A-A	Via Prisciano	Giorno	2,5s - 3s - 2,5s - 3,5s	Auto - Auto	Attuale
2	VP_S1_D_A-A	Via Prisciano	Giorno	2,5s - 3s - 2,5s - 3,5s	Auto - Auto	Contromisura 1
3	VP_S2_D_A-A	Via Prisciano	Giorno	2,5s - 3s - 2,5s - 3,5s	Auto - Auto	Contromisura 2
4	VP_ATT_D_A-M	Via Prisciano	Giorno	2,5s - 3s - 2,5s - 3,5s	Auto - Moto	Attuale
5	VP_S1_D_A-M	Via Prisciano	Giorno	2,5s - 3s - 2,5s - 3,5s	Auto - Moto	Contromisura 1
6	VP_S2_D_A-M	Via Prisciano	Giorno	2,5s - 3s - 2,5s - 3,5s	Auto - Moto	Contromisura 2
1	VP_ATT_N_A-A	Via Prisciano	Notte	2,5s - 3s - 2,5s - 3,5s	Auto - Auto	Attuale
2	VP_S1_N_A-A	Via Prisciano	Notte	2,5s - 3s - 2,5s - 3,5s	Auto - Auto	Contromisura 1
3	VP_S2_N_A-A	Via Prisciano	Notte	2,5s - 3s - 2,5s - 3,5s	Auto - Auto	Contromisura 2
4	VP_ATT_N_A-M	Via Prisciano	Notte	2,5s - 3s - 2,5s - 3,5s	Auto - Moto	Attuale
5	VP_S1_N_A-M	Via Prisciano	Notte	2,5s - 3s - 2,5s - 3,5s	Auto - Moto	Contromisura 1
6	VP_S2_N_A-M	Via Prisciano	Notte	2,5s - 3s - 2,5s - 3,5s	Auto - Moto	Contromisura 2
1	MO_ATT_D_A-A	Piazzale delle Medaglie d'Oro	Giorno	2,5s - 3s - 2,5s - 3,5s	Auto - Auto	Attuale
2	MO_S1_D_A-A	Piazzale delle Medaglie d'Oro	Giorno	2,5s - 3s - 2,5s - 3,5s	Auto - Auto	Contromisura 1
3	MO_S2_D_A-A	Piazzale delle Medaglie d'Oro	Giorno	2,5s - 3s - 2,5s - 3,5s	Auto - Auto	Contromisura 2
4	MO_ATT_D_A-M	Piazzale delle Medaglie d'Oro	Giorno	2,5s - 3s - 2,5s - 3,5s	Auto - Moto	Attuale
5	MO_S1_D_A-M	Piazzale delle Medaglie d'Oro	Giorno	2,5s - 3s - 2,5s - 3,5s	Auto - Moto	Contromisura 1
6	MO_S2_D_A-M	Piazzale delle Medaglie d'Oro	Giorno	2,5s - 3s - 2,5s - 3,5s	Auto - Moto	Contromisura 2
1	MO_ATT_N_A-A	Piazzale delle Medaglie d'Oro	Notte	2,5s - 3s - 2,5s - 3,5s	Auto - Auto	Attuale
2	MO_S1_N_A-A	Piazzale delle Medaglie d'Oro	Notte	2,5s - 3s - 2,5s - 3,5s	Auto - Auto	Contromisura 1
3	MO_S2_N_A-A	Piazzale delle Medaglie d'Oro	Notte	2,5s - 3s - 2,5s - 3,5s	Auto - Auto	Contromisura 2
4	MO_ATT_N_A-M	Piazzale delle Medaglie d'Oro	Notte	2,5s - 3s - 2,5s - 3,5s	Auto - Moto	Attuale
5	MO_S1_N_A-M	Piazzale delle Medaglie d'Oro	Notte	2,5s - 3s - 2,5s - 3,5s	Auto - Moto	Contromisura 1
6	MO_S2_N_A-M	Piazzale delle Medaglie d'Oro	Notte	2,5s - 3s - 2,5s - 3,5s	Auto - Moto	Contromisura 2

The experimental design was based on a series of microsimulation trials, each with a duration of 60 s. During each microsimulation, participants were exposed to a sequence of approaching vehicle platoons characterised by progressively increasing inter-platoon temporal gaps and were free to decide whether and when to initiate the crossing. If a participant decided to cross the road, the relevant data were recorded and the simulation proceeded to the subsequent microsimulation. Conversely, if the participant decided not to cross, the simulation automatically terminated after 60 s, the non-crossing decision was recorded, and the system advanced to the next microsimulation. Between two consecutive microsimulations, a neutral waiting room was introduced to allow participants to return to a predefined starting position. This procedure ensured that each microsimulation began from identical initial spatial conditions, thereby maintaining consistency across trials and participants. In each trial, participants were required to perform the pedestrian crossing task, which consisted of observing the approaching traffic and deciding whether and when to initiate the crossing according to their own judgement and perceived safety.

The two zebra crossings considered in the study represent real-world urban contexts and were faithfully reproduced within the virtual environment to ensure spatial and perceptual coherence with the existing infrastructure. This configuration allowed participants to experience realistic crossing situations while maintaining full experimental control over traffic conditions and infrastructural features.

iv. Traffic and Interaction Modelling

The traffic interaction was characterised by the presence of successive vehicle platoons travelling at a constant speed of 45 km/h, following predefined trajectories and not exhibiting any collaborative behaviour toward pedestrians. This speed was selected as representative of regular urban traffic flow and was adopted to evaluate pedestrians' perceived safety conditions under consistent and controlled traffic dynamics. Each approaching traffic condition was implemented using vehicle platoons composed of a fixed number of vehicles, travelling with a constant intra-platoon temporal spacing. The temporal gap between successive platoons was not treated as a discrete experimental factor; instead, it was implemented as a progressively increasing sequence of exposure conditions, as illustrated in the following Table 4. Specifically, pedestrians were sequentially exposed to increasing temporal gaps between consecutive platoons, starting from shorter values and gradually increasing according to a predefined temporal order. This approach was adopted to reproduce a realistic traffic stream and to observe pedestrian decision-making under gradually changing crossing opportunities, rather than under isolated and artificially fixed gap conditions.

Table 4 - Temporal GAP between successive vehicle platoons.

gap tra veicoli (45 km/h) [s]		
corsia vicina		
2,5	3	3,5
gap tra veicoli (45 km/h) [m]		
corsia vicina		
31,25	37,50	43,75

Within the approaching traffic conditions, a specific experimental factor was the type of leading vehicle in the platoon. The platoon configuration was designed such that the leading vehicle, representing the first and most perceptually salient element encountered by the pedestrian, could be either a passenger car or a motorcycle, while the remaining vehicles in the platoon were consistently passenger cars. This configuration allowed the investigation of the Vehicle Size Effect and differences in visual salience on pedestrian behaviour, isolating the influence of the first approaching vehicle under otherwise identical traffic conditions.

All the above conditions were tested for both pedestrian crossings at Via Prisciano and Piazzale delle Medaglie d'Oro, enabling the analysis of behavioural differences associated with visibility conditions, approaching traffic composition, and type of infrastructural safety measure adopted. The trajectories followed by approaching vehicles replicated the real traffic movements associated with the two crossings under study. Specifically, for Via Prisciano, vehicles approached along a straight roadway segment, whereas for Piazzale delle Medaglie d'Oro, vehicle trajectories followed a curved alignment reflecting the actual geometry of the urban environment.

v. Session Completion and Debriefing

At the conclusion of the experimental session, participants were debriefed and asked to report any discomfort, simulator sickness symptoms, or anomalous events experienced during the trials. This information was used to verify data quality and to identify potential exclusions or sensitivity analyses.

2.3.4 Data Collection

Data collection was fully integrated within the virtual reality pedestrian simulator and implemented to ensure high temporal resolution, repeatability, and consistency across all experimental conditions. The acquisition system was designed to automatically record both behavioural decisions and kinematic variables during each microsimulation, without any direct intervention by the experimenter. For each microsimulation, the primary outcome variable recorded was the pedestrian crossing decision, defined as a binary variable indicating whether the participant initiated the crossing or not. This variable represents the main dependent variable of the experimental design and constitutes the basis for the analysis of gap acceptance behaviour (Miller, 1947; Razzaq & Shubber, 2022). When a participant decided to cross, additional quantitative variables were recorded to characterise the decision-making process and the associated risk conditions (Ni et al., 2016; Tageldin et al., 2017). In particular, the waiting time was measured as the elapsed time between the start of the microsimulation and the instant at which the pedestrian initiated the crossing manoeuvre. This variable provides a direct measure of hesitation and decision latency under different traffic and environmental conditions. The Time to Zebra (TTZ) was computed at the exact moment the pedestrian started the crossing. TTZ was defined as the residual temporal distance between the pedestrian and the first approaching vehicle of the platoon, calculated based on the instantaneous vehicle speed and distance from the crosswalk. TTZ represents a key indicator of perceived safety and urgency at the decision moment and was later used for both descriptive and inferential analyses. The temporal gap accepted by the pedestrian was also recorded. Since participants were exposed to a sequence of approaching platoons with progressively increasing platoon gaps, the accepted gap was identified as the specific temporal interval between platoons at which the pedestrian chose to cross. In cases where the pedestrian did not cross during the 60 s duration of the microsimulation, the trial was terminated automatically, and the non-crossing outcome was recorded together with the maximum exposed gap.

In addition to behavioural variables, the simulator continuously logged kinematic and positional data for both pedestrians and vehicles. For the approaching vehicles, the system recorded the instantaneous speed, position along the trajectory, and temporal information throughout the simulation. These data were used to reconstruct vehicle trajectories and to verify the consistency of traffic conditions across trials. All data were time-stamped and associated with metadata describing the experimental condition, including crossing location, Via Prisciano or Piazzale delle Medaglie d'Oro, scenario configuration, S0, S1, or S2, lighting condition, daytime or nighttime, and leading vehicle type, passenger car or motorcycle. This structure enabled the aggregation and comparison of observations across different infrastructural, environmental, and traffic configurations.

Finally, questionnaire subjective data were collected after the simulation sessions, including perceived safety, realism of the simulator, effectiveness of infrastructural countermeasures, and cyber sickness symptoms. These subjective measures were stored separately but linked to the behavioural dataset through anonymous participant identifiers, allowing integrated analyses between objective behaviour and subjective perception. Overall, the adopted data collection framework provided a comprehensive and robust dataset, suitable for advanced statistical modelling of pedestrian decision-making processes and for the evaluation of infrastructural countermeasures under controlled yet realistic traffic conditions.

2.3.5 Participants

The experimental study initially involved a total of 48 participants. Participants were recruited on a voluntary basis within the academic community of the Department of Civil, Computer Science and Aeronautical Technologies Engineering of Roma Tre University, including undergraduate and graduate students, academic staff, and researchers. The sample was predominantly male, consisting of 31 males (64%) and 17 females (36%). Participants' ages ranged from 20 to over 60 years, with a strong prevalence of young adults. Regarding educational background, the sample exhibited a medium-to-high level of education. All participants had completed at least secondary education, and approximately 50% held a university degree, including postgraduate qualifications up to the doctoral level. This composition reflects the academic recruitment context and the predominance of students and young adults within the sample. All participants declared the absence of sensory, motor, or balance impairments that could affect task performance. No participant reported neurological disorders or conditions incompatible with simulator use. No participant interrupted the simulation due to symptoms of simulator sickness; therefore, no exclusions were required on this basis. Data cleaning was subsequently performed at the manoeuvre level to remove anomalous or inconsistent observations, ensuring a robust and representative final dataset for analysis.

2.4 Motorcycle Simulation

2.4.1 Instrument

The experimental activity was conducted using a set of instruments specifically selected to recreate realistic, controlled, and immersive riding scenarios, with the aim of analysing participants' behaviour under simulated traffic conditions. The instrumentation adopted in this study consisted of the Honda Riding Trainer (HRT) motorcycle simulator, reported in the following Figure 24, integrated with a Meta Quest 3S virtual reality headset, and a dedicated computing system for simulation management and data processing.

The Honda Riding Trainer (HRT) represents one of the core experimental tools used in this study, in combination with a virtual reality headset. Developed by Honda in 2005, the HRT is a compact, cost-effective, and transportable motorcycle riding simulator, originally designed for road safety education and for enhancing riders' perceptual, attentional, and decision-making skills. The simulator consists of a physical riding station that faithfully reproduces the ergonomics of a real motorcycle, including a seat, handlebars, and realistic control devices such as throttle, brakes, clutch, turn indicators, headlight controls, and horn. A pedal unit is also included, with pedals for clutch and braking. In the present study, the simulator was operated in automatic riding mode, which excludes the use of pedals and gear shifting in order to simplify vehicle control and reduce task complexity for participants. The HRT is equipped with a front monitor that allows real-time visualisation of the riding scenario. However, in this experimental setup, the monitor was not used by the participant for scenario visualisation, but only by the operator for monitoring and managing the simulation. The riding scenario was instead rendered directly within the HMD worn by the participant, ensuring a higher level of immersion and perceptual realism.

Figure 24 - Honda Riding Trainer (HRT).

To enhance the immersive quality of the simulation, the HRT was integrated with a Meta Quest 3S virtual reality HMD, as reported in the following Figure 25, which constituted a fundamental component of the experimental apparatus. The headset enabled participants to experience the riding scenario within a three-dimensional immersive environment, providing a natural and realistic visual perception. The use of the VR HMD allowed the rider to interact with the simulated environment in a manner that closely resembles real-world riding conditions, supporting accurate depth perception, peripheral vision, and spatial awareness.

Figure 25 - Motorcycle simulator spatial configuration.

The HRT simulator was connected to a dedicated PC running a Windows operating system, responsible for executing the simulation software and managing real-time data processing. Within the experimental framework, Unity was adopted as the graphics engine and development environment for creating and managing interactive three-dimensional riding scenarios. In this configuration, the HRT provided the physical input commands, while Unity handled the visual rendering, interaction logic, and scenario dynamics. The integration of the VR HMD within Unity was achieved through the installation and configuration of a dedicated virtual reality software package, enabling accurate tracking of head movements and seamless visual feedback within the headset.

The VR system supported advanced features such as real-time head tracking, ensuring a fluid synchronisation between the participant's physical movements and the corresponding visual updates in the virtual environment. In this setup, the HMD functioned not merely as a display device, but as an active component of the simulation, capable of translating physical user inputs into immersive visual responses.

The HRT was not originally designed for direct integration with external simulation environments. Therefore, a custom interface was developed to enable communication between the physical simulator and Unity. Physical inputs generated by the HRT controls (e.g., throttle, brakes, steering) were captured through a USB connection and mapped to the corresponding control parameters of the virtual motorcycle within Unity. Custom C# scripts were developed to process these input signals and translate them into coherent vehicle behaviour in the virtual environment. Each control input was calibrated to ensure realistic and proportional responses, such as progressive acceleration, proportional braking, and smooth steering dynamics. Unity generated the visual scenario and transmitted it directly to the VR headset, allowing participants to experience the simulation from a first-person perspective. When a physical action was performed on the simulator (e.g., braking), the corresponding signal was immediately transmitted to Unity, triggering the appropriate response in the virtual motorcycle. This ensured a high level of consistency between physical actions and virtual outcomes, preserving the realism of the riding experience.

2.4.2 Experimental Protocol

The study focused on motorcycle–pedestrian interactions occurring in proximity to the uncontrolled pedestrian crossing of Via Prisciano, with the aim of analysing the rider's behaviour during the approach phase, the perception of the pedestrian, and the response to the pedestrian's presence. The analysis targeted behavioural and performance-related variables such as speed adaptation, deceleration patterns, and stopping behaviour, which collectively reflect riders' attention allocation and response strategies in the presence of pedestrians.

i. **Participant Preparation and Briefing**

Before the start of each experimental session, participants received a standardised briefing outlining the general objectives of the study, the functioning of the motorcycle simulator, and the overall structure of the experimental trials. Participants were instructed to drive the motorcycle as they would under normal real-world conditions, without adopting overly cautious or deliberately risky behaviour. To minimise expectancy effects, participants were not informed in advance about the specific interaction events under investigation. Informed consent was obtained from all participants in accordance with established ethical research guidelines.

ii. Familiarisation Phase

A dedicated familiarisation phase was conducted prior to data collection to allow participants to adapt to the simulator environment, embodiment responsiveness, and visual immersion. During this phase, participants completed one or more practice trials in a scenario that included pedestrian crossings located in areas different from those used in the formal experiment. Data collected during the familiarisation phase were not included in the experimental dataset. The practice scenario featured urban road segments with different types of interaction events, allowing participants to become accustomed to the simulator controls, the virtual environment, and the task demands. The familiarisation phase was considered complete once participants demonstrated stable riding behaviour and reported an adequate level of comfort with the simulator.

iii. Experimental Scenarios and Driving Tasks

The motorcycle–pedestrian interaction was implemented through the three infrastructural scenarios previously described for the Via Prisciano crossing, designed to assess the effectiveness of alternative safety strategies:

- Baseline scenario (S0), representing the current "as-is" configuration;
- Scenario 1 (S1), incorporating a first set of countermeasures aimed at improving safety conditions at the crossing;
- Scenario 2 (S2), incorporating a second set of countermeasures to evaluate the impact of further interventions on motorcyclists' behaviour and safety.

Within each infrastructural scenario, three crossing-event conditions were implemented by manipulating the timing of the pedestrian's entry into the carriageway relative to the rider's approach. The reference variable used to define these conditions was the Time to Zebra (TTZ), which represents the temporal margin available to the rider to reach the zebra crossing at the moment the pedestrian initiates the crossing manoeuvre. The three event conditions were:

i. No pedestrian crossing;
ii. Pedestrian crossing with TTZ = 2.5;
iii. Pedestrian crossing with TTZ = 3.5 s.

By combining the three infrastructural scenarios (S0, S1, S2) with the three crossing-event conditions, a total of nine experimental motorcycle–pedestrian scenarios were generated for Via Prisciano.

iv. Traffic and Interaction Modelling

For the vehicle–pedestrian interaction scenarios, pedestrian behaviour was systematically controlled using a dynamic Time-to-Zebra (TTZ) triggering mechanism. Pedestrians were continuously present in the scene and positioned near the crosswalk, while the initiation of the crossing manoeuvre was governed by the driver's approach conditions. When the user vehicle entered a control area extending 100 m upstream of the pedestrian crossing, an automated system tracked the vehicle and continuously computed the Time to Zebra (TTZ) based on its instantaneous speed and trajectory. The pedestrian crossing behaviour was triggered when the computed TTZ reached a predefined threshold, corresponding to different levels of urgency. To ensure scenario consistency and to avoid unrealistically delayed pedestrian activation, a fallback condition was implemented: if the predefined TTZ threshold was not reached due to a low vehicle speed, the pedestrian crossing behaviour was initiated when the distance between the vehicle and the zebra crossing became less than 15 m. This approach ensured a consistent and controlled exposure of drivers to pedestrian crossing events, while preserving the realism of vehicle–pedestrian interactions and avoiding artificial pedestrian appearance effects.

v. Session Completion and Debriefing

At the conclusion of the experimental session, participants were debriefed and asked to report any discomfort, simulator sickness symptoms, or anomalous events experienced during the trials. This information was used to verify data quality and to identify potential exclusions or sensitivity analyses.

2.4.3 Data Collection

During the experimental sessions, a comprehensive data collection framework was implemented to record both objective driving performance variables and subjective assessments. Data acquisition was fully integrated into the Unity-based driving simulator architecture and was designed to ensure high temporal resolution, accuracy, and consistency across all experimental scenarios and interaction types. The driving simulator continuously recorded vehicle state and motion variables throughout each simulation trial, with data acquisition performed automatically by the simulation software and its associated performance measurement modules.

The data acquisition strategy varied according to the type of interaction under analysis. Data were collected along predefined trigger sections spaced at an inter-distance of 1.0 m, distributed along a 100 m approach segment upstream of the pedestrian crossing.

The following objective variables were recorded:

- Section identifier: alphanumeric code associated with each predefined trigger section;
- Vehicle position: spatial coordinates (X, Y, Z) expressed in a fixed reference frame;
- Lateral offset: lateral deviation of the vehicle from the reference trajectory;
- Vehicle speed;
- Elapsed time: time elapsed from the beginning of the trial at the instant the vehicle crossed each specific trigger section.

In the presence of motorcycle–pedestrian collisions, the following additional variables were recorded:

- Collision time: elapsed time from the beginning of the trial at the moment of collision;
- Motorcycle speed at impact;
- Pedestrian position at impact;
- Motorcycle position at impact.

These continuously recorded variables formed the basis for the subsequent computation of surrogate safety measures such as Time to Collision (TTC), Minimum Time to Collision (MTTC), Post-Encroachment Time (PET), Time to Zebra (TTZ), Gap Time, and deceleration-based indicators. Importantly, these indicators were not directly recorded, but rather derived offline from the raw kinematic and positional data collected during the simulations

Following data collection, a set of time-based, kinematic, and spatial indicators was computed in order to quantify driver behaviour, conflict severity, and safety-related outcomes across the different interaction scenarios. These indicators were derived from the raw vehicle trajectory, speed, and timing data and are commonly adopted in the analysis of traffic conflicts and surrogate safety measures.

2.4.4 Participants

The experimental study initially involved a total of 52 participants. Participants were recruited on a voluntary basis within the academic community of the Department of Civil, Computer Science and Aeronautical Technologies Engineering of Roma Tre University, including undergraduate and graduate students, academic staff, and researchers. The sample was predominantly male, consisting of 29 males (56%) and 23 females

(44%). Participants' ages ranged from 20 to 59 years, with a strong prevalence of young adults. Regarding educational background, the sample exhibited a medium-to-high level of education. All participants had completed at least secondary education, and approximately 75% held a university degree, including postgraduate qualifications up to the doctoral level. This composition reflects the academic recruitment context and the predominance of students and young adults within the sample. With regard to the type of motorcycle primarily ridden, 55% reported using a 125 cc motorcycle, 16% a 50 cc motorcycle, 12% a 150 cc motorcycle, and 18% a motorcycle with an engine capacity greater than 150 cc. In terms of annual mileage, 37% reported riding between 1,000 and 2,000 km per year, 27% less than 1,000 km, 24% between 2,000 and 5,000 km, and 12% more than 5,000 km. Concerning riding frequency, 39% stated that they ride several times per week, 29% every day, while 16% ride occasionally and another 16% only for leisure or during weekends. Regarding prior experience with simulation, 51% of the participants had already experienced driving in a simulator. However, only 8% reported previous experience with a motorcycle simulator specifically. Experience with HMDs was reported by 39% of the sample, and only 10% had previously used a motorcycle simulator with an HMD, indicating that immersive motorcycle simulation was largely unfamiliar to the majority of participants.

All participants declared the absence of sensory, motor, or balance impairments that could affect task performance. No participant reported neurological disorders or conditions incompatible with simulator use. No participant interrupted the simulation due to symptoms of cyber sickness; therefore, no exclusions were required on this basis. Data cleaning was subsequently performed at the manoeuvre level to remove anomalous or inconsistent observations, ensuring a robust and representative final dataset for analysis.

3 Simulation studies RU PoliTO

The research was structured into two complementary studies. The first study examined the *Corso Vittorio Emanuele II* corridor with the aim of investigating driver-VRU interactions along the corridor and understanding how these evolve across different segments. Driving simulation experiments were employed to identify the primary factors contributing to collisions involving VRUs (pedestrians and cyclists) and evaluate the impact of various pedestrian behaviours on driver response.

The second study shifts the focus to a specific intersection (*Corso Vittorio Emanuele II – Corso Inghilterra*), exploring driver–VRU interactions in a concentrated conflict area and evaluating potential countermeasures for cyclist crossings. The aim of this intersection-based study is to identify and discuss measures that can reduce risk for VRUs and improve safety performance.

3.1 Driving simulation experiments of *Corso Vittorio Emanuele II* corridor

3.1.1 Introduction

Collision diagrams were produced to reconstruct a detailed historical crash patterns along the *Corso Vittorio Emanuele II* corridor between vehicle and VRUs. Considering the crashes recorded between 2006 and 2020, the spatial distribution of events highlights a concentration of crashes at strategic locations, such as the intersections with *Corso Vinzaglio*, *Corso Re Umberto*, *Via Sacchi*, and *Via Borsellino*. Moreover, most events occurred during daytime and were more frequently recorded on the service road than on the main carriageway Figure 26. The distribution of VRU-related crashes varies by user category, but the overall evidence consistently points to service roads as the most critical environment, where uncontrolled interactions between vehicles and VRUs are more likely and where multiple risk situations can emerge.

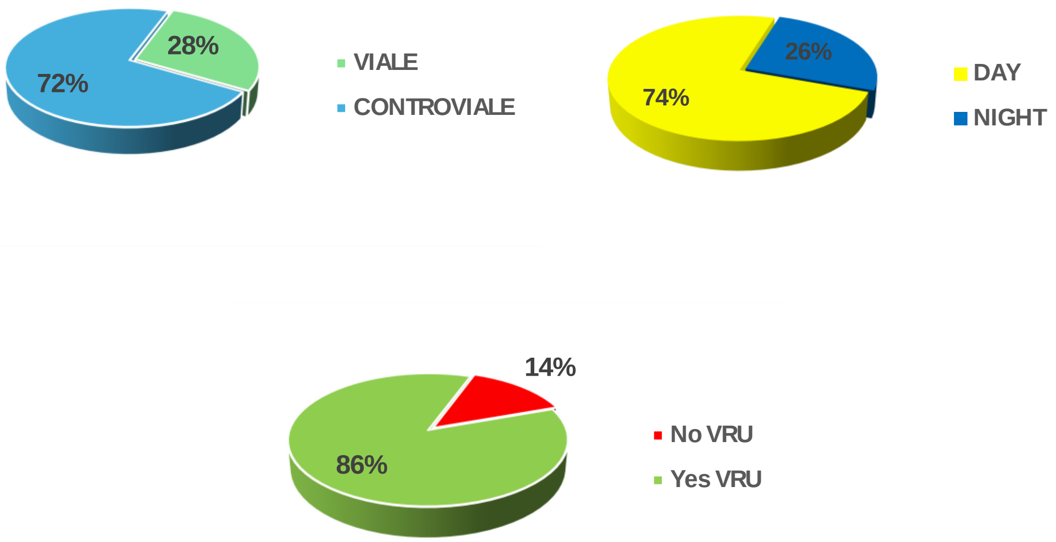

Figure 26. Location, Lighting condition and VRUs involvement of occurred crashes.

3.1.2 Simulated road scenario

The reconstructed virtual corridor of *Corso Vittorio Emanuele II* corridor extends from the *Piazza Rivoli* roundabout to the intersection with *Via Nizza*, with a total length of 2.15 km excluding the length of the intersections. The virtual environment has been designed to reflect real traffic conditions as closely as possible, incorporating all typical urban features. The virtual corridor includes twelve intersections, eleven of which correspond to existing crossings along the main carriageway (Figure 27). Seven of these were selected for detailed analysis based on collision diagrams and observational criteria defined within the project. To realistically represent driver behaviour and driver-VRU interactions, the model incorporates bus stops, traffic control devices, traffic signals and typical pedestrian and vehicle flows. Attention was given to accurately reproducing facilities relevant to VRUs, such as pedestrian and bicycle crossings and lanes, bicycle boxes, and shared lanes. In total, the virtual environment incorporates 57 pedestrian crossings, 29 bicycle crossings, 15 dedicated bicycle lanes, one shared pedestrian-bicycle lane, six advanced bicycle stop lines and seven shared vehicle-bicycle lanes.

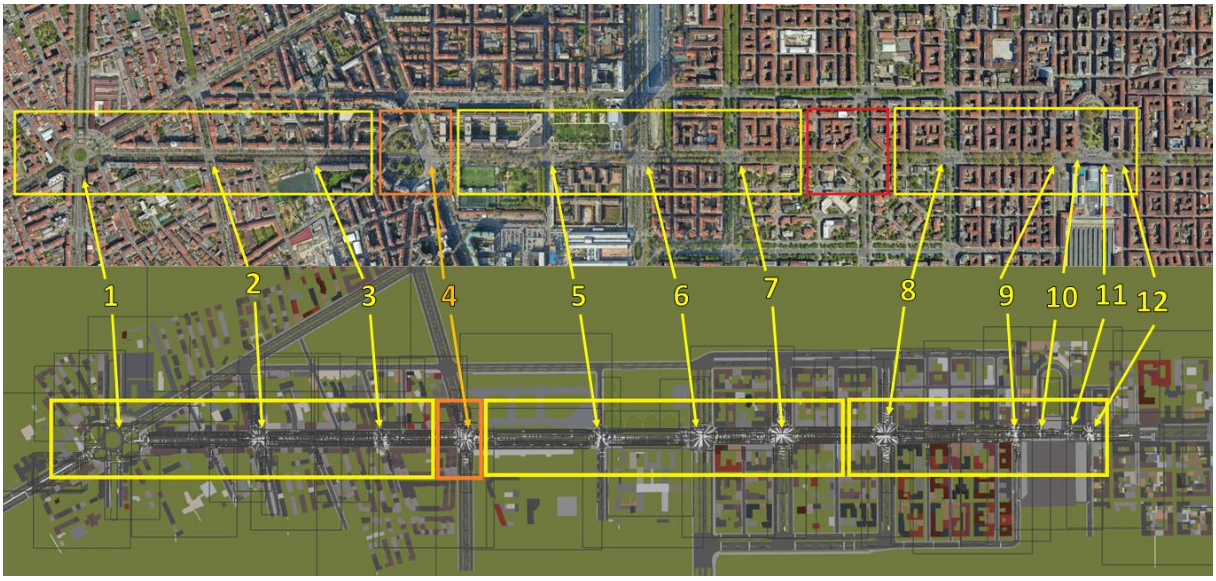

Figure 27. Real and modelled *Corso Vittorio Emanuele II* corridors comparison (yellow boxes = totally replicated in the digital model, orange boxes = partially replicated, red boxes = not replicated)

Figure 28. Comparison between real and modelled cross-section of *Corso Vittorio Emanuele II* corridor.

To identify possible types of interactions between vehicles and VRU, geometrical characteristics and configurations of service roads were analysed in detail. The following Table 5 and Table 6 show the longitudinal vehicle-VRUs interaction along service road segments and transversal vehicle-VRUs interactions in correspondence of the main intersections respectively.

Table 5. Longitudinal vehicle-VRUs interaction along *Corso Vittorio Emanuele II* service road segments.

Interaction type	Graphical scheme	Locations
No longitudinal interaction	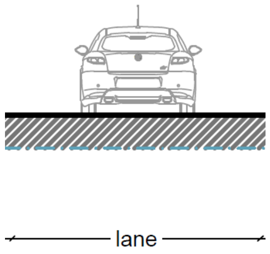	From *Piazza Rivoli* to *Corso Ferrucci* (both service roads) From *Corso Ferrucci* to *Corso Inghilterra* (W-E service road)
Longitudinal interaction in shared lanes	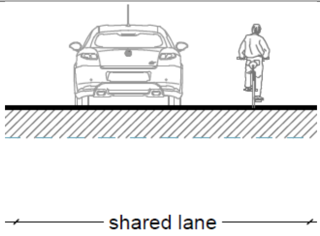	From *Corso Inghilterra* to *Via Sacchi* (W-E service road) From *Corso Ferrucci* to *Corso Inghilterra* (W-E service road) From *Via Sacchi* to *Corso Re Umberto* (E-W service road) From *Corso Vinzaglio* to *Corso Inghilterra* (E-W service road)
Longitudinal interaction with bicycle lanes	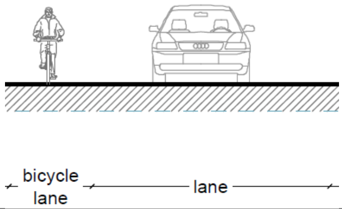	From *Corso Re Umberto* to *Corso Vinzaglio* (E-W service road) From *Corso Inghilterra* to *Corso Ferrucci* (W-E service road)

Table 6. Transversal vehicle-VRUs interactions in correspondence of *Corso Vittorio Emanuele II* main intersections

Interaction type	Graphical scheme	Locations
Transversal interaction only with pedestrians	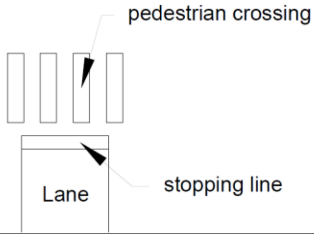	Intersection with *Corso Racconigi* (both service roads) Intersection with *Via Cesana* (both service roads Intersection with *Corso Inghilterra* (right service road) Intersection with *Corso Re Umberto* (left service road)
Transversal interaction with both pedestrians and cyclists	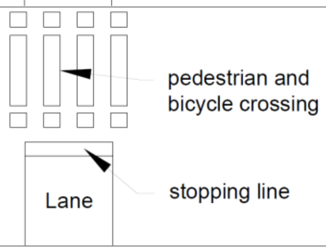	Intersection with *Via Borsellino* (right service road)
Transversal interaction with pedestrian (with bike box)	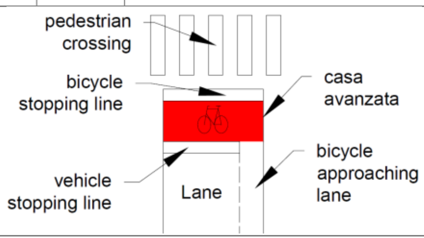	Intersection with *Corso Inghilterra* (left service road) Intersection with *Corso Vinzaglio* (right service road)

<table>
<tr><td><u>Transversal interaction with both cyclists and pedestrian (with bike box)</u></td><td>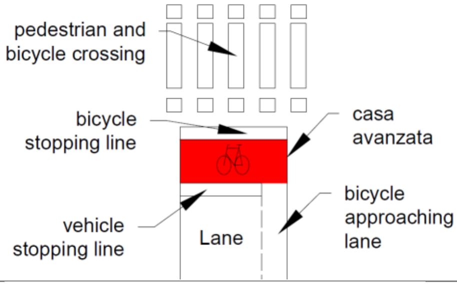
</td><td>Intersection with Via Borsellino (E-W service road)
Intersection with Corso Re Umberto (W-E service road)</td></tr>
<tr><td><u>Transversal interaction with both cyclists and pedestrians (with bike box and additional gap between crossing and stopping line)</u></td><td>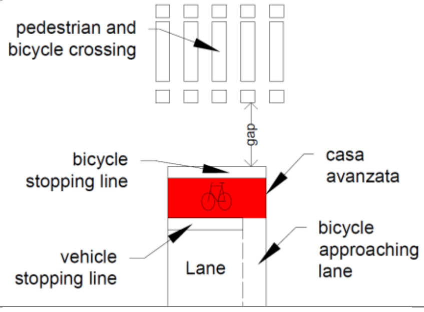
</td><td>Intersection with Corso Vinzaglio (E-W service road)</td></tr>
<tr><td><u>Transversal interaction with both cyclists and pedestrians (with bike box and separated crossings)</u></td><td>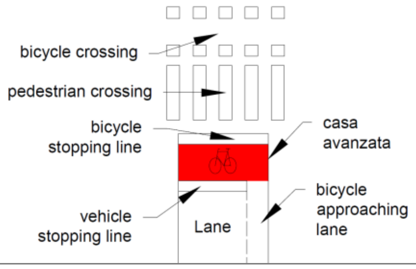
</td><td>Intersection with Via Sacchi (W-E service road)</td></tr>
</table>

3.1.3 Experimental design

The experimental procedure was based on a within-subjects design, comprising two independent sub-experiments which analysed different aspects of vehicle-VRU interactions.

The first sub-experiment focused on pedestrian-related factors and was defined by three variables:

i. pedestrian behaviour (yielding priority, non-yielding priority);
ii. time gap acceptance by pedestrians (3s, 6s);
iii. lighting conditions (day, night).

Conducted along the first two corridor segments between Piazza Rivoli and the intersection with *Via Cesana*, this sub-experiment examined how drivers responded to pedestrians either yielding or not yielding while crossing the service road. Different Time Gap Acceptance by Pedestrians (PTGA) values were introduced to represent varying levels of pedestrian risk-taking, enabling an assessment of driver reactions to crossings occurring at different temporal distances from the approaching vehicle. Non-yielding behaviour was included to reflect realistic pedestrian behaviour, particularly in locations without nearby mid-block crossings.

The second sub-experiment took place along three corridor segments between *Corso Inghilterra* and *Via Sacchi*. It was designed to capture the more complex interaction scenarios that are typical of urban environments with shared lanes. This sub-experiment considered four factors:

i. interaction type (simple, complex)
ii. crossing visibility (at crosswalk, far from the crosswalk)
iii. lighting conditions (day, night)
iv. crossing start side of the pedestrian (left, right).

Interactions were classified as either simple or complex depending on whether the driver was exposed to a single conflict involving either a pedestrian or a cyclist, or simultaneous longitudinal and transversal conflicts involving both user types. Crossings were simulated at and away from marked crosswalks, and from both sides of the road, to evaluate their influence on interaction dynamics and conflict severity.

To reduce the effects of learning and anticipation, the interactions were distributed across multiple locations within each section of the corridor. Four locations (A, B, C, and D) were used in the first sub-experiment (Figure 29 and Figure 30) and three (E, F, and G) in the second (Figure 31, Figure 32, and Figure 33), ensuring variability in the presentation of scenarios and enhancing the robustness of the behavioural observations.

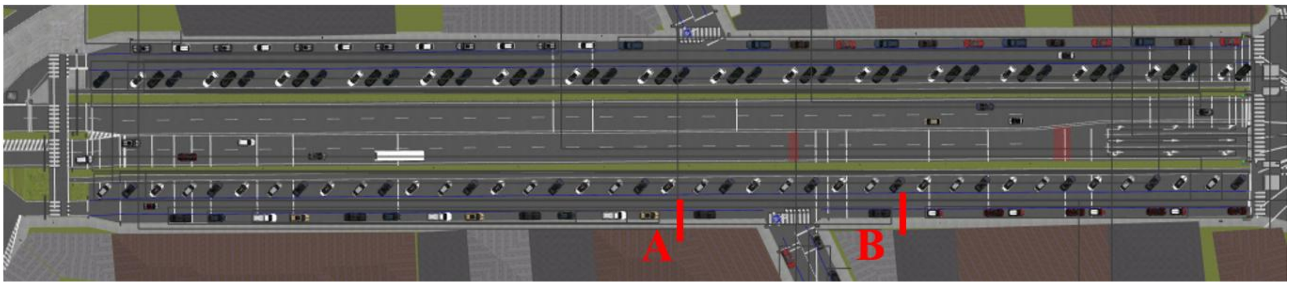

Figure 29. Corridor first segment between modelled *Piazza Rivoli* and intersection with *Corso Racconigi* (A-B locations).

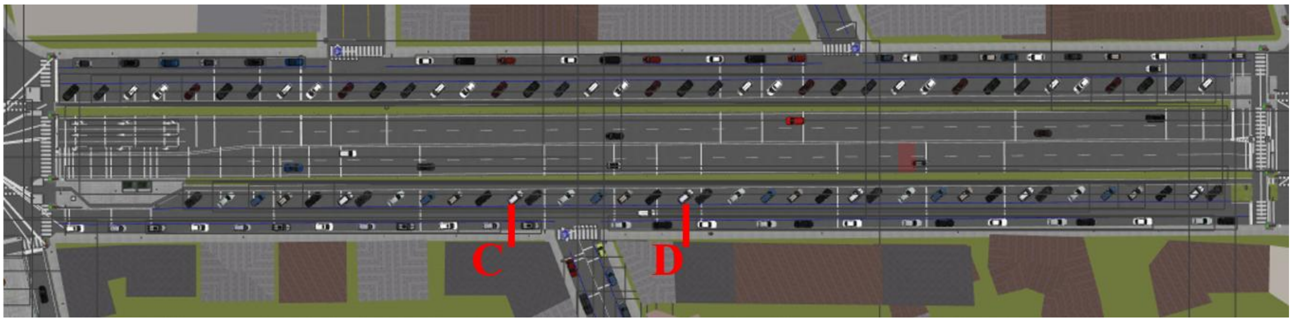

Figure 30. Corridor second segment between modelled intersections with *Corso Racconigi* and with *Via Cesana* (C-D locations).

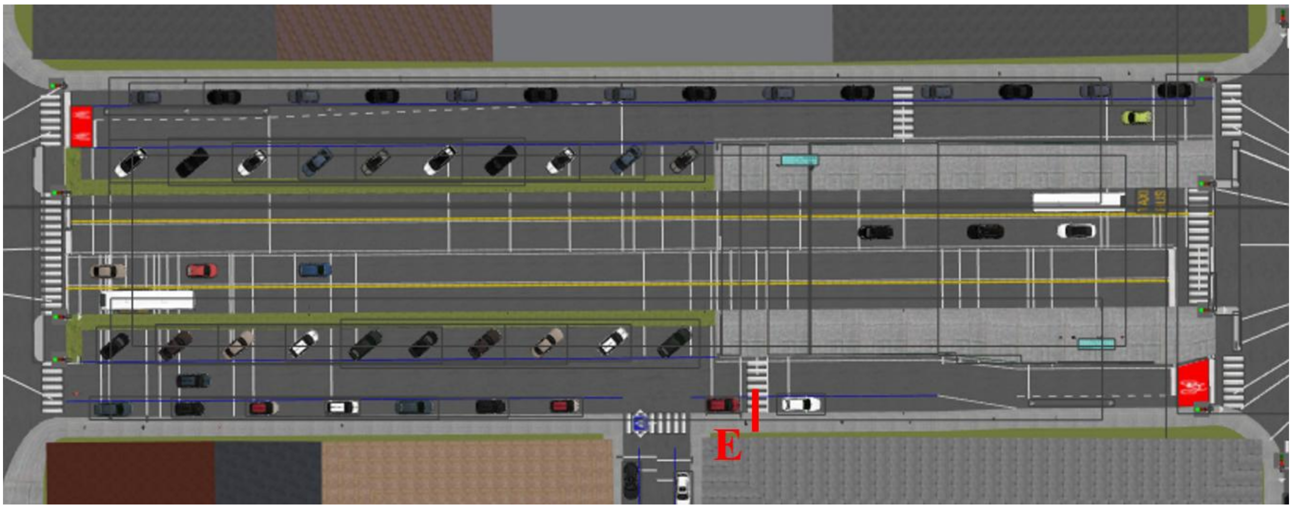

Figure 31. Corridor segment between modelled intersection with *Corso Inghilterra* and *Corso Vinzaglio* (location E).

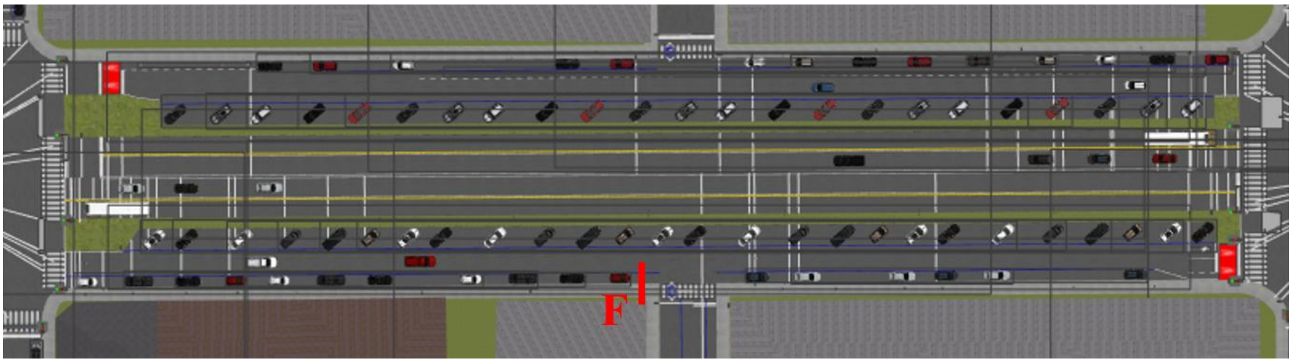

Figure 32. Corridor segment between modelled intersections with *Corso Vinzaglio* and *Corso Re Umberto* (location F).

Figure 33. Corridor segment between modelled intersections with Corso Re Umberto and with Via Sacchi (location G).

Participants were required to drive the entire length of the virtual *Corso Vittorio Emanuele II* corridor, travelling along the west-east (W-E) service road from Piazza Rivoli to the intersection with *Via Nizza*. Each scenario was structured into two consecutive sections (Figure 34), each presenting different vehicle-VRU interactions. In line with real-world conditions, the first section had a speed limit of 30 km/h, while the second section had a lower limit of 20 km/h due to the presence of shared lanes.

Figure 34. Experimental sections (*Corso Vittorio Emanuele II* corridor).

The first section covered the stretch of the corridor between *Piazza Rivoli* and the intersection with *Via Cesana*, and was characterised by a conventional cross-section with two main carriageway lanes in each direction, single-lane service roads and physically separated cycle lanes. In this section, vehicle-pedestrian interactions occurred at predefined mid-block locations (A, B, C and D) along the service road, with pedestrians crossing from right to left. The scenarios differed in terms of the factors previously described (pedestrian behaviour, PTGA, and lighting conditions). Concerning the pedestrian behaviour, in the "yielding priority" condition (Figure 35), pedestrian starts moving (t_0) and approaches the through vehicle lane stopping at the lane strip (t_1). Consistently with the rules, pedestrian gives priority to the vehicle and finishes crossing after the vehicle has passed (t_2).

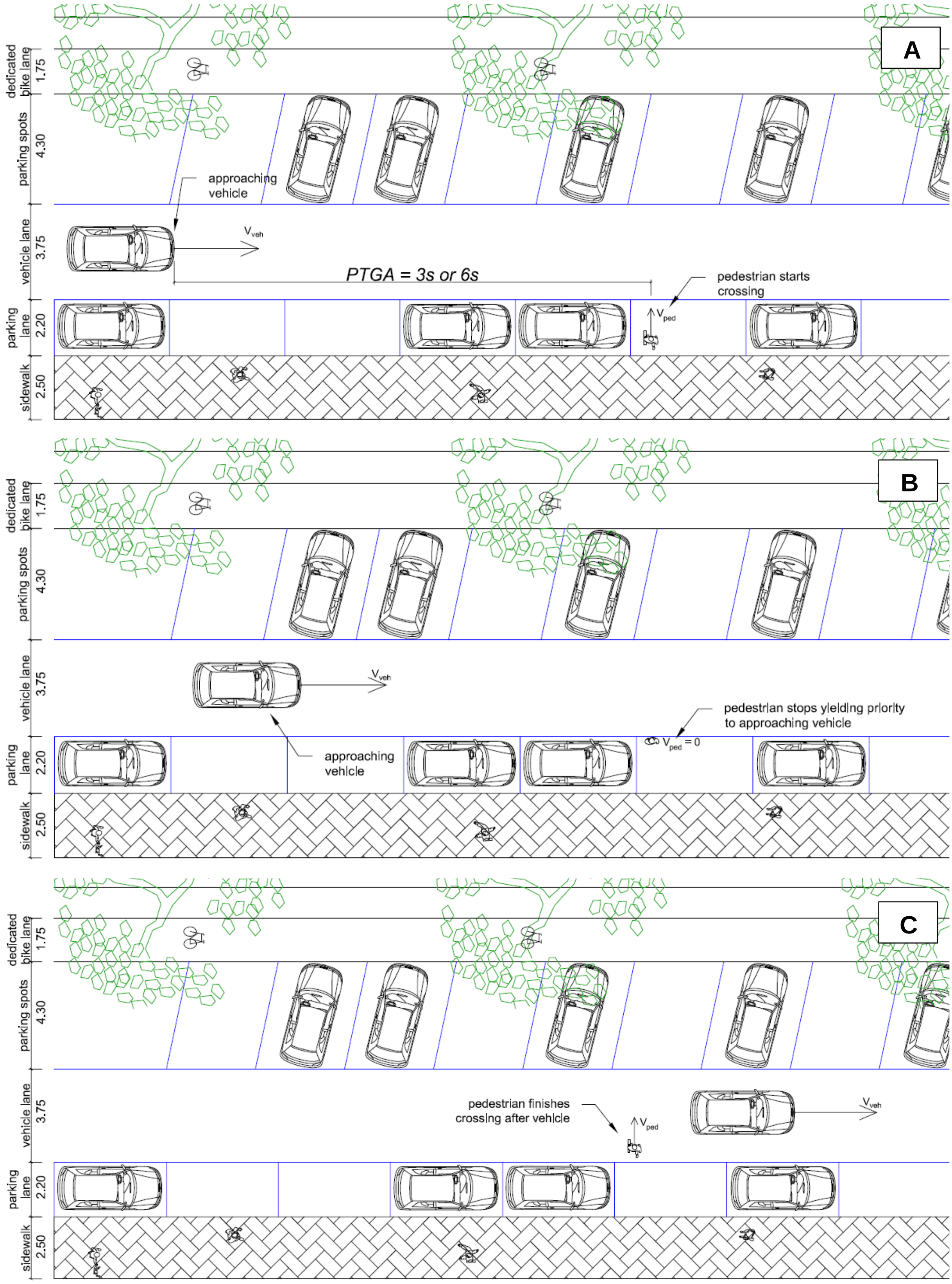

Figure 35. Yielding priority behaviour scheme: (A) t_0 pedestrian starts crossing, (B) t_1 pedestrian stops at lane strip, (C) t_2 pedestrian finishes crossing.

In the "non-yielding priority" situation, pedestrian does not interrupt the crossing manoeuvre under any circumstances (Figure 36). Even if not complying with regulations, it summarises the actual behaviour of some individuals.

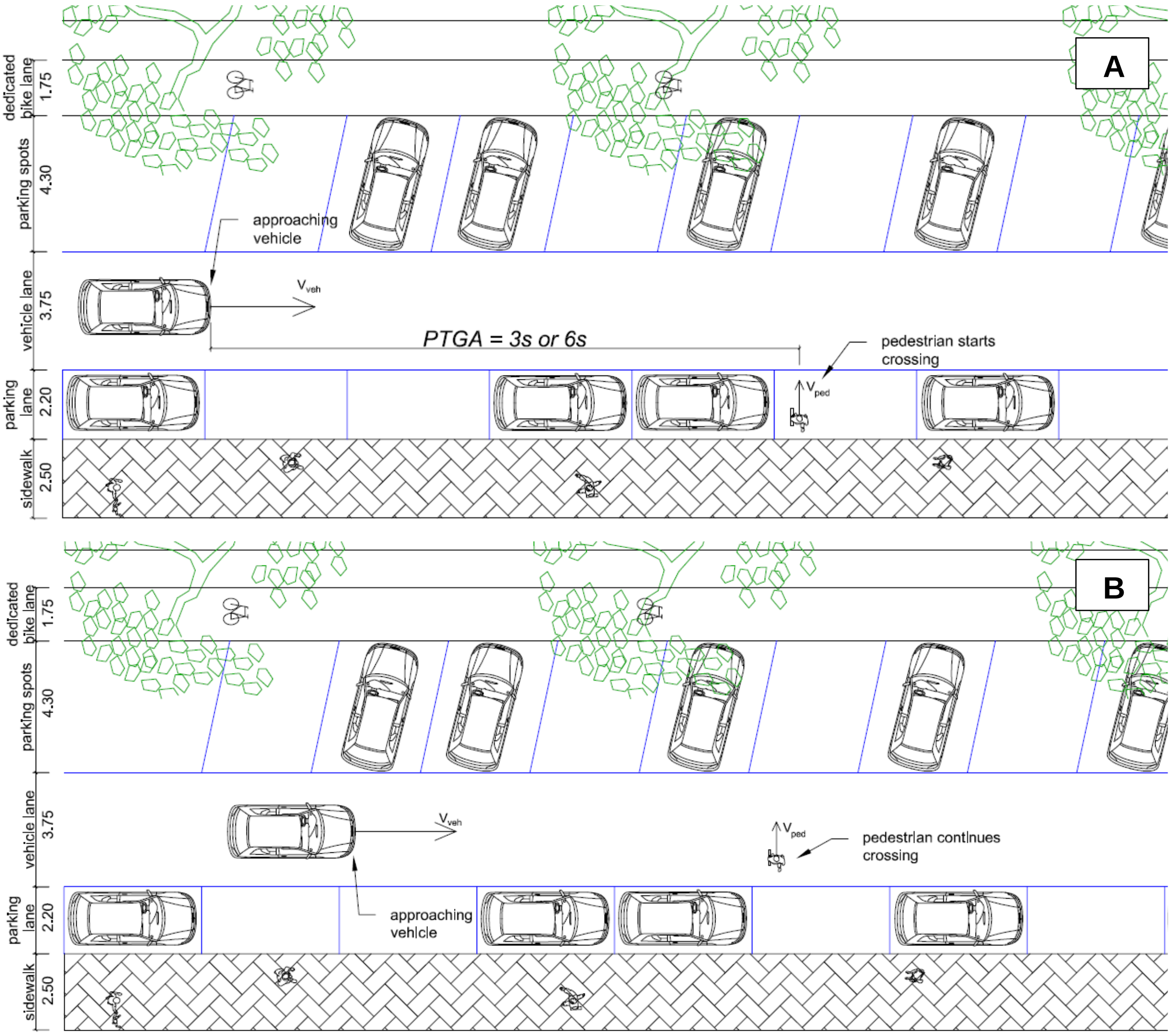

Figure 36. Non-yielding priority behaviour scheme: (A) t_0 pedestrian starts crossing, (B) t_1 pedestrian continues crossing.

The second section extends from the intersection with *Corso Inghilterra* to *Via Sacchi*. It comprises three consecutive corridor segments, each with a progressively more complex layout. These segments feature shared lanes and reduced segregation between vehicles and VRUs. In this section, vehicle-VRU interactions occur at mid-block crossings and in the absence of formal crossing facilities at locations D, E, and F. Depending on the scenario, pedestrians approach from either side of the roadway. The configuration of the service road varies across the segments, alternating between fully shared lanes and combinations of shared and reserved bicycle lanes. The following Table 7 summarises the experimental factors considered in each following analysis.

Table 7. Experimental factors considered in the section 2.

Experimental factors	Sub 2.1		Sub 2.2		Sub 2.3		Sub 2.4		Sub 2.5	
Interaction Type	Simple pedestrian	Complex	Simple pedestrian	Complex	Simple pedestrian		Simple pedestrian		Simple cyclist	
Lighting condition	DAY	NIGHT	DAY	NIGHT	DAY	NIGHT	DAY	NIGHT	DAY	NIGHT
Crossing visibility	Crosswalk		Far from crosswalk		Crosswalk	Far from crosswalk	Crosswalk		-	
Pedestrian crossing start side	Left		Right		Right		Left	Right	-	

The second sub-experiment defined five specific interaction patterns to isolate and analyse the effects of individual factors on driver-VRU interactions. The first interaction pattern focused on interactions at marked crosswalks involving pedestrians crossing from the left. Both simple and complex interaction configurations (Figure 37), as well as day and night conditions, were examined. The aim was to assess whether the presence of a cyclist travelling on the right influences the severity of conflicts between drivers and pedestrians, and in particular whether interactions involving cyclists lead to riskier situations when pedestrians approach from the left.

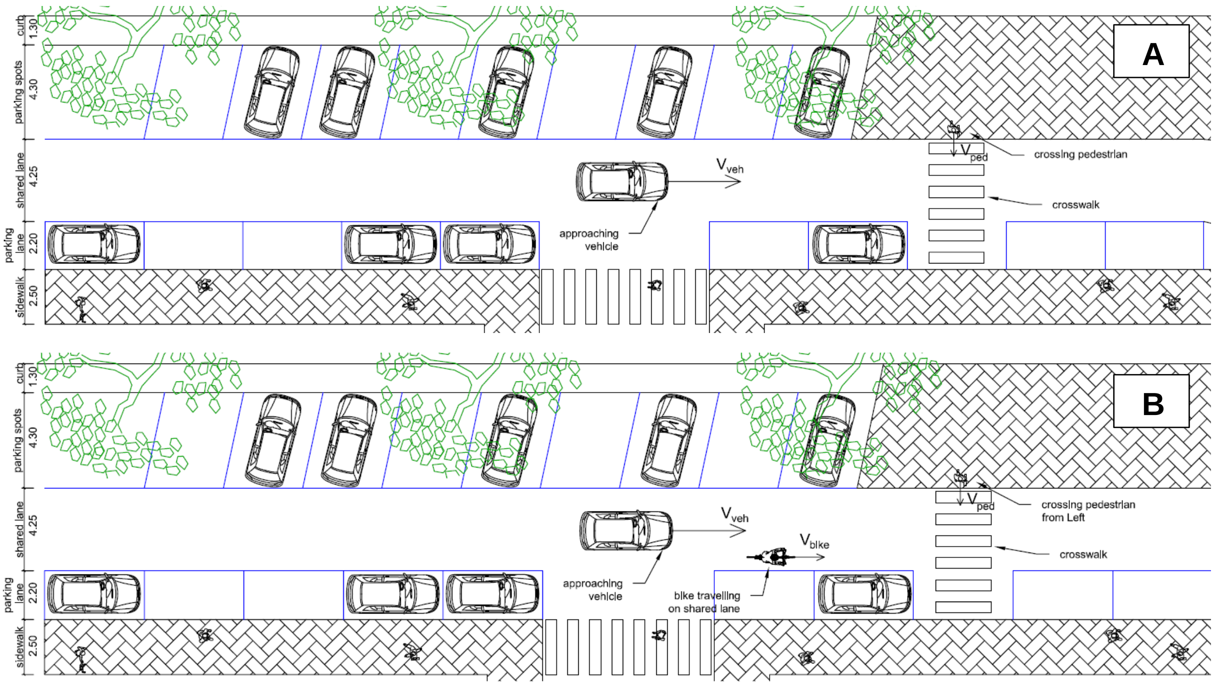

Figure 37. First pattern: (A) simple interaction, (B) complex interaction.

The second interaction pattern involves pedestrians crossing from the right at locations away from marked crosswalks. As in the previous case, both lighting conditions and interaction types were considered (Figure 38). Here, the focus was on evaluating the cyclist's influence on conflict severity in a more localised setting, where both the pedestrian and cyclist interact with the driver from the same side of the road.

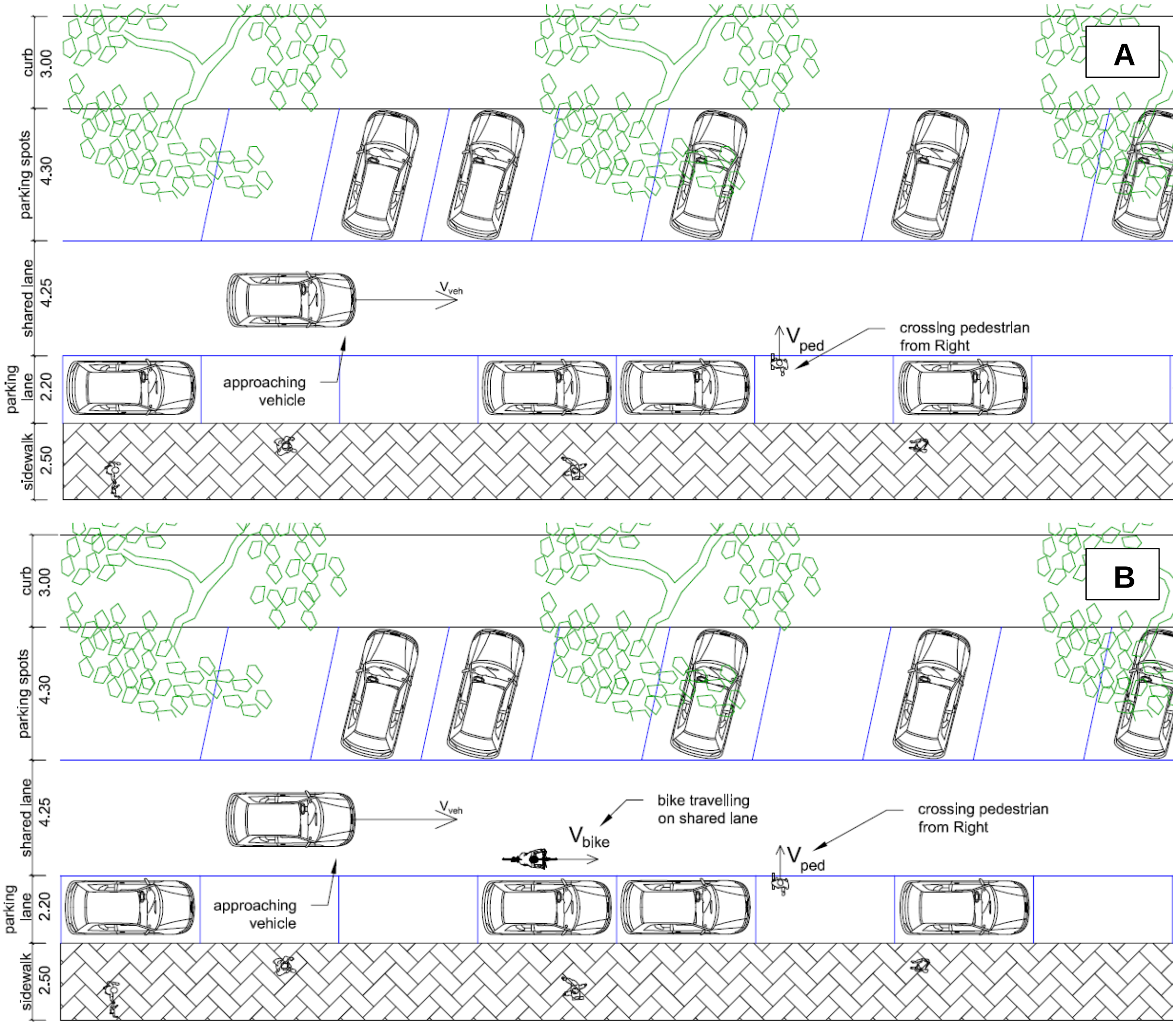

Figure 38. Second pattern: (A) simple interaction, (B) complex interaction.

The third interaction involves driver and pedestrian, investigating the effects of crossing visibility and lighting conditions. Crossings were simulated at both marked and unmarked locations during the day and at night, with the aim of identifying potential relationships between conflict severity and the presence of road signs and pavement markings (Figure 39).

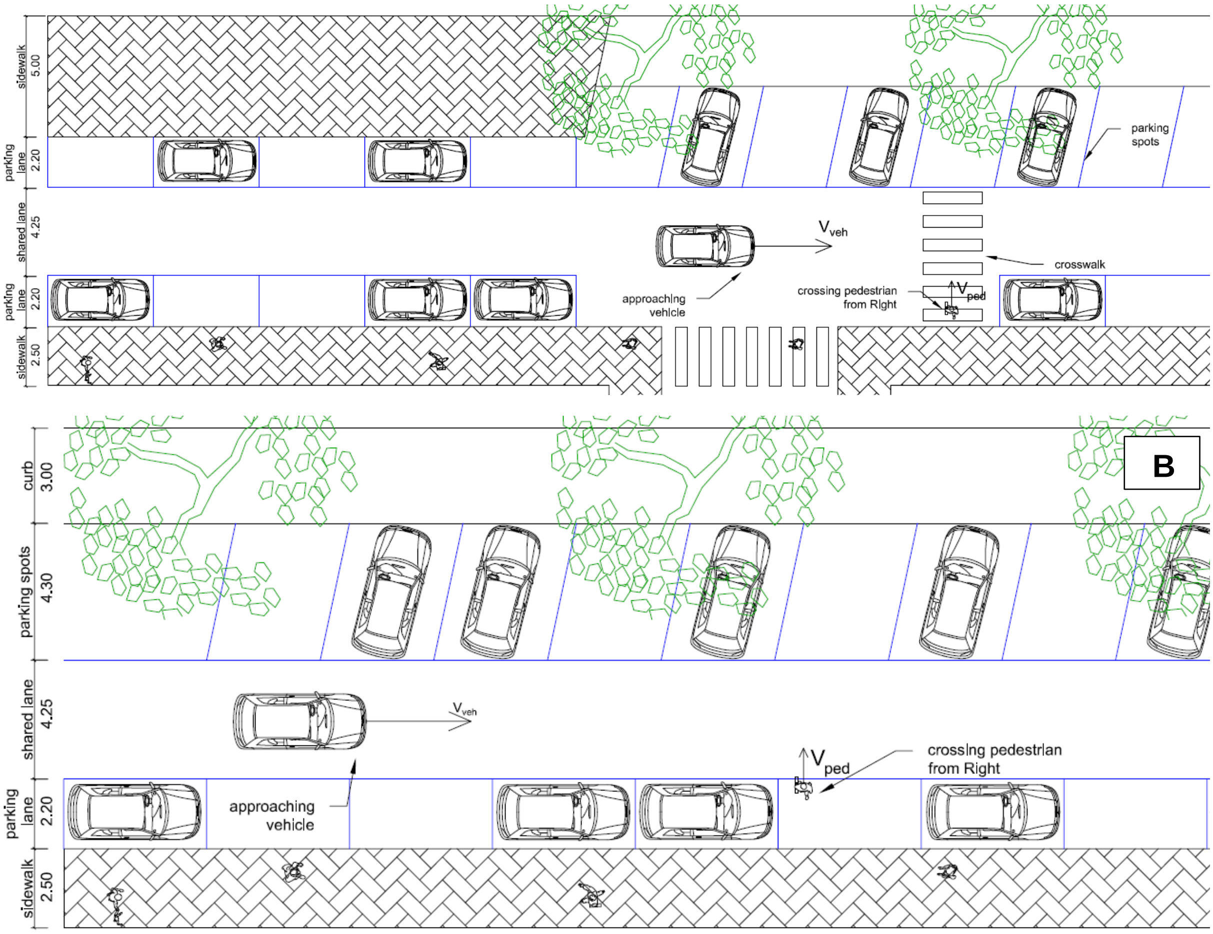

Figure 39. Third pattern: (A) pedestrian interaction at crosswalk, (B) pedestrian interaction far from crosswalk.

The fourth interaction focuses on simple mid-block pedestrian crosswalk, examining the combined effects of lighting conditions and the side from which the pedestrian started to cross (Figure 40). This configuration was designed to explore how the side from which pedestrians enter the roadway may affect the interaction severity.

The fifth interaction configuration addressed the conflicts between drivers and cyclists in shared lanes. It focused specifically on driver behaviour in the presence of cyclists and how lighting conditions may influence these interactions.

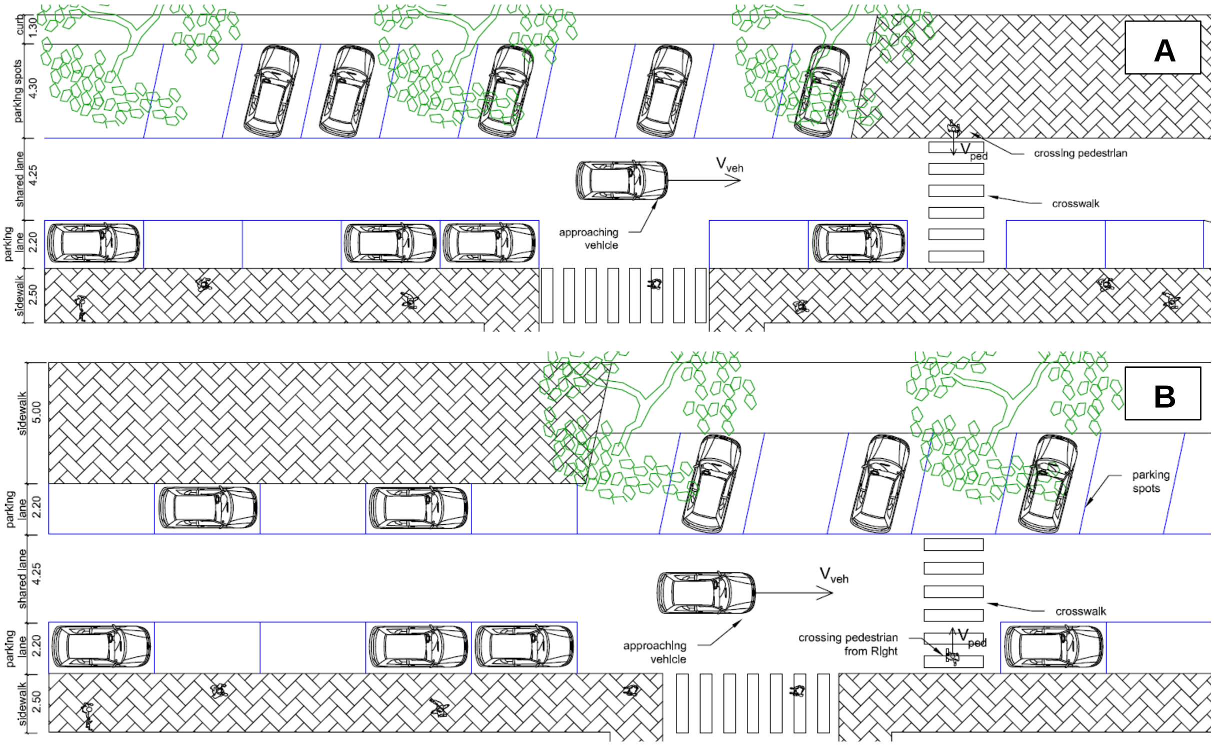

Figure 40. Fourth pattern: (A) pedestrian crossing from left, (B) pedestrian crossing from right.

3.1.4 Experimental protocol, participants and measured variables

Participants were recruited on a voluntary basis. On the day of the test, participants completed a brief pre-driving protocol, which included answering a health screening questionnaire and signing a privacy consent form. Before beginning the experimental tasks, each participant undertook a short familiarisation drive to become accustomed to the simulator, which also took about five minutes. The experimental protocol consisted of eight driving scenarios, divided into two separate sessions: one conducted under daytime conditions and the other under nighttime conditions. Each scenario lasted approximately seven minutes. After the experiment, participants completed a post-simulation questionnaire to assess their perceived simulation sickness. Each driving session lasted around 45 minutes, resulting in a total driving time of approximately 90 minutes per participant.

A total of 32 participants took part in the study, with an equal number of male and female drivers. All participants held a valid driving licence and were aged between 25 and 65 years. Demographic characteristics, particularly gender and age, were therefore included as variables in the subsequent analysis. Table 8 summarises the composition of the sample and reports mean values and standard deviations for the main characteristics collected, including age, driving experience (in years and kilometres driven per year) and number of crashes. Participants were also grouped by gender and into three age categories to enable comparative analysis.

Table 8. Mean (M) and Standard deviation (SD) of participants characteristics.

	N.	Age [years]			Driving Experience [km/years]		Driving Experience [years]		Number of crashes	
		Min	M	Max	M	SD	M	SD	M	SD
Males	16	25	42.6	65	11088.2	7366	24.4	15.3	1.5	1.9
Females	16	25	39.4	58	10750	7143.4	21.4	12.5	1	1
25-35 years	13	25	27.2	33	6700	5597.2	9.5	2.9	0.2	0.4
36-52 years	10	36	44.5	52	11100	6208.4	26.4	5.4	2	2
53-65 years	9	53	59.8	65	17222.2	5651.9	41.1	7.3	2.3	1.7
Total	32	25	41.8	65	11034.4	7110.4	23.7	14.2	1.4	1.7

Several quantitative measures were adopted to analyse interactions between drivers and vulnerable road users (VRUs), using a set of established surrogate safety measures (SSMs) and behavioural indicators. For the first sub-experiment, three SSMs were selected to characterise driver-pedestrian interactions:

- Minimum Time-to-Collision (MTTC);
- Post-Encroachment Time (PET);
- Proportion of Stopping Distance (PSD).

MTTC was used to quantify the temporal proximity of conflicting road users on a collision course, with lower values indicating more critical interactions. PET measured the temporal separation between successive road users occupying the same conflict area. This allowed events to be classified as collisions, conflicts or undisturbed passages, based on established thresholds. PSD was employed to evaluate drivers' ability to stop safely in response to pedestrian crossings by comparing the available stopping distance with the minimum acceptable stopping distance, given the vehicle's speed and deceleration limits.

Additionally, a binary variable (Stop_NoStop) was introduced to identify instances where drivers stopped to give way to pedestrians, enabling a clear distinction to be made between stopping and non-stopping behaviours in various pedestrian interaction scenarios.

In the second sub-experiment, MTTC and PET were used again to assess the severity of transversal driver-pedestrian interactions. For longitudinal driver-cyclist interactions, overtaking behaviour was analysed by measuring the overtaking speed (Over_Speed) and the minimum lateral distance (min_distance) between cars and bicycles. The overtaking speed is defined as the average vehicle speed during the passing manoeuvre while the minimum car-bicycle distance was calculated during overtaking using a simplified geometric representation of both vehicles as indicated in Figure 41.

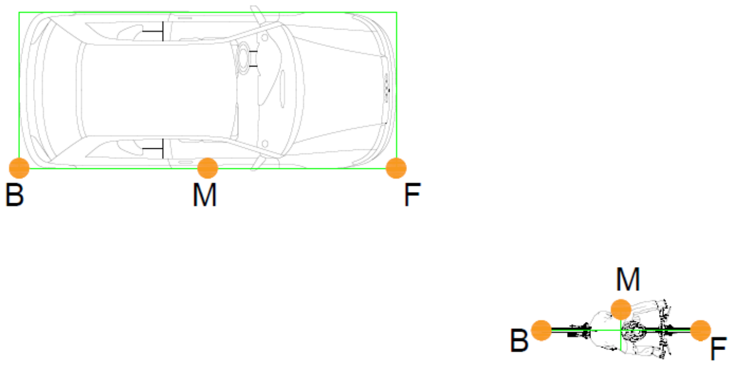

Figure 41. Vehicle and bike shapes schematisation and key point representation, in which B corresponds to the rear edges, M corresponds to the vehicle side midpoint and the cyclist's elbow, and F is referred to the front edges. During each overtaking manoeuvre, distances between all combinations of these points were computed, and the minimum value was selected as the representative car-bicycle distance.

The effects of the experimental factors on the measured variables were estimated using linear mixed-effects models (LMMs) fit by maximum likelihood. This approach is well suited to experiments involving repeated measurements, as it can handle both categorical and continuous variables while accounting for variability between individuals through random effects.

For analysing the binary outcome variable "Stop_NoStop", a logistic regression model was adopted. This method is appropriate for assessing the probability of an event occurring and allows both categorical and continuous predictors to be included.

3.2 Driving simulation experiments of *Corso Vittorio Emanuele II* – Corso Castelfidardo intersection

3.2.1 Introduction

This experiment evaluated the vehicle-cyclist interactions at the urban intersection formed by *Corso Vittorio Emanuele II*, *Corso Castelfidardo* and *Corso Inghilterra* in Turin. This intersection is part of the *Corso Vittorio Emanuele II* corridor arranged as a multi-carriageway section, comprising a central roadway with two lanes in each direction for higher speed through traffic and two lateral service roads for local access. These components are physically separated by tree-lined medians and kerbs, resulting in a complex yet clearly structured road system for motor vehicles. In this intersection the configuration of the cycling infrastructure is quite complex and characterised by a pronounced geometric asymmetry: in some areas, cyclists are provided with dedicated, protected paths; in others, they are directed onto indirect routes with chicanes, or must merge abruptly into shared lanes. This discontinuity undermines the predictability of the intersection environment and does not align with the principles of a self-explanatory road, since the available cues do not consistently guide users towards intuitive interpretations of flow direction and priority. Consequently, the absence of clear, coherent design guidelines can generate uncertainty regarding right-of-way and anticipated manoeuvres, creating favourable conditions for the vehicle-cyclist conflicts highlighted in the previous section.

Moreover, the crash analysis identified two main cluster of crashes between vehicles and bicycle. In the first cluster (Figure 42-A), collisions were consistently front-side and concentrated in a highly specific area. The typical triggering mechanism was a vehicle executing a left-turn manoeuvre that intersected the cyclist's trajectory. In the second pattern (Figure 42-B), the crash configuration remained front-side, but the triggering mechanism was more strongly linked to cyclist behaviour. Several cases involved cyclists not complying with traffic signals or stop controls, thereby creating an unexpected conflict with a vehicle.

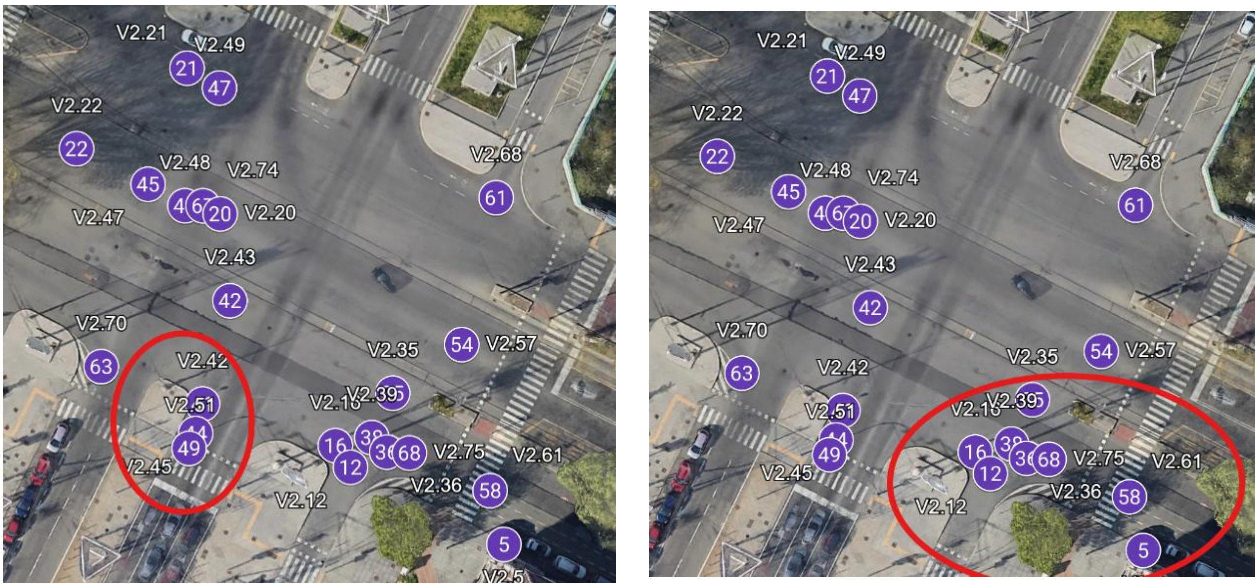

(A) (B)

Figure 42. Clusters of crash events in Corso Vittorio Emanuele II – Corso Castelfidardo intersection: (A) first cluster, (B) second cluster.

3.2.2 Simulated road scenario

The intersection was recreated in a driving simulation environment using SCANeR Studio (AVSimulation). The virtual model was developed using cartographic sources and satellite imagery to accurately reproduce the road layout and surrounding urban setting, including elements such as lane widths, curvature, pavement markings, buildings, and other contextual features that contribute to the realism of the scenario (Figure 43). Before finalising the model, an on-site observation campaign was carried out to collect information that could not be reliably derived from static aerial data. This fieldwork involved measuring the duration of the red, yellow and green phases for different movements in order to document the signal timings, and also involved observing how vehicles typically enter and clear the junction in order to support the calibration of background traffic. Particular attention was devoted to cyclist behaviour, since this directly influences the conflict scenarios investigated in the study. The observations revealed that when the bicycle facility is not straightforward, but instead comprises S-curves or chicanes, cyclists often deviate from the marked alignment, opting for a more direct, linear route through the intersection instead.

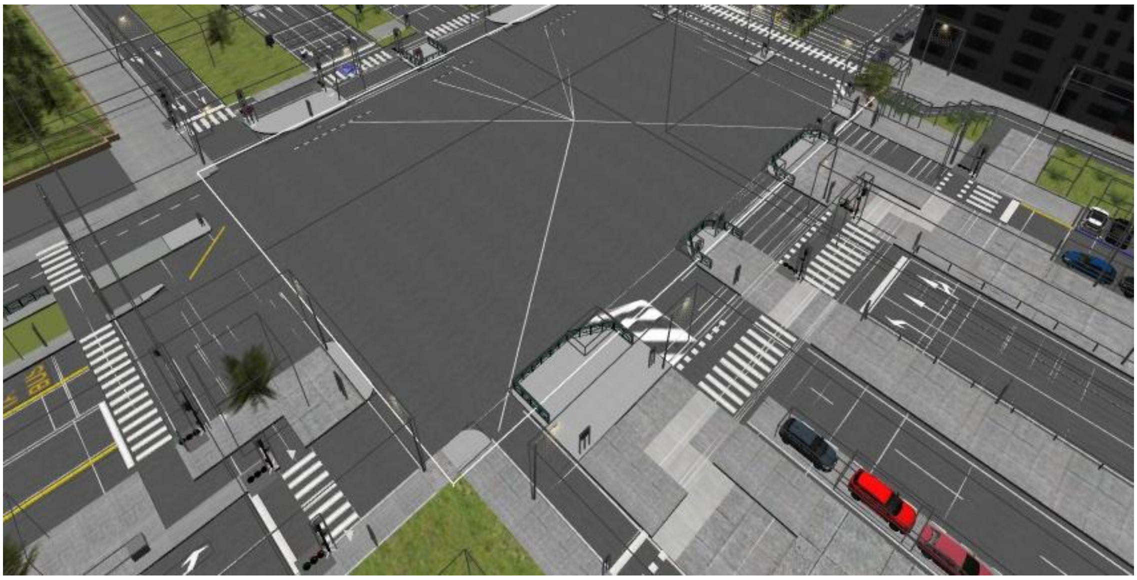

Figure 43. Virtual reconstruction of the studied intersection

To evaluate the safety implications of the infrastructure design, two intersection configurations were implemented in the simulator. The first scenario reproduced the existing conditions, maintaining the current geometric characteristics and related issues identified in the analysis. The second scenario represented a countermeasure based on a geometric redesign intended to make the bicycle layout consistent and symmetric across the entire intersection. In this alternative configuration, cyclists are provided with a dedicated, protected crossing placed alongside the pedestrian crossing, with straight trajectories that align with the protected lanes on the side roads. This removes the indirect chicane segments that contribute to uncertainty in the current layout. Although the redesign applies to the entire intersection, the expected benefits differ depending on the manoeuvre considered. For the first critical manoeuvre, the intervention removes the chicane to improve symmetry and reduce ambiguity about the intended cyclist path. From the driver's perspective, the redesigned, signal-controlled bicycle crossing increases the visibility of the conflict area and enables potential interactions to be recognised earlier. Additionally, by reducing the distance between the stop line and the conflict point, the redesign tends to limit vehicle speed at the critical location since drivers have less space to accelerate before reaching the crossing.

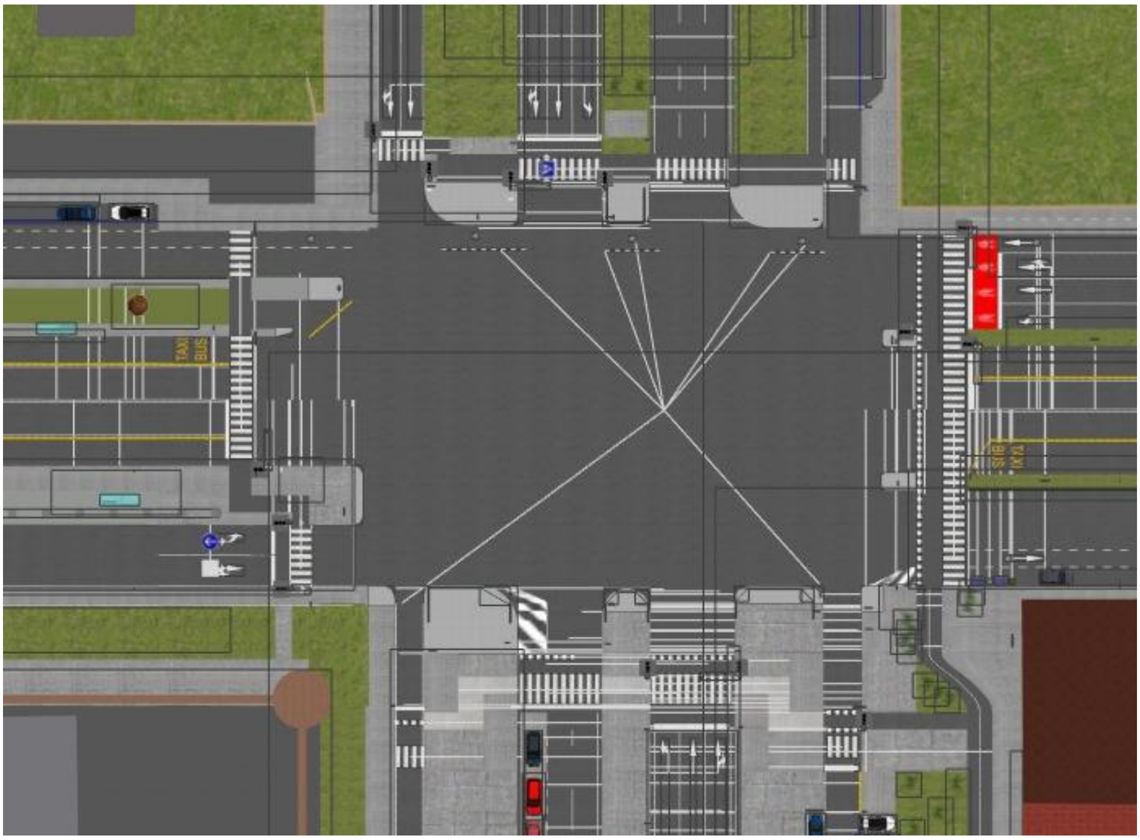

(A)

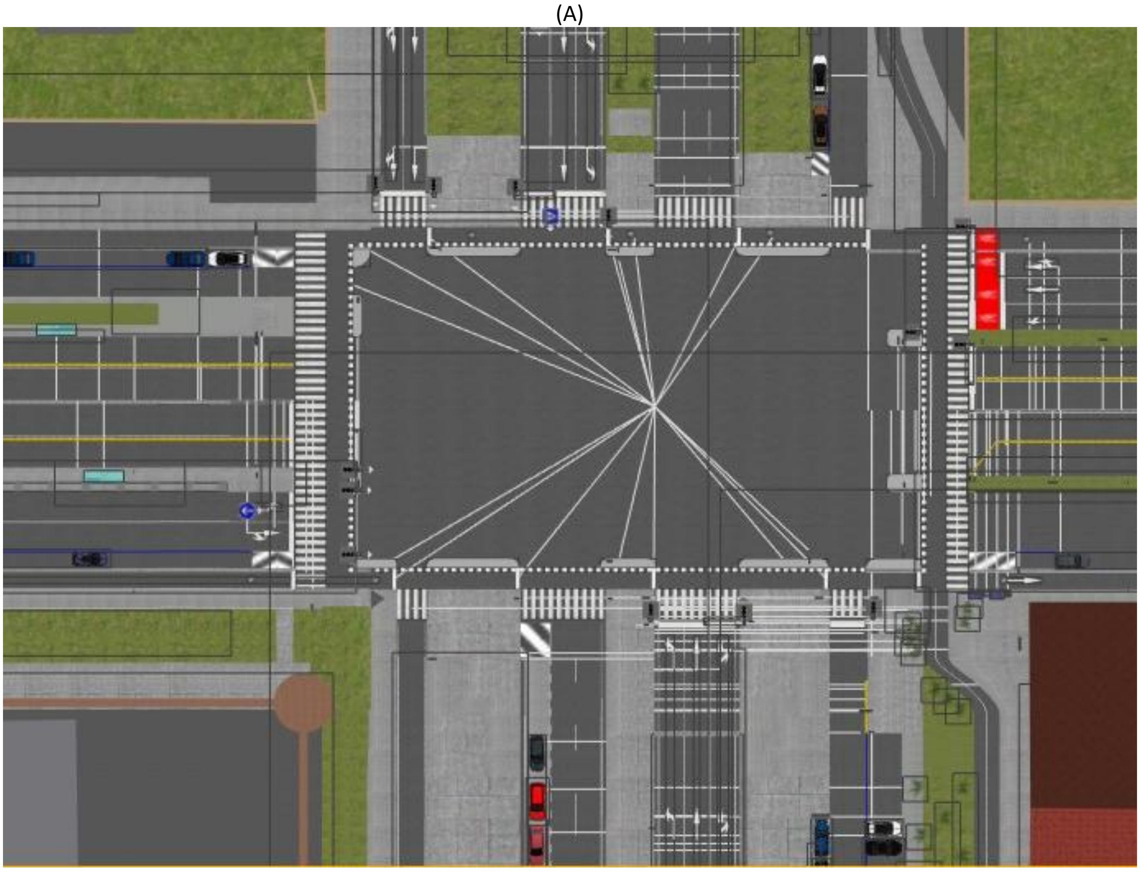

(B)

Figure 44. Comparison between (A) actual intersection configuration and (B) intersection with the countermeasure.

3.2.3 Experimental design

The analysis of the different types of conflict emerging from the identified crash clusters was divided into three separate manoeuvres. Each manoeuvre addressed a different conflict situation and involved a different group of participants. A between-subjects approach was adopted for the manoeuvre variable, meaning that each driver performed only one manoeuvre. Within each manoeuvre scenario, the experimental conditions were organised using a standard two-level factorial design in experimental statistics, enabling the simultaneous assessment of multiple factors and their influence on outcomes. This design was used to quantify the effects of three key safety-related variables:

- intersection layout (comparing the current configuration with the redesigned countermeasure);
- cyclist behaviour (represented through two speed profiles: aggressive at 20 km/h versus prudent at 8 km/h);
- lighting conditions (comparing day and night driving environments).

Combining these three factors results in eight distinct scenario variants for each manoeuvre (Table 9). Running all eight scenarios for every participant, in addition to the familiarisation and training drives, would have resulted in excessive repetition, increasing the risk of fatigue and potentially biasing behavioural responses, thereby reducing the reliability of the data. To limit this effect, the study applied a blocking strategy in which the eight scenarios were split into two balanced sets of four. The allocation to blocks followed a statistically controlled structure rather than a purely random split to ensure that the experimental design remained mathematically balanced. Participants were then randomly assigned to one of the two blocks, meaning each driver experienced only half of the full set of scenarios (Table 10). As the design preserves orthogonality, the main effects of the factors can still be estimated across the full sample by combining data from both blocks, even though individual participants completed only four scenarios.

Table 9. Scenarios generated by the combination of factors.

Manoeuvre	Factor A	Factor B	Factor C	ID Scenario
1	Real	Aggressive	Day	1.1
			Night	1.2
		Prudent	Day	1.3
			Night	1.4
	Countermeasure	Aggressive	Day	1.5
			Night	1.6
		Prudent	Day	1.7
			Night	1.8
2	Real	Aggressive	Day	2.1
			Night	2.2
		Prudent	Day	2.3
			Night	2.4
	Countermeasure	Aggressive	Day	2.5
			Night	2.6
		Prudent	Day	2.7
			Night	2.8
3	Real	Aggressive	Day	3.1
			Night	3.2
		Prudent	Day	3.3
			Night	3.4
	Countermeasure	Aggressive	Day	3.5
			Night	3.6
		Prudent	Day	3.7
			Night	3.8

Table 10. Blocking generation (w = woman; m = man)

Manoeuvre	Block	Factor 1 A:A	Factor 2 B:B	Factor 3 C:C	ID Scenario	Participants		
1	1	1	1	-1	1.2	4w+4m	8w+8m	24w+24m
		-1	-1	-1	1.8			
		-1	1	1	1.5			
		1	-1	1	1.3			
	2	1	1	1	1.1	4w+4m		
		1	-1	-1	1.4			
		-1	-1	1	1.7			
		-1	1	-1	1.6			
2	1	1	1	-1	2.2	4w+4m	8w+8m	
		-1	-1	-1	2.8			
		-1	1	1	2.5			
		1	-1	1	2.3			
	2	1	1	1	2.1	4w+4m		
		1	-1	-1	2.4			
		-1	-1	1	2.7			
		-1	1	-1	2.6			
3	1	1	1	-1	3.2	4w+4m	8w+8m	
		-1	-1	-1	3.8			
		-1	1	1	3.5			
		1	-1	1	3.3			
	2	1	1	1	3.1	4w+4m		
		1	-1	-1	3.4			
		-1	-1	1	3.7			
		-1	1	-1	3.6			

The simulated conflict situations were reconstructed to closely match the crash dynamics identified in the cluster analysis and the behaviours observed during fieldwork. Each manoeuvre represents a specific pattern of interaction between the driver and the cyclist, with defined trajectories and trigger conditions that reflect the most common and consistent conflict mechanisms at the study intersection.

In the manoeuvre 1, the participant drives along *Corso Castelfidardo*, approaching the junction in the left-hand lane with the intention of turning left at the traffic lights to enter *Corso Vittorio Emanuele II* towards *Piazza Rivoli*. A conflict then emerges with a cyclist travelling perpendicular to *Corso Vittorio Emanuele II*, moving from one side road to the other towards *Porta Nuova* railway station. Here cyclists do not follow the designed chicane alignment, instead they proceed on a direct, straight trajectory and ignoring both the bicycle markings and the traffic signal. Figure 45 shows the simulated critical car-bicycle interaction where a cyclist proceeding on straight trajectory during the green phase that authorises the driver to turn left.

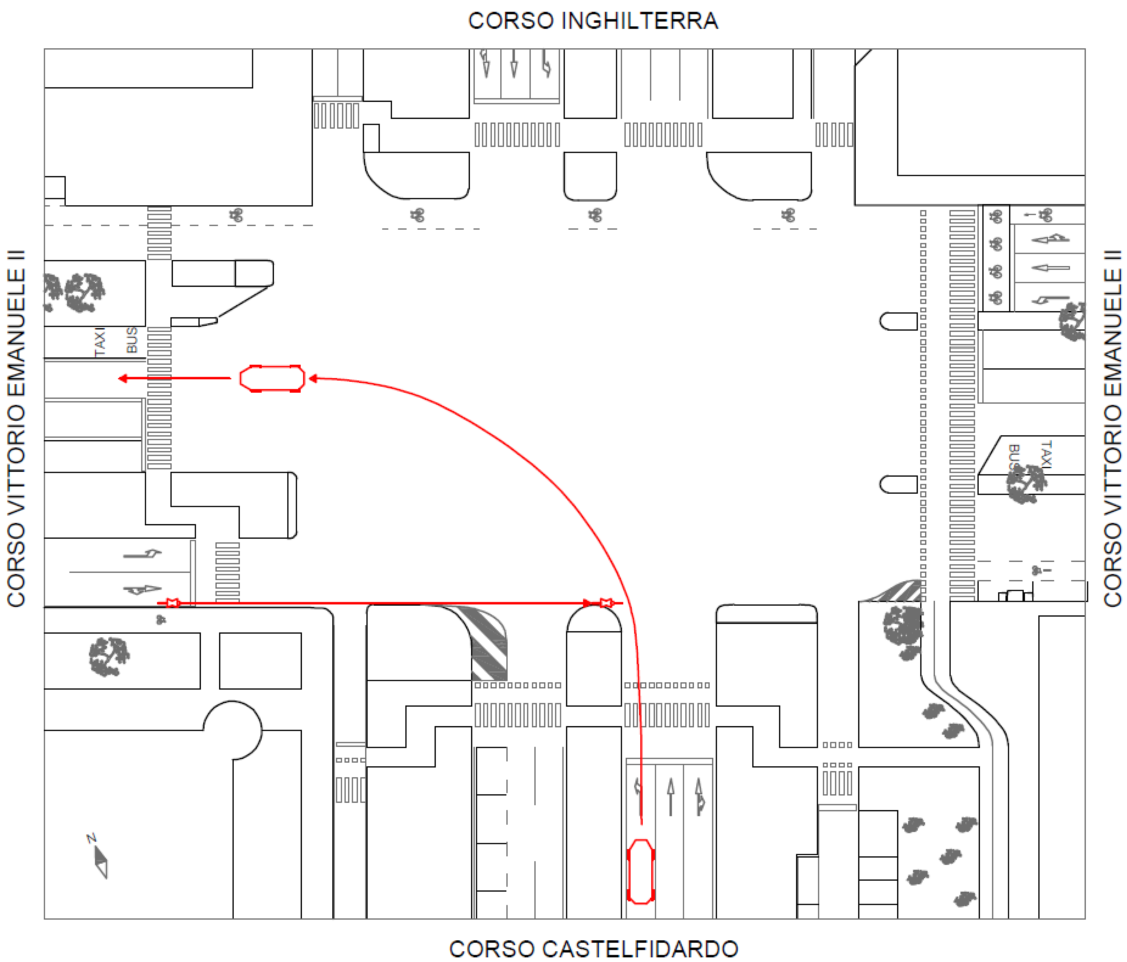

Figure 45. Manoeuvre 1 scheme.

The manoeuvre 2 simulates the left-turn crossing interaction observed in second road crash cluster. Here, the driver approaches from *Corso Inghilterra* intending to turn left into the side road of *Corso Vittorio Emanuele II* towards *Porta Nuova* railway station. The operational conditions are designed to replicate the local signal settings, in which the green interval for the manoeuvre is short and the stop line is positioned several metres before the intersection. This combination may encourage drivers to accelerate to complete the manoeuvre before the traffic light phase ends. A cyclist initiates the conflict by accelerating from the corner area between *Corso Vittorio Emanuele II* and *Corso Castelfidardo* and entering the bicycle crossing to reach the opposite side. The cyclist runs the red light under the assumption that the intersection is clear and crosses the vehicle path at the most critical moment (Figure 46).

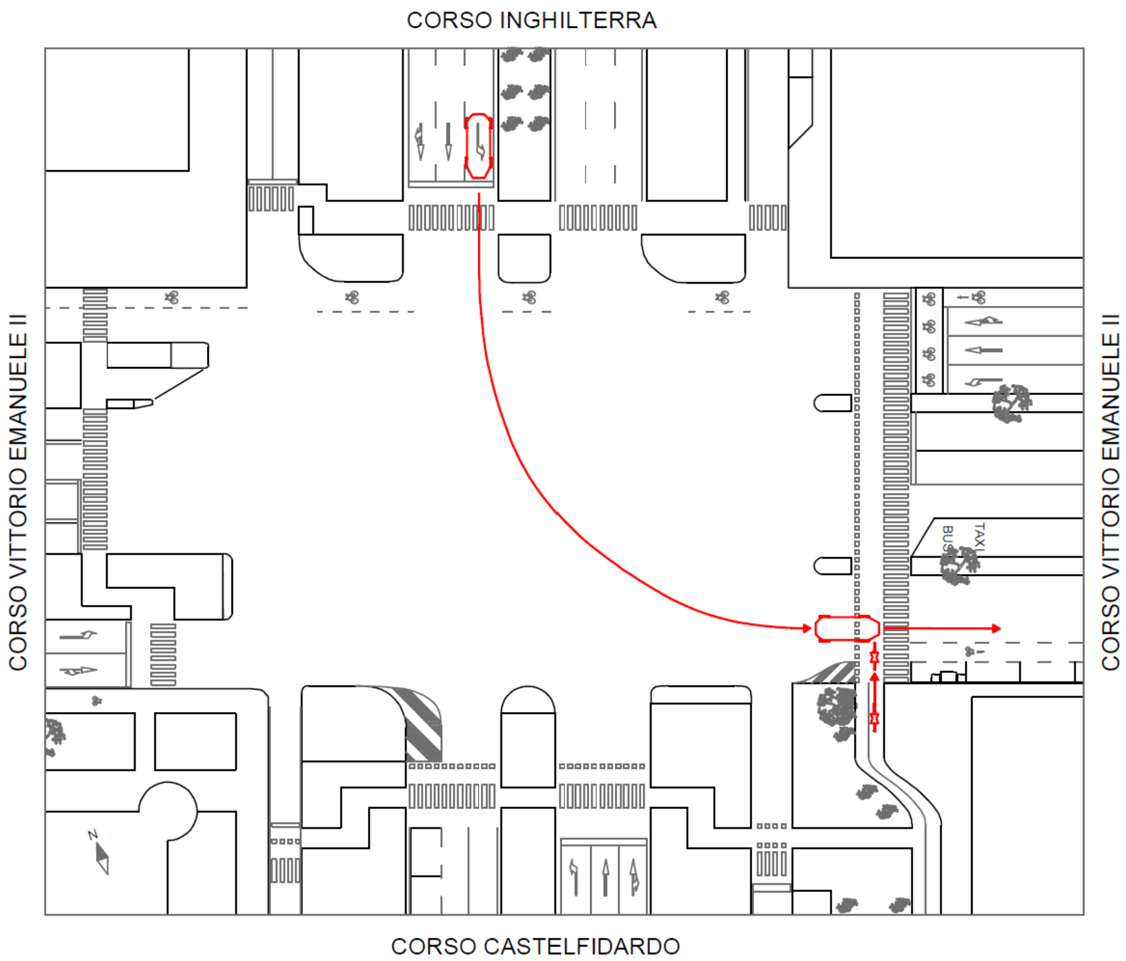

Figure 46. Manoeuvre 2 scheme.

The manoeuvre 3 addresses another behaviour linked to second road crashes cluster. In this scenario, the participant drives along the side road of *Corso Vittorio Emanuele II* towards Porta Nuova railway station. Before the intersection the side road is not shared with bicycles, while after it becomes a car-cyclist shared lines. A conflict occurs when a cyclist coming from *Corso Castelfidardo* needs to merge into the shared lane.

Rather than using the designed chicane, the cyclist takes a shortcut through the parking strip separating the cycle lane from the pavement. This results in a sudden and unprotected entry into the traffic lane, directly in front of the coming vehicle (Figure 47).

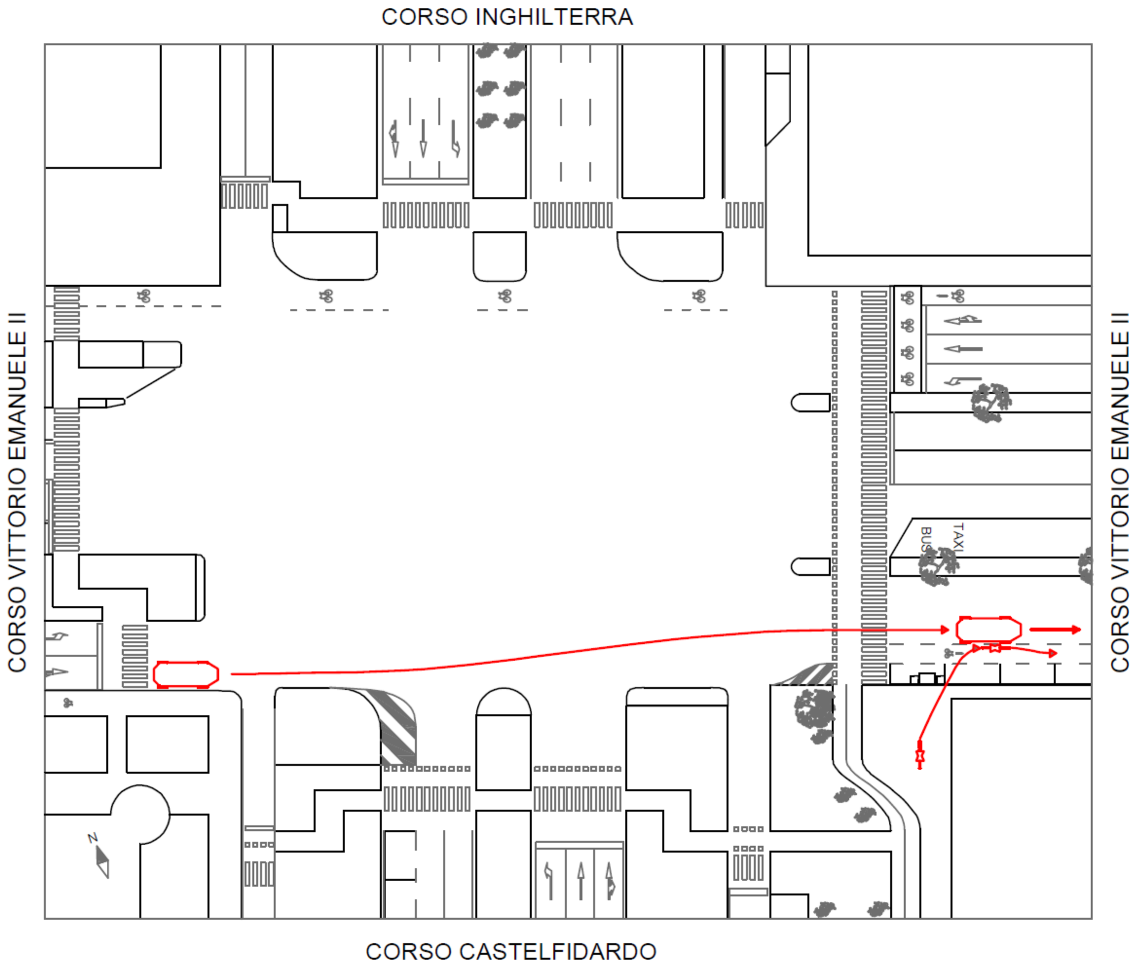

Figure 47. Manoeuvre 3 scheme.

Figure 48, Figure 49, and Figure 50 show a comparison of the actual road configuration with the countermeasure scenario for each of the three simulated conflicting points (manouvers).

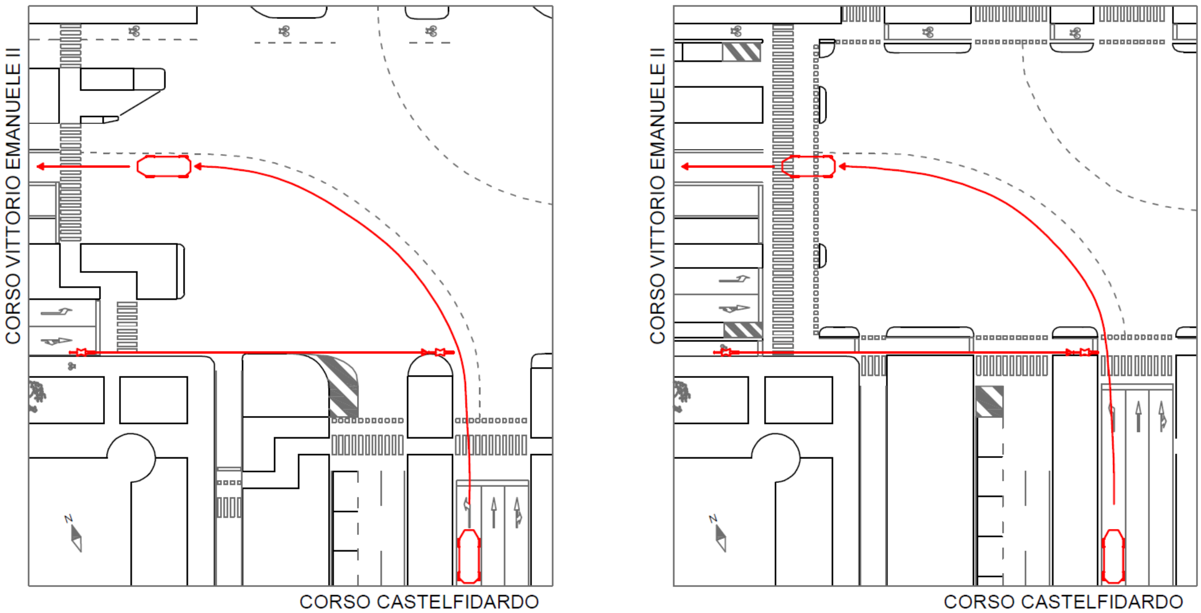

(A) (B)

Figure 48. Comparison of manoeuvre 1 in (A) actual road configuration and (B) countermeasure scenario.

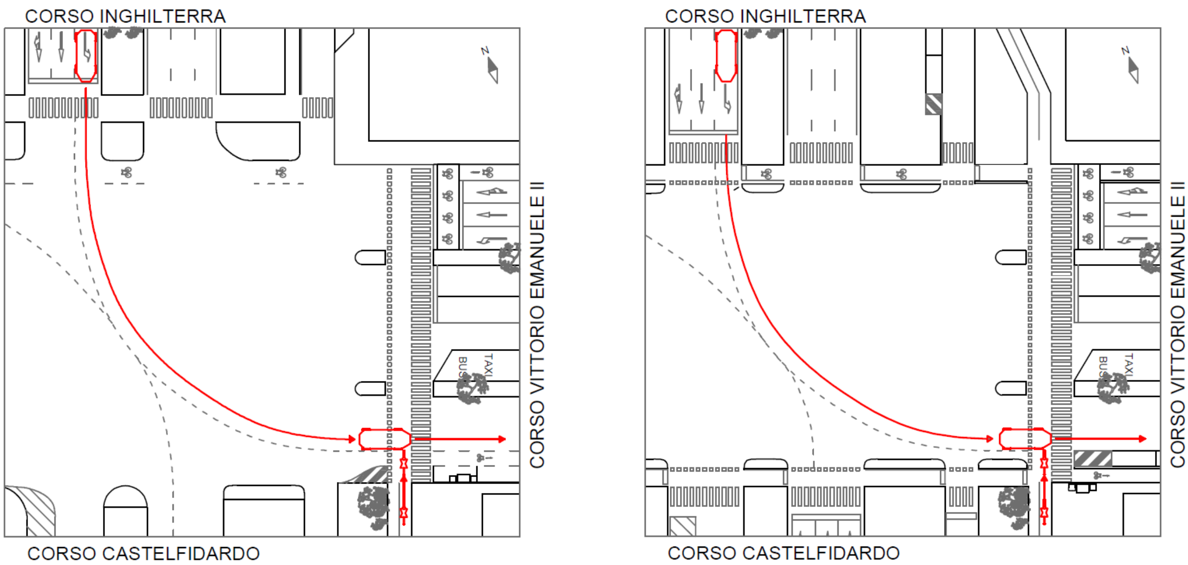

(A) (B)

Figure 49. Comparison of manoeuvre 2 in (A) actual road configuration and (B) countermeasure scenario.

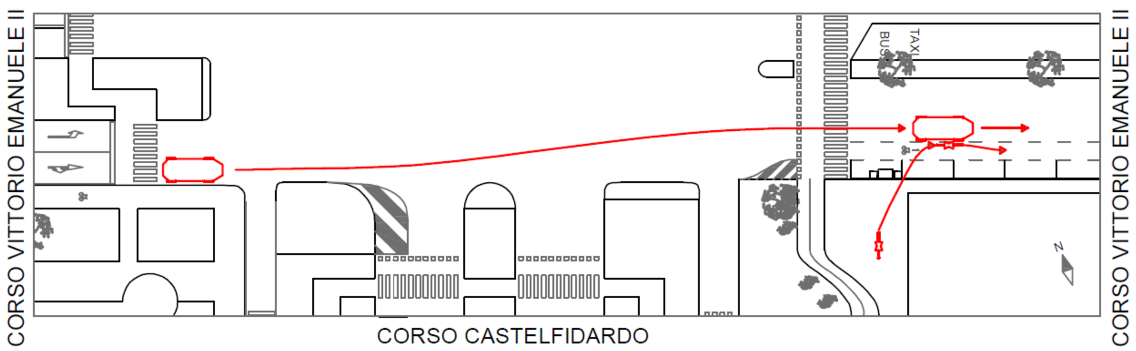

(A)

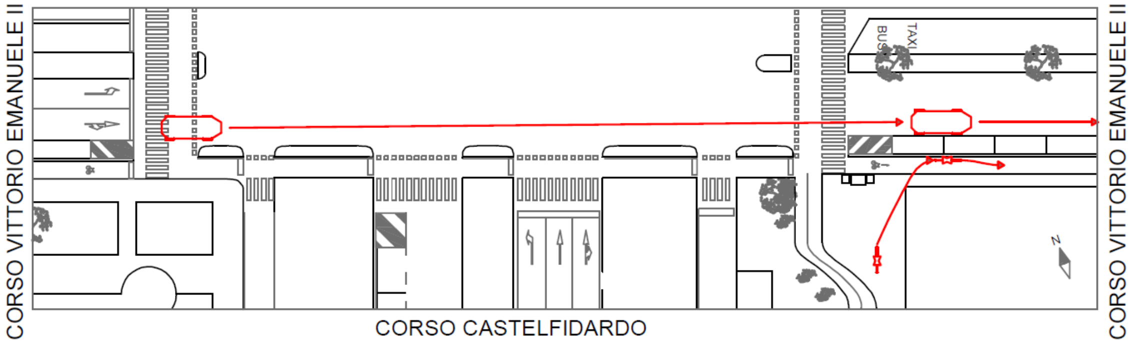

(B)

Figure 50. Comparison of manoeuvre 3 in (A) actual road configuration and (B) countermeasure scenario.

3.2.4 Experimental protocol, participants and measured variables

The experimental protocol was divided into four consecutive phases. Prior to attending the road safety laboratory, participants were enrolled remotely and asked to complete an online pre-drive questionnaire. This initial step collected demographic information, driving style and behavioural traits that could impact safety-related responses. Once participants arrived at the laboratory, the pre-simulation phase began with the completion of informed consent and privacy documentation. They then received a short briefing on how to operate the driving simulator, including information about possible discomfort or simulator sickness. They then completed a training drive to become familiar with the steering wheel and pedal sensitivity.

During the simulation phase, participants were introduced to the manoeuvre they were required to perform, after which they drove through the scenarios they had been randomly assigned. After each scenario, they completed the NASA-TLX questionnaire to report their perceived mental workload while performing the driving task in that specific condition. Finally, in the post-simulation phase, participants completed the Simulation Sickness Questionnaire.

A total of forty-nine participants took part in the study. Sixteen drivers were assigned to each of the three manoeuvres, and an additional participant was included in Manoeuvre 3. To ensure a diverse sample, recruitment was balanced by gender, resulting in 25 men and 24 women (Table 11). Participants were also grouped by age into two categories. Around half of the sample were classified as “junior” drivers, aged 37 years or younger, while the rest were “senior” drivers, aged 38 years or older. All participants held a valid driving licence. For the experimental trials, each driver was assigned a randomly selected sequence of scenarios drawn from the predefined blocks described earlier.

Table 11. Summary of total participants (SD = standard deviation)

		Age		Driving experience (years)	
Gender	**Number of drivers**	**Mean**	**SD**	**Mean**	**SD**
Men (M)	25	38.9	11.6	20.5	11.6
Women (W)	24	37.3	10.9	37.3	10.9

Considering that each conflict differs in terms of geometry, timing and driver task demands, safety performance was quantified using manoeuvre-specific indicators. For this reason, the set of observed variables was tailored to the risk mechanisms underlying each manoeuvre.

In manoeuvre 1, where the dominant risk is a potential side impact when the ego vehicle accelerates through the turn, safety was primarily captured by the minimum TTC (MTTC) between the ego vehicle and the cyclist. This core indicator was complemented by ego vehicle speed at the interaction point, steering correction magnitude as a proxy for control effort and evasive response occurrence. Evasive behaviour was coded as a binary outcome to determine whether an avoidance action occurred. It was then characterised by its form to distinguish between braking, steering, a combined response or no evasive action, to reflect the driver's instinctive reaction to the conflict.

In manoeuvre 2, the MTCC and the speed at the conflict point (*speed_cp*) were used as key safety indicators. However, an additional variable was introduced to describe the speed management of the drivers, expressed as the difference between the maximum speed achieved within the intersection and the speed at the conflict location. This provided a measure of whether drivers reduced their speed before reaching the potential impact area.

The manoeuvre 3 involved a cyclist entering unexpectedly from an unconventional location, resulting in a conflict. Therefore, the selected indicators focused on rapid driver response and sudden speed changes. To maintain comparability across manoeuvres, the MTTC and conflict-point speed were used again, while speed variation was computed between the moment the vehicle entered the intersection and the conflict point. Due to the sudden nature of the event, peak deceleration at the conflict point was included as a key descriptor of the driver's reaction.

As the experimental design produced repeated observations from the same participants, the resulting dataset has a correlated structure, meaning that measurements within a driver are not independent. To account for this dependency and separate within-driver effects from between-driver variability, the primary analytical framework was based on LMM refined through a backward elimination process. Statistical significance was evaluated using a threshold of 0.05. All statistical analyses were performed in Jamovi software.

4 Simulation studies RU UniPD

4.1 Simulation Scenario

The riding simulation scenario was developed to accurately reproduce a real urban traffic configuration that had previously been identified as a hazardous road location (HRL). This identification was based on accident data analyses presented in Deliverable 1 and on field inspections documented in Deliverable 2, which highlighted a high level of conflict between motor vehicles and vulnerable road users. The selected scenario corresponds to the intersection between Via Gattamelata and Via Modena, located in the city of Padua. The choice of this site was further supported by stakeholder consultations conducted within the framework of the PRIN ARCADE research project (e.g., local traffic police), ensuring that the simulated environment reflects both empirical evidence and local expertise regarding critical safety issues.

Similarly to other RUs, this intersection geometry reflects the actual layout of the study area, with particular attention paid to lane widths, curb alignments, visibility constraints, and surrounding urban elements. Particular care was devoted to replicating the real spatial configuration that influences drivers' perception and decision-making processes, such as the presence of roadside obstacles. This detailed geometric reconstruction, enabled through the use of software such as Google Earth Pro and FormIt, ensured a high degree of ecological validity and allowed the simulator to reproduce realistic driving dynamics consistent with the actual intersection. To note, no parking areas are available in the surroundings of the selected intersection.

Via Gattamelata is an important road artery of the city, characterized by heavy traffic during peak hours (7:00 – 9:30; 17:30 – 20:00). This site possesses specific characteristics on the zebra crossing area, such as red-colored concrete in correspondence of the intersection and the pedestrian crossing area, covering the whole intersection between the two contiguous blocks. This area has no horizontal traffic signs (except for pedestrian crossings, both permanent and yellow-colored temporary crossings) and is provided with a feeble lightning system at night. Road separator curbs allow drivers only to turn right from each driving direction. Adjunctively, Via Gattamelata is provided with a red-colored non-separated bicycle lane from the vehicle lane with no road curbs. Bicycle lanes are identified by red concrete, but the color appears to be ruined by time and heavy traffic. At the intersection area, the road lane "merges" with the intersection-colored area, potentially causing a reduced identification on specific road users' lanes for pedestrians, cyclists and drivers. Overall, road lightning seems also limited during the night and there is no appropriate lightning system dedicated to pedestrian crossings and bicycle lanes (Figure 51, Figure 52, Figure 53).

Figure 51 - Streetview of the HRL selected from the Padua RU ("Gattamelata-Modena")

Figure 52 - Streetview of the HRL selected from the Padua RU ("Gattamelata-Modena").

Considering the features of the selected intersection, the analysis focused on evaluating the role of two specific road characteristics: (1) the absence of a dedicated separator between vehicle and bicycle lanes and (2) the absence of horizontal signage near pedestrian crossings.

To systematically assess the effectiveness of the related infrastructural safety measures, four distinct scenarios were implemented in the riding simulation: two representing the existing state of the intersection (control condition) and two incorporating the implementation of infrastructural countermeasures (experimental condition). Each condition was tested under two lighting conditions (daytime and nighttime),

Figure 53 - Streetview of the HRL selected from the Padua RU ("Gattamelata-Modena").

for a total number of riding scenarios equal to four.

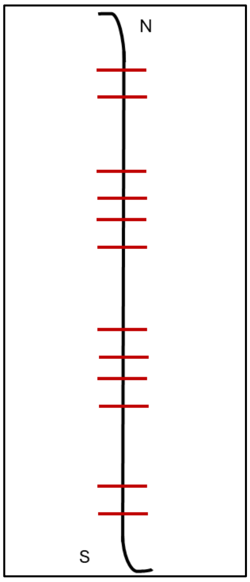

Figure 54 - graphical representation of the driving scenario

The scenario was developed in **Scaner Studio**, integrating building shapes imported from Google Earth Pro and additional objects (e.g., curbs) specifically created in FormIt. The same track was used for all four scenarios.

The total length of the track was **5449.723 m**, whereas the driver travelled 4762.106 m. Along the track, the driver encountered 24 crossing areas distributed across 12 road intersections (two per intersection, one for each contiguous block). In the graphical representation on the right (Figure 54), the horizontal red bars indicate the intersections.

Each intersection was located 250 m from the subsequent one, with three 784 m straight road segments dividing the four main intersection blocks. Each intersection reproduced the original layout: it was introduced by two triangular road separators, and, at the red-concrete intersection, the two roads were further divided by a rectangular curb acting as a road separator, allowing pedestrian crossings within each block.

The experiment required drivers to assume the perspective of a motorcyclist, simulating the riding activity on board of a **50cc motorcycle simulator**. Specifics about the simulator are provided in the following sections. Therefore, the focus was on motorcycle-cyclist interaction (at crossings and along the track) as well as on motorcycle-pedestrian interaction (at crossings).

4.1.1 Control and Experimental Condition

The two conditions differed in the presence of a bicycle-lane road separator along the entire track in the experimental condition (height = 0.40 m), as well as horizontal square signage near pedestrian crossings indicating permitted crossings for both pedestrians and bicycles at those locations.

Figure 51 Screenshot of the HRL in the simulation (Control-Day on the left; Experimental-Day on the right)

Each of the three scenarios was simulated under both **daytime** and **nighttime** lighting conditions. The inclusion of lighting variability allowed the analysis of the interaction between infrastructural design and environmental visibility, recognizing the significant role played by illumination in urban driving behavior and risk perception. Nighttime scenarios were calibrated to reproduce realistic lighting conditions in peak hours (8:30 am and 6 pm), in order to assess potential changes in gap acceptance, speed profiles, and safety margins with and without countermeasures.

Figure 52 - Screenshot from the driver perspective (Control-Day on the left; Experimental-Night on the right)

4.2 Instruments

4.2.1 The environment: welcome into the CAVE

The experiment took place in a **CAVE Automatic Virtual Environment** at the Department of General Psychology. The CAVE is equipped with a 180° curved screen (radius 370 cm, height 210 cm, ~18 m² projection area, acoustically transparent micro-perforated fabric) elevated 20 cm from the ground. It employs three Epson EB-L1050 ultra-short-throw laser projectors (WUXGA 1920x1200, 4K enhancement, >2,500,000:1 contrast) with warping and blending via an M-FRAME PRO3 processor, driven by an ASUS workstation (Intel i9-9900K, RTX 2080 Ti, 32 GB RAM) running Windows 10. The adjacent "Control Room" houses graphics generation, video processing, remote controls, four PTZ IR cameras for subject monitoring, and 5.1 surround audio. This immersive setup renders SCANeR Studio scenarios across the curved display for full perceptual realism, with the HRT positioned centrally.

Figure 57 - Picture of the experimental setting

4.2.2 The simulation: the Honda Riding Trainer and SCAnER Studio

The instrumentation used in this study consisted of the Honda Riding Trainer (**HRT**) motorcycle simulator, shown in Figure 57 and 58, integrated with the SCANeR Studio simulation environment in the CAVE. The Honda Riding Trainer (HRT) represents one of the core experimental tools in this study, used in combination with a virtual reality headset. Developed by Honda in 2005, the HRT is a compact, cost-effective, and transportable fixed motorcycle simulator originally designed for road safety education and to enhance riders' perceptual, attentional, and decision-making skills.

The simulator features a physical riding station that accurately reproduces the ergonomics of a real Honda motorcycle, including seat, handlebars, and realistic control devices such as throttle, brakes, clutch, turn indicators, headlight controls, and horn. A pedal unit is also provided, with pedals for clutch and braking. In this study, the simulator was operated in automatic riding mode, which disables the use of pedals and gear shifting to simplify vehicle control and reduce task complexity for participants.

Figure 538 - The Honda Riding Trainer (HRT) toolbar

The HRT is equipped with a front monitor that allows real-time visualization of the riding scenario. However, in this experimental setup, the monitor was used only by the operator for monitoring and managing the simulation. The riding scenario was rendered directly within the SCANeR Studio simulation software. SCANeR Studio is a modular simulation platform integrated with the Honda Riding Trainer in this study, enabling high-fidelity rendering of riding scenarios directly within its environment for enhanced immersion. It supports the development of faithful terrains with precise road geometries, behavioral dynamics scripting via built-in coding tools, and real-time communication with MATLAB Simulink to control driving parameters in stream - such as limiting speed to 60 km/h in this experiment to ensure consistency with the riding tool. This setup ensures realistic perceptual cues while simplifying scenario management in the CAVE.

4.2.3 Monitoring the heartbeat: Plux CardioBAN

Figure 59 - The PluX Cardioban BLE

The **cardioBAN BLE** is a compact wireless wearable (31x71x11 mm, 27 g) for real-time acquisition of single-lead ECG (±2.5 mV range) and motion data via integrated triaxial accelerometer (±8 g) and gyroscope (±500 dps) (Figure 59). It streams raw signals up to 1 kHz with 16-bit resolution over Bluetooth 5.1 (up to 10 m range), with internal memory for ~10 hours of logging and a rechargeable 155 mAh LiPo battery offering 10 hours of continuous use. Compatible exclusively with Biosignals Studio software, it includes a

Bluetooth dongle, USB cable, and disposable electrodes for comfortable, dynamic monitoring in research settings. This tool was used in the experiment to monitor cardiac activity along the experimental sessions, focusing on Heart Rate and Heart Rate Variability (HRV) in the time domain during presentations of pedestrian/cyclist crossings

4.3 Experimental Protocol

The experimental study was conducted following a standardized test protocol designed divided into multiple phases. The protocol was structured to ensure reliability, internal consistency, and comparability across different infrastructural configurations, lighting conditions, and interaction types, while minimizing learning effects and behavioral bias by randomizing experimental order.

4.3.1 Sampling and Briefing

Participant sampling targeted individuals holding a category B driving license, with at least one prior experience in riding a motorcycle and no major cardiac conditions that could affect data collection or interpretation. Eligible volunteers were contacted via email and invited to complete an online Qualtrics survey. The survey gathered sociodemographic information, driving habits, previous experience with different modes of transportation, prior exposure to extended reality (XR) technologies, and potential susceptibility to simulation sickness (e.g. travel sickness, major visual problems). Participants also completed the Mind Reading Belief Scale (Realo et al., 2003; Sangiuliano Intra et al. 2018), the Driving Behavior Questionnaire (Reason et al., 1990; Smorti & Guarnieri, 2016), and the Barratt Impulsiveness Scale (Fossati et al., 2001; Patton et al., 1995), providing a comprehensive profile of their cognitive, affective, and behavioral characteristics relevant to the experimental aims.

4.3.2 Experimental phase, familiarization, riding scenario and riding tasks

The experimental protocol consisted of two sessions on separate days, spaced at least 72 hours apart. To align with laboratory availability and participants' schedules while respecting circadian rhythms, daytime riding scenarios were conducted during daylight hours, and nighttime scenarios in the late afternoon. On the first day, participants were welcomed at the Department of General Psychology and escorted to the CAVE laboratory, where they were introduced to the virtual environment. They first read and signed an informed consent form, with the right to withdraw at any time without explanation. Participation was voluntary and uncompensated (no financial reward or academic credits). Baseline measures were then collected, including state levels of depression, anxiety, and stress (DASS-21; Bottesi et al., 2015; Lovibond & Lovibond, 1995) and simulation sickness (SSQ; Balk et al., 2013; Kennedy et al., 1993). Each participant was then assigned a unique alphanumeric code to ensure data anonymization thereafter.

General information about the experimental procedure was then detailed to the participant, who was free to ask questions or seek clarification as needed. Afterwards, the cardioBAN BLE was positioned along the left midclavicular line, below the left clavicle. This placement was selected to minimize invasiveness across participants of different genders and sensitivities. Once the experiment introduction and cardioBAN installation were complete, the experimenter left the room and moved to the control room, where they could control the simulation, monitor participant activity, and—if needed—communicate with the participant. A dedicated **familiarization phase** was conducted prior to data collection to allow participants to adapt to the simulator environment, vehicle dynamics, control responsiveness, and visual immersion. During this phase (≈ 5 mins), drivers completed a practice route not included in the experimental dataset, featuring urban road segments without critical interaction events. The familiarization phase was considered complete once the participant demonstrated stable vehicle control and reported adequate comfort with the HRT simulator.

After the familiarization phase, 3 minutes of **heartbeat baseline** recording were collected to stabilize the cardiac signal before any experimental stimulation. This good practice was performed before both the first and second riding scenarios each day. As anticipated, each participant completed two riding scenarios per session, balanced across daytime (day or night in the simulation). The order of scenarios was assigned pseudorandomly to ensure balance across scenario types (day/night and control/experimental), then inverted for the second session. For example, if a participant began with the Control-Day scenario followed by Experimental-Day on the first day, they would start with Experimental-Night and conclude with Control-Night on the second day.

The riding activity required participants to ride a 50cc motorcycle through an urban environment, constructed by combining twelve instances of the same Hazardous Road Location (HRL). The track followed the structure depicted in Figure 54, sequencing HRLs along a straight four-lane road (two lanes per direction). To reduce familiarity effects, six of the twelve HRLs were rotated 180°, allowing participants to approach them from both directions without requiring return trips via curves or roundabouts. This design minimized the risk of simulation sickness in the CAVE environment, as prior studies and pilot tests had demonstrated the need to control for this potential confound.

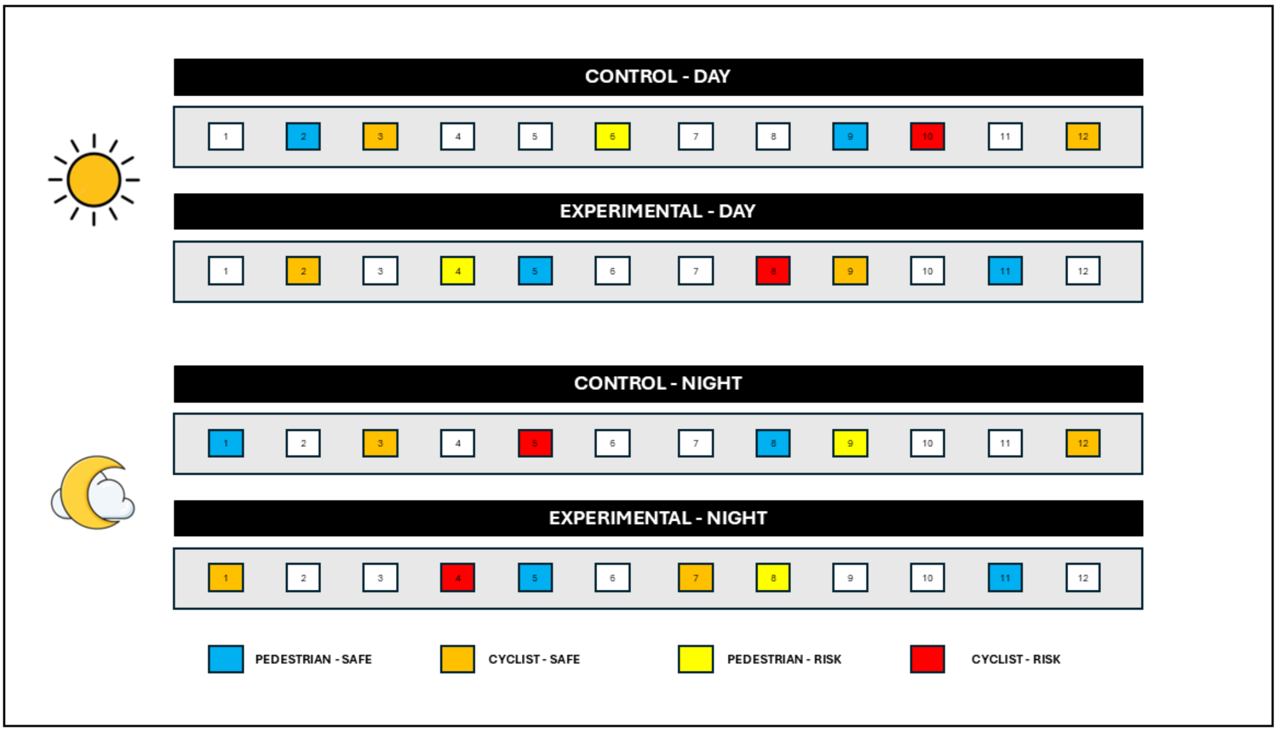

Figure 60 - Graphical representation on the randomization of crossing events across the four riding scenarios.

The reference track remained consistent across all riding scenarios, but riding direction (north to south or vice versa) varied within daytime conditions, and pedestrian/cyclist crossings were positioned at different intersections across scenarios. Figure 60 illustrates crossing locations for each scenario using a color-coded scheme. In each scenario, participants encountered six right-side crossings at designated areas—three by pedestrians and three by cyclists—with one of each type designated as "risky" based on parameters detailed below, yielding four "safe" and two "risky" crossings overall. Crossings occurred when the calculated Pedestrian Time Gap Acceptance (PTGA) between the vulnerable road user (VRU) and the rider exceeded a predefined PTGA threshold. This allowed us to use the **minimum Time to Contact (TTC)** as a reliable risk indicator in the investigation of the motorcyclist-pedestrian/cyclist interaction at crossings. The PTGA thresholds and crossing speeds used in this study are presented in Table 12.

Table 12 - PTGA thresholds and crossing speeds per type of crossing

VRU	PTGA threshold	Crossing speed
Pedestrian		
Safe crossing	**5,50 sec**	**3,56 km/h**
Risky crossing	**3,75 sec**	**4,00 km/h**
Cyclist		
Safe crossing	**5,25 sec**	**7,50 km/h**
Risky crossing	**3,50 sec**	**8,50 kh/h**

The four scenarios were populated with low-to-medium motorized traffic (e.g., buses, vehicles, motorcycles), particularly in the oncoming direction relative to the participant's travel. Importantly, medium-density traffic was imposed on the bicycle lane to examine the impact of the longitudinal road separator on **Standard Deviation of Lateral Position (SDLP)** and, consequently, cyclists' safety. At the same time, the virtual environment was populated with pedestrians along the crosswalks, who lacked the ability to cross the road in order to avoid unpredictable simulation events apart from the predefined experimental stimuli.

Throughout each scenario, participants were instructed to drive along the track as they would in a real urban environment, reacting to road events accordingly. They retained active control of brakes, throttle, and accelerator, with maximum speed limited to 60 km/h via a dedicated Simulink model. Each scenario took approximately 6–7 minutes to complete on average. After finishing the first riding activity, participants completed the Qualtrics survey again, including the NASA-TLX (Hart, 2006) and SSQ. The protocol then proceeded identically for the second scenario: a new heartbeat baseline was recorded, followed by the riding task and final questionnaires assessing NASA-TLX, SSQ, and Sense of Presence (IPQ; Himmels et al., 2020; Schubert et al., 2001) to evaluate immersion and involvement in the virtual environment.

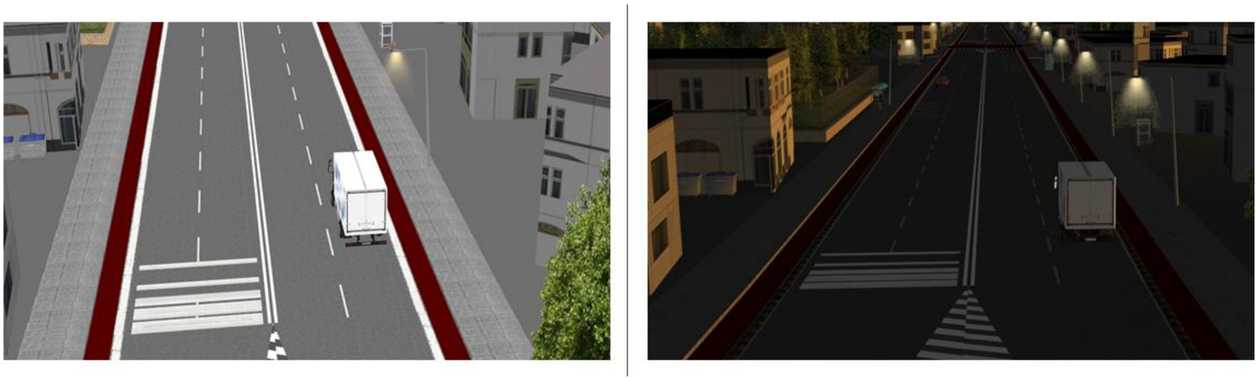

Figure 61: Screenshots from the virtual environment (Control-Day on the left, Experimental-Night on the right)

At the end of the first session, no specific information about the project's aims was provided to participants. In contrast, a full debriefing was conducted at the conclusion of the second session—at least three days after the first and structured identically—during which participants were informed about the study's specific objectives and the broader aims of the ARCADE project.

4.3.3 Parameters of interest

The **Minimum Time to Collision (MinTTC)** serves as a key surrogate indicator of risky interactions between motorcyclists and pedestrians/cyclists at crossings, representing the shortest time at which a collision would occur if their current speeds and trajectories remain unchanged. Lower MinTTC values signal heightened collision risk, reflecting closer proximity and reduced safety margins during VRU crossings. In this study, varying Pedestrian Time Gap Acceptance (PTGA) thresholds directly modulates crossing initiation (see Table

1): shorter PTGA prompts earlier, riskier crossings (yielding lower MinTTC), while longer PTGA delays crossings for safer gaps (higher MinTTC), enabling a more precise control over interaction dynamics and behavioral responses.

The **Standard Deviation of Lateral Position (SDLP)** serves as a reliable surrogate measure of motorcyclist-cyclist interaction risk along the track, quantifying lane-keeping variability and potential lane incursions toward the bicycle lane. Elevated SDLP indicates unstable steering and greater proximity to cyclists, signaling heightened collision risk under divided-road conditions. In this study, the road separator's presence is hypothesized to promote more stable trajectories—keeping motorcyclists farther from the bike lane—resulting in reduced SDLP, whereas control scenarios without separators should elicit larger SDLP due to unconstrained lateral drift and reduced perceived barriers.

Heart Rate (HR) and Heart Rate Variability (HRV), extracted from Cardioban ECG signals serve as robust psychophysiological indicators of stress and autonomic activation during motorcycle riding. HR elevations reflect sympathetic nervous system arousal in response to stressors like risky VRU crossings, while reduced HRV (particularly in time-domain measures) signals autonomic imbalance, cognitive load, and diminished vagal tone under high-demand conditions. In this study, these metrics captured real-time emotional and physiological responses to experimental manipulations (e.g., PTGA variations), enabling differentiation between safe and risky events. Analysis windows were applied post-baseline stabilization to isolate scenario-specific changes, providing objective evidence of activation beyond subjective reports.

4.4 Participants

28 individuals participated in this study (13 women), all holding a valid category B driving license. Participants, drawn from adults and young adults in the academic communities of the Department of General Psychology and Department of Developmental Psychology at the University of Padua (50% undergraduate/graduate students, 50% researchers/professionals), had a mean age of 27.8 years (SD = 4; range: 20–34). They averaged 19.2 years of education (SD = 2.2; range: 15–24) and had held their B license for 8.82 years on average (SD = 4.28; range: 2–16). Weekly, 71% drove a four-wheeled vehicle ≥3 times, 75% rode a bicycle ≥3 times, but 50cc motorcycle use was rare overall. Lifetime road accidents included 14% as pedestrians (n=4), 32% as four-wheeled drivers (n=9), 57% as passengers (n=16), and 18% as cyclists (n=5). Only 7% (n=2) had no prior extended reality (XR) experience, and 11% (n=3) reported side effects from XR systems. No participants had neurological or cardiac disorders incompatible with simulator use, though 32% noted eyesight issues, 21% headaches/migraines, and 21% travel sickness. No severe simulation sickness occurred

during riding sessions, with zero dropouts due to this; all 28 completed the experiment except one who missed the daytime session (n=27).

References

Bella, F. (2008). Driving simulator for speed research on two-lane rural roads. *Accident; Analysis and Prevention, 40*(3), 1078–1087. https://doi.org/10.1016/j. aap.2007.10.015

Bella, F., Silvestri M. (2015). Effects of safety measures on driver's speed behavior at pedestrian crossings. *Accident analysis and prevention* 08/2015; 83:111-124. DOI:10.1016/j.aap.2015.07.016

Bella, F., Silvestri M. (2017). Interaction driver–bicyclist on rural roads: Effects of cross-sections and road geometric elements. *Accident Analysis and Prevention*. Volume 102, 1 May 2017, Pages 191-201. DOI: 10.1016/j.aap.2017.03.008.

Calvi, A., & D'Amico, F. (2006). Quality control of road project: Identification and validation of a safety indicator. *Advances in Transportation Studies International Journal, 9*, 47–66.

Calvi, A. (2015). Does roadside vegetation affect driving performance? Driving simulator study on the effects of trees on drivers' speed and lateral position. *Transportation Research Record, 2518*, 1–8. https://doi.org/10.3141/2518-01

Calvi, A. (2018). Investigating the effectiveness of perceptual treatments on a crest vertical curve: A driving simulator study. *Transportation Research Part F: Traffic Psychology and Behaviour, 58*, 1074–1086. https://doi.org/10.1016/j.trf.2018.06.002

Calvi, A., Bella, F., & D'Amico, F. (2018). Evaluating the effects of the number of exit lanes on the diverging driver performance. *Journal of Transportation Security, 10* (1–2), 105–123. https://doi.org/10.1080/19439962.2016.1208313

Calvi, A., D'Amico, F., Ferrante, C., & Bianchini Ciampoli, L. (2020). A driving simulator validation study for evaluating the driving performance on deceleration and acceleration lanes. *Advances in Transportation Studies, 50*, 67–80. http://doi.org/10.54941/ahfe1002434.

Gettman, D., & Head, L. (2003). Surrogate Safety Measures from Traffic Simulation Models. *Transportation Research Record Journal of the Transportation Research Board*, *1840*(1), 104–115. https://doi.org/10.3141/1840-12

Li, S., Anis, M., Lord, D., Zhang, H., Zhou, Y., & Ye, X. (2024). Beyond 1D and oversimplified kinematics: A generic analytical framework for surrogate safety measures. *Accident Analysis & Prevention*, *204*, 107649. https://doi.org/10.1016/j.aap.2024.107649

Mahmud, S. M. S., Ferreira, L., Hoque, Md. S., & Tavassoli, A. (2017). Application of proximal surrogate indicators for safety evaluation: A review of recent developments and research needs. *IATSS Research*, *41*(4), 153–163. https://doi.org/10.1016/j.iatssr.2017.02.001

Miller, A. J. (1974). A note on the analysis of Gap-Acceptance in traffic. *Journal of the Royal Statistical Society Series C (Applied Statistics)*, *23*(1), 66. https://doi.org/10.2307/2347055

Ni, Y., Wang, M., Sun, J., & Li, K. (2016). Evaluation of pedestrian safety at intersections: A theoretical framework based on pedestrian-vehicle interaction patterns. *Accident Analysis & Prevention*, *96*, 118–129. https://doi.org/10.1016/j.aap.2016.07.030

Razzaq, A. K., & Shubber, K. H. H. (2022). Effect of waiting time on gap acceptance Characteristics of change direction U-Turn opening. *Mathematical Modelling and Engineering Problems*, *9*(3), 825–830. https://doi.org/10.18280/mmep.090332

Tageldin, A., Zaki, M. H., & Sayed, T. (2017). Examining pedestrian evasive actions as a potential indicator for traffic conflicts. *IET Intelligent Transport Systems*, *11*(5), 282–289. https://doi.org/10.1049/iet-its.2016.0066

Balk, S. A., Bertola, D. B., & Inman, V. W. (2013, June). Simulator sickness questionnaire: twenty years later. In *Driving assessment conference* (Vol. 7, No. 2013). University of Iowa.

Bottesi, G., Ghisi, M., Altoè, G., Conforti, E., Melli, G., & Sica, C. (2015). The Italian version of the Depression Anxiety Stress Scales-21: Factor structure and psychometric properties on community and clinical samples. *Comprehensive psychiatry*, *60*, 170-181.

Fossati, A., Di Ceglie, A., Acquarini, E., & Barratt, E. S. (2001). Psychometric properties of an Italian version of the Barratt Impulsiveness Scale-11 (BIS-11) in nonclinical subjects. *Journal of clinical psychology*, *57*(6), 815-828.

Hart, S. G. (2006, October). NASA-task load index (NASA-TLX); 20 years later. In Proceedings of the human factors and ergonomics society annual meeting (Vol. 50, No. 9, pp. 904-908). Sage CA: Los Angeles, CA: Sage publications.

Himmels, C., Rock, T., Venrooij, J., & Riener, A. (2020). Presence questionnaires in driving simulation. *PRESENCE: Virtual and Augmented Reality*, *29*, 261-275.

Lovibond, P. F., & Lovibond, S. H. (1995). The structure of negative emotional states: Comparison of the Depression Anxiety Stress Scales (DASS) with the Beck Depression and Anxiety Inventories. *Behaviour research and therapy*, *33*(3), 335-343.

Patton, J. H., Stanford, M. S., & Barratt, E. S. (1995). Factor structure of the Barratt impulsiveness scale. *Journal of clinical psychology*, *51*(6), 768-774.

Realo, A., Allik, J., Nőlvak, A., Valk, R., Ruus, T., Schmidt, M., et al. (2003). Mind-reading ability: Beliefs and performance. *Journal of Research in Personality, 37*(5), 420–445. doi: 10.1016/S0092-6566(03)00021-7

Reason, J., Manstead, A., Stradling, S., Baxter, J., & Campbell, K. (1990). Errors and violations on the roads: a real distinction? *Ergonomics*, *33*(10-11), 1315-1332.

Sangiuliano Intra, F., Tagliabue, S., Di Dio, C., Marchetti, A., & Massaro, D. (2018). Psychometric Properties of Mind-reading Belief Scale on an Italian Sample and Correlation with the Self-Construal. Studia Psychologica, 60(2), 94-107.

Schubert, T., Friedmann, F., & Regenbrecht, H. (2001). The experience of presence: Factor analytic insights. *Presence: Teleoperators & Virtual Environments*, *10*(3), 266-281.

Smorti, M., & Guarnieri, S. (2016). Exploring the factor structure and psychometric properties of the Manchester Driver Behavior Questionnaire (DBQ) in an Italian sample. *TPM. Testing, Psychometrics, Methodology in Applied Psychology*, *23*(2), 185-202.